

**FREDERICO VASCONCELLOS GUATIMOSIM**

**MECHANICAL BEHAVIOUR AND STRUCTURAL  
PERFORMANCE OF RECYCLED FOAMED BITUMEN  
STABILIZED MATERIALS**

São Paulo  
2015

**FREDERICO VASCONCELLOS GUATIMOSIM**

**MECHANICAL BEHAVIOUR AND STRUCTURAL  
PERFORMANCE OF RECYCLED FOAMED BITUMEN  
STABILIZED MATERIALS**

Dissertation presented for the degree of  
Master of Science (Engineering) at the  
Polytechnic School of the University of  
São Paulo.

São Paulo  
2015

**FREDERICO VASCONCELLOS GUATIMOSIM**

**MECHANICAL BEHAVIOUR AND STRUCTURAL  
PERFORMANCE OF RECYCLED FOAMED BITUMEN  
STABILIZED MATERIALS**

Dissertation presented for the degree of  
Master of Science (Engineering) at the  
Polytechnic School of the University of  
São Paulo.

Research Area:  
Transportation Engineering

Advisor: Prof. Kamilla Vasconcelos,  
PhD

São Paulo  
2015

Este exemplar foi revisado e corrigido em relação à versão original, sob responsabilidade única do autor e com a anuência de seu orientador.

São Paulo, \_\_\_\_\_ de \_\_\_\_\_ de \_\_\_\_\_

Assinatura do autor: \_\_\_\_\_

Assinatura do orientador: \_\_\_\_\_

#### Catálogo-na-publicação

Guatimosim, Frederico

Mechanical Behaviour and Structural Performance of Recycled Foamed Bitumen Stabilized Materials / F. Guatimosim -- versão corr. -- São Paulo, 2015. 109 p.

Dissertação (Mestrado) - Escola Politécnica da Universidade de São Paulo. Departamento de Engenharia de Transportes.

1.Pavimentação (Reabilitação) 2.Reciclagem 3.Avaliação Laboratorial 4.Avaliação de Campo I.Universidade de São Paulo. Escola Politécnica. Departamento de Engenharia de Transportes II.t.

I dedicate this thesis to my grandfather, José Silvério, best human being I've ever met, without whom none of this would have been possible...

## **ACKNOWLEDGEMENTS**

First and foremost, I would like to thank my parents Henrique and Thereza Christina for everything they have done for me. Without their guidance and love I wouldn't have been able to achieve all that I have, for my success is a mere result of theirs.

I'd like to thank my sister, Mariana, for her kind words and caring. The road has been lighter by your side.

For my uncle Rodrigo and my aunt Flavia, for all the support, attention and incentive through all the steps that have brought me here. Your support motivates me and gives me confidence to move forward.

I'd like to thank my grandmother, Maria Thereza for always thinking I am two steps ahead, when I am actually one step behind trying to catch up.

I would like to thank all the personnel from the Laboratory of Pavement Technology of University of São Paulo for their valuable support in the experimental laboratory tests. I'd like to thank Diomária taking care of all of us students as a mother, Erasmo for helping me with the hard work, Vanderlei for all the patience to help me prepare the tests and the support while performing and Robson and Edson for all the talks and valuable lessons you taught me even when we were just passing time.

I would also like to thank ValmirBonfim from Fremix, whose lecture brought me in contact with the BSM theme, and whose support has been vital for this dissertation development.

I'd like to thank Wendell Pereira and Cristian Amaro, for all their field support and availability.

For my bosses Anselmo and Renato, for helping me throughout and allowing me to spend so many days out of the office without ever complaining.

At last, I'd like to thank Dave Collings, Wynand van Niekerk and Professor Kim Jenkins for all their valuable support, kind attention and amazing hospitality. Part of my fondness for this thesis comes from how fondly I remember Africa.

## RESUMO

Em busca de soluções estruturais para restauração de pavimentos rodoviários que sejam eficientes, mas ao mesmo tempo que sejam econômicas e impactem o mínimo possível na dinâmica de operação da malha rodoviária, tem sido difundida a metodologia de reciclagem a frio de pavimentos com a estabilização com espuma de asfalto. A redução de custos devido a reutilização de material e a menor necessidade de transporte de insumos, além da possibilidade de realização da restauração em um curto espaço de tempo, têm contribuído para a crescente utilização do processo. Este trabalho tem como objetivo avaliar o desempenho e o comportamento mecânico de uma mistura reciclada estabilizada com espuma de asfalto, para melhor entender os efeitos do confinamento e do teor de umidade do material, visto que este passa por um processo de cura quando já em serviço. Foi acompanhado um trecho experimental onde o pavimento foi restaurado com a aplicação de uma base reciclada estabilizada com espuma de asfalto. O segmento foi monitorado através do controle tecnológico de execução e de levantamentos deflectométricos com FWD. Verificou-se que as deflexões após quase 24 meses da execução do trecho reduziram consideravelmente. Paralelamente, foram realizados ensaios de resistência à tração por compressão diametral, módulo de resiliência triaxial e de deformação permanente para diferentes procedimentos de cura para verificação do efeito da saída da água nas mudanças de comportamento mecânico do material. Verificou-se ainda o efeito das tensões de confinamento no módulo de resiliência de materiais estabilizados com espuma de asfalto e determinaram-se os parâmetros de cisalhamento do material através de ensaios Triaxiais Monotônicos. Pode-se concluir que a cura é uma consideração importante tanto com relação a sua duração, quanto com relação ao seu efeito no comportamento do material.

**Palavras-chave:** Reciclagem a frio; Espuma de asfalto; Rigidez; Deformação Permanente; Estado de Tensão

## ABSTRACT

Seeking for pavement rehabilitation solutions that result in efficient and capable structures, that bring economic advantages, and the smallest possible impact to the road network operation, cold recycling with foamed asphalt stabilization has been gaining acceptance and growing steadily. The possibility of economic benefits due to material reuse and the decrease in transportation costs, allied to the reduced time needed to open to traffic, have contributed to the increase in this technique's use. This study has the objective of evaluating the performance of cold recycled mixes stabilized with foamed asphalt, for a better understanding on the effects of confining stresses, and material moisture content, since it undergoes the curing process when in service. An experimental test section with foamed stabilized recycled material used as the base course was monitored through quality control and quality assurance and FWD tests. It was observed that deflections, after nearly 24 months, have decreased significantly. In laboratory, Indirect Tensile Strength, Triaxial Resilient Modulus, and Permanent Deformation Tests were conducted for samples cured through different procedures, to evaluate the stress dependency and the effect of moisture decrease on the material behaviour. As a complementing test to evaluate the effect of confinement on material mechanical behaviour and to characterize the shear properties in foamed stabilized materials, a Monotonic Triaxial Test was performed. Based on the results obtained, one can conclude that the curing is a critical consideration in terms of timing and its influence on pavement performance. Triaxial tests showed the stress dependency of this bitumen stabilized material, while permanent deformation results indicated some potential for damage in the early stages after construction. Also, foamed bitumen stabilized materials stress dependency indicate that its mechanical behaviour is similar to unbound granular materials. On the field evaluation, FWD data indicated the decrease in deflection with time, resulting in an increase of the layers stiffness.

**Keywords:** Cold Recycling, Foamed Asphalt, Stiffness, Permanent Deformation, Stress Dependency.



## FIGURES LIST

Figure 1 – Optimum water content determination as a function of the expansion rate and half life of the foamed bitumen (Wirtgen, 2012). .....	12
Figure 2 – Curing time and long-term performance of different materials (SANRAL, 2014). .....	19
Figure 3 – (a) Specimen with the rubber membrane inside the pressurized chamber; (b) Servo-pneumatic test machine. ....	22
Figure 4 – Pavement layer thickness using cold in-situ foamed bitumen recycling (Milton and Earland, 1999). ....	27
Figure 5 – Layer Thickness of <i>in situ</i> and <i>ex situ</i> (plant mix) foamed bitumen recycled material, with 100 mm of asphalt surfacing required for all cases (Nunn and Thom, 2002). ....	28
Figure 6 – Criteria for Determining Allowed Capacity from PN (Asphalt Academy, 2009). ....	32
Figure 7 – Flow chart of the PN design methodology (adapted from Austroads, 2011) .....	33
Figure 8 – Position of analysis for each layer and parameter (SANRAL, 2014) .....	34
Figure 9 – Location of the Trial Section. ....	38
Figure 10 – Existing structure in Highway SP-070 prior to rehabilitation.....	39
Figure 11 – Location of the KMA 220 mix plant. ....	41
Figure 12 – Foamed Stabilized Recycled Mixture Gradation. ....	43
Figure 13 – Gradation for Recycled mixture containing 100% RAP + Crushed CTB and 1% Hydrated lime. ....	45
Figure 14 – Proposed pavement structure.....	47

Figure 15 – Structural analysis results for a segmented recycled layer using Rubicon Toolbox Software. ....	49
Figure 16 – Structural analysis results for a unified recycled layer using Rubicon Toolbox Software. ....	50
Figure 17 – Pavement milling of the Trial Section. ....	51
Figure 18 – Location of FWD evaluation points. ....	52
Figure 19 – (a) Existing pavement structure; (b) Recycled pavement structure. ....	52
Figure 20 – (a) Recycled layer execution; (b) Compaction with the TCR (15 tons) ...	53
Figure 21 – (a) Sand Equivalent Test; (b) FWD evaluation of stipulated points. ....	55
Figure 22 – Deflection bowls for the 90th percentile of D0 for the FWD tests performed on diferente layers on rehabilitation day. ....	56
Figure 23 – Deflection bowls for the 90th percentile of D0 for different FWD evaluations. ....	57
Figure 24 – Maximum deflection (D0) evaluation of the trial section on different occasions. ....	58
Figure 25 – Backcalculated Elastic Modulus for the BSM layer along the curing period. ....	60
Figure 26 – Flow chart with a summary of laboratory proceedings ....	61
Figure 27 – Material (a) reception; (b) homogenization; (c) separation; (d) storage..	63
Figure 28 – Moisture Density relation determination (Specimens with 152 x 127 mm) .....	64
Figure 29 – (a) specimen with 152 x 127 mm; (b) material drying in the oven; (c) specimen with 200 x 100 mm; (d) sample of oven dried material. ....	65
Figure 30 – LCPC compaction machine; .....	66

Figure 31 – LCPC Traffic Simulator operating at ambient temperature.....	67
Figure 32 – Percentage of rutting accumulated in the wheel path in terms of the number of load cycles. ....	69
Figure 33 – Specimen preparation and triaxial test: (a) bottom capping; (b) Top capping; (c) capped specimen with top cap positioned; (d) specimen during the test .....	72
Figure 34 – Resilient Modulus for dry cured specimens with different periods in terms of the confining stress ( $\sigma_3$ ).....	73
Figure 35 – Specimen tested without curing resulting in (a) deformation along the diametral line; (b) material crumbling when removed from test apparatus. ....	74
Figure 36 – Resilient Modulus for humid cured specimens with different periods in terms of the confining stress ( $\sigma_3$ ).....	75
Figure 37 – Resilient Modulus obtained for stress combination of $\sigma_d = 0,309$ MPa and $\sigma_3 = 0,103$ MPa.....	76
Figure 38 – (a) Specimen positioning for ITS test; (b) specimen after failure. ....	78
Figure 39 – ITS results for different curing periods and procedures.....	79
Figure 40 – (a) Specimen during the monotonic triaxial test; (b) effect of air confinement on latex membrane. ....	80
Figure 41 – Gradation envelope for the BSM material used in the Monotonic Triaxial Test. ....	82
Figure 42 – Mohr-Coulomb failure envelope. ....	84

## TABLES LIST

Table 1 – Gradation envelope for BSM (Asphalt Academy, 2002). .....	42
Table 2 – Initial designed mixture for the recycled layers.....	44
Table 3 – ITS tests for the mixture containing 100% RAP + Crushed CTB an 1% of Hydrated Lime .....	45
Table 4 – Gradation for Recycled mixture containing 100% RAP + Crushed CTB and !% Hydrated lime. ....	46
Table 5 – Material properties defined for structural analysis modelling on Rubicon Toolbox Software. ....	48
Table 6 – ITS results from mixture quality control. ....	54
Table 7 – Construction quality control results.....	54
Table 8 – Accumulated Permanent Deformation per curing, based on the LCPC Simulator tests.....	69
Table 9 – Stress combinations for the Resilient Modulus Tests .....	71
Table 10 – Resilient modulus Increase Rate per different curing periods. ....	76
Table 11 – Residual moisture content and resilient modulus equations.....	76
Table 12 – Gradation of the BSM mixture used for the Montonic Triaxial Tests.....	81
Table 13 – Monotonic Triaxial Test results.....	83
Table 14 – FWD data and backcalculation results for measurements made on September/2013, on top of the remaining infrastructre. ....	98
Table 15 – FWD data and backcalculation results for measurements made on September/2013, on top of the bottom BSM layer.....	100

Table 16 – FWD data and backcalculation results for measurements made on September/2013, on top of the top BSM layer.....102

Table 17 – FWD data and backcalculation results for measurements made on December/2013.....104

Table 18 – FWD data and backcalculation results for measurements made on October/2014.....106

Table 19 – FWD data and backcalculation results for measurements made on June/2015.....108

## SUMMARY

1	INTRODUCTION .....	1
1.1	PROBLEM IDENTIFICATION .....	2
1.2	OBJECTIVES .....	3
1.3	DISSERTATION OUTLINE .....	4
2	RECYCLING IN ASPHALT PAVEMENT REHABILITATION .....	5
2.1	COLD RECYCLING .....	8
2.2	RECYCLED LAYERS.....	9
2.3	ASPHALT BINDERS IN COLD RECYCLING.....	10
2.4	INPUTS USED IN RECYCLING WITH FOAMED BITUMEN .....	14
2.5	CURING OF BSM .....	18
2.6	BSM MECHANICALPERFOPRMANCE.....	20
2.6.1	Indirect Tensile Strength Test.....	21
2.6.2	Triaxial Resilient Modulus Testing .....	21
2.6.3	Monotonic Triaxial Testing.....	23
2.6.4	FWD Testing.....	24
2.7	MIXTURE AND STRUCTURAL DESIGN OF BSM LAYERS .....	25
2.7.1	Departamento Nacional de Infraestrutura de Transportes (DNIT) .....	25
2.7.2	Departamento de Estradas e Rodagem do Paraná (DER-PR).....	26
2.7.3	Transportation Research Laboratory (TRL) – United Kingdom.....	26
2.7.4	Department of Transport and Main Roads (TMR), Queensland – Australia .....	28
2.7.5	City of Canning – Australia .....	29
2.7.6	New Zealand Transport Agency – New Zealand .....	29
2.7.7	TG2 2009 – Structural Design Method – South Africa .....	30
2.7.8	SAPEM 2014 – South African Pavement Engineering Manual .....	34
3	TRIAL SECTION.....	37
3.1	TRIAL SECTION CHARACTERIZATION.....	38
3.2	REHABILITATION SOLUTION .....	40
3.3	REHABILITATION PROJECT .....	41
3.4	TRIAL SECTION CONSTRUCTION .....	50
3.5	FWD MONITORING.....	55
3.6	FWD BACKCALCULATION .....	58
4	LABORATORY ANALYSIS.....	61
4.1	TRIAL SECTION MATERIAL .....	62
4.2	MOISTURE DENSITY RELATION .....	64

4.3	PERMANENT DEFORMATION EVALUATION.....	65
4.4	TRIAXIAL RESILIENT MODULUS .....	69
4.5	INDIRECT TENSILE STRENGTH TEST.....	77
4.6	MONOTONIC TRIAXIAL TEST .....	79
5	SUMMARY AND CONCLUSIONS.....	85
6	SUGGESTIONS FOR FUTURE RESEARCH.....	89
7	REFERENCES LIST.....	91
	APPENDIX .....	98

## 1 INTRODUCTION

In Brazil, a country of continental dimensions where the main transportation mode is through roads, the good performance of the road network in attending user needs is critical for social and economic development. With a total of over 1.7 million kilometres of roadways, of which only 12.5% are paved (DNIT, 2014), most of the country's goods and people are transported into a few major highways. This scenario increases the traffic and creates logistic issues for production transport.

The country's economic growth in the last two decades associated with the lack of proper maintenance and expansion of the network, has led to an increase in the road traffic and a gradual deterioration of the existing pavements. Although pavement materials deteriorate with time and weathering, the increase of load repetitions tends to accelerate this process, and rise the frequency of rehabilitations.

To attend the traffic demands, the pavement structures should be increasingly efficient, minimizing interventions, rehabilitations and reconstruction of damaged roadways.

The growth of urban areas in a higher pace than that of the public transportation results in saturation of city accesses and highways capacity. The impact of an accident or a lane interdiction for maintenance may affect significantly the logistics of the network operation and the lives of all users relying on it.

The development and application of structural solutions that increase the pavements life expectancy, reducing operational impacts and maintenance costs are sought after ever more avidly.

Due to the operational difficulties encountered in rehabilitation campaigns, allied to financial restrictions, mitigatory solutions are often applied, resulting in more interventions and long-term higher costs.



The search for solutions of good structural performance and low maintenance and application costs has recently led to the propagation and spreading of recycling techniques, especially those using material stabilization with foamed bitumen.

The possibility of reusing the milled material from the deteriorated pavement, also reducing transportation costs, further support the acceptance of recycling processes from a financial perspective. The time needed for construction counts as another benefit, reducing operational impacts. From the technical point of view, recycling allows you to quickly rehabilitate deeper layers, providing a powerful tool to eliminate structural distresses.

## 1.1 PROBLEM IDENTIFICATION

Although foamed bitumen stabilization of recycled pavements is not a new technology, it is still far from being a worldwide standardly applied technique. Even though the mechanical behaviour of the stabilized layer is associated with that of asphalt mixtures due to the binder presence, it seems to be closer to that of granular materials, but with higher cohesion (Jenkins, 2000; Fu and Harvey, 2007; Jooste and Long, 2007; Collings and Jenkins, 2011; Schwartz and Khosravifar, 2013).

As a rehabilitation technique, the mechanical behaviour of materials in the field is of great importance, especially to the understanding of its best applications. In the recycled material mixing process, there is water addition both as the foaming agent, as well as the mixing and compaction moisture. After paving the layer, it can be observed that as water comes out as part of the curing process, material stiffness increases leading to lower structure deformability levels.

An important question is how the materials performance changes along the curing period, and what impacts these changes may have in the pavements response to traffic demands over time. Looking into the curing effect, and assuming that the foamed bitumen stabilized material, also referred to as

BSM (Asphalt Academy, 2009; Wirtgen, 2012), behaves as a granular material, it can be questioned what the effects of a greater material deformability in the early stages would have in the long term performance.

This thesis aims to evaluate the foamed bitumen stabilized material behaviour both in the field and in the laboratory, comparing the resilient modulus from backcalculated FWD data and triaxial resilient modulus testing. Laboratory testing was also conducted with the objective of analyzing the effects of confinement and the similarities between foamed stabilized materials and granular materials. The curing effect is also analyzed as how it impacts the material stiffness and permanent deformation susceptibility through triaxial testing and laboratory traffic simulator, respectively.

## 1.2 OBJECTIVES

The main objective of this study is to evaluate the behaviour of foamed bitumen stabilized materials both in the field and in the laboratory. The field evaluation was done with FWD tests in a trial section in the Ayrton Senna Highway, in the State of São Paulo. For the laboratory analyses, Indirect Tensile Stress tests were conducted, as well as Triaxial Resilient Modulus, Permanent Deformation, and Monotonic Triaxial tests.

The specific objectives of this thesis are:

- Compare the resilient modulus obtained from the triaxial resilient modulus tests and the backcalculated FWD data;
- Quantify the effect of confinement through the triaxial resilient modulus test and evaluate if it behaves like a granular material;
- Evaluate the curing influence in the materials mechanical behaviour with triaxial resilient modulus and permanent deformation analyses.

### 1.3 DISSERTATION OUTLINE

This dissertation is organized in 6 chapters, as described below:

Chapter 1 – Introduction of the studied theme, where the reader is presented to the objectives of the research and the proposed methodology to assess it.

Chapter 2 – Literature review on recycling techniques, at first as a general theme and afterwards more specifically, to provide means for the research development and analysis.

Chapter 3 – Trial section characterization and evaluation. Presentation of the trial section, material characterization, discussion of the rehabilitation procedure, presentation of execution quality control data and field monitoring through deflectometric analysis.

Chapter 4 – Laboratory analysis of BSM mechanical behavior through mixture characterization and execution of Triaxial Resilient Modulus Tests, Permanent Deformation Tests, Indirect Tensile Strength Tests, Monotonic Triaxial Tests and discussion on the obtained results.

Chapter 5 – Presentation of all findings and final conclusions, with the assessment of the research objectives attainment,

Chapter 6 – Suggestion of topics for future research involving the studied theme.

## **2 RECYCLING IN ASPHALT PAVEMENT REHABILITATION**

Pavement deterioration through time is caused by several reasons such as repeated traffic loading, weathering, and even low quality construction and proceedings. The early deterioration leads to a search for efficient rehabilitation techniques that allow us to increase the design life of the pavement, with proper serviceability level, attending the users' needs.

Throughout service life, a road will keep, in most cases, its original structure and components, although the materials response and characteristics may change with time. In this sense, the recovery of initial material properties, and consequently the original structural response, would lead to pavement rehabilitation.

Some changes that may happen in the degradation process cannot be reversed, especially considering limited amounts of financial resources for that purpose. On the other hand, it is still possible to reuse these materials by changing its characteristics to fit new functions and technical purposes.

Degraded materials that can be found in existing pavements may be non-stabilized or contaminated granular layers, cracked cemented treated layers, soil layers, or even asphalt concrete. The most common material to be reused in road paving is the Reclaimed Asphalt Pavement (RAP) obtained through cold milling of asphalt layers.

Recycling these materials may be done by incorporating new aggregates, rearranging the existing ones for a better gradation, or adding chemical additives and stabilizers.

One alternative to granular stabilization is the addition of chemicals, such as cement and hydrated lime, or asphalt binder. These agents create bonds between the aggregates through cementation, calcification or particle adhesion, making the layer stiffer, less susceptible to moisture damage, and with more predictable elastic behaviour.

The more common rehabilitation techniques use asphalt mixture overlays above the existing structure, local repairs with material substitution in different structure levels, or even full reconstruction of entire segments.

The use of recycling techniques has been growing since the early 1970's, driven by the oil business crisis and the high costs of its by-products, as the asphalt binder. Before the crisis, the costs involved in milling, stock piling, processing and application of a recycled layer were far higher than those to execute new hot mix asphalt layers (Roberts et al., 1996).

Overlaying asphalt layers may not be a proper long-term solution, as pathologies in the existing structure tend to resurface in the new ones (Tang et al., 2012). Not only that, but consecutive overlays can result in significant geometry modifications, which may lead to safety issues and profile problems, especially in bridge and superstructure transitions. To avoid these geometry alterations, cold milling of degraded asphalt surface is often used. For this reason, RAP is a common and abundant resource.

Although reconstruction is an effective solution, as previous problems will be sorted and will not reappear, it is a very lengthy and costly solution, involving, most the times, the use of new materials and the disposal of the existing ones.

Recycling allows you to reuse the existing materials, reducing the impacts generated by extraction and transportation of new ones. Some other recycling advantages when compared to conventional techniques are: (i) reduction of natural resources and fuel, (ii) reuse of high quality materials that would have been disposed of, (iii) reduction of working vehicles in the job site and surroundings, (iv) minimization of lane closure time (Stroup-Gardiner, 2011).

There are different recycling methods: (i) hot and cold (nowadays, even warm), and (ii) in plant for later application, or in situ for immediate application.

Hot mix recycling can be done either in plant or in situ. In the first case, the RAP may be cold milled and taken to a plant, while in the second case it has

to be obtained by hot or cold milling and mixed with the addition of new materials by specific equipment that applies and finishes the layer in one single pass (Castro Neto, 2000). Both processes use aggregate heating as the way of reducing moisture, activating the old binder around the RAP with the intention of creating a better mix between aggregates and the binder.

Therefore, hot mix recycling dispenses a higher cost due to the amount of energy necessary, being primarily used for recycling surface layers with low distress levels (Stroup-Gardiner, 2011).

Cold recycling techniques on the other hand, do not involve the drying and heating of materials, which makes it feasible for different applications, as detailed in section 2.1. This process is commonly used to treat distresses in deeper pavement layers, as it can be done with a bigger variety of materials (Bang et al., 2011). Some examples are the recycled layers with (i) cement, (ii) hydrated lime, (iii) asphalt emulsion, (iv) foamed bitumen, and (v) granular stabilization.

The milled material processing, and the gradation of the new material, can be done in plant, or in situ. For a plant recycling process, the material is collected through milling, or from other stockpile, taken to the plant to be treated, graded and mixed to the new materials. In this process, there is more control of the process, with the possibility of combining different material sources to obtain the desired design gradation. The different materials may come from different places, or even from the same road, in the case of roads that have been repeatedly rehabilitated creating great structure variability. On the other hand, the need for transportation from the plant to the job site means an added cost in the process (Wirtgen, 2012).

In situ recycling is a continuous process, meaning that pavement is milled, crushed, mixed with stabilizing agents, applied and conformed in a single pass. Once the road possesses layers with consistent depths and materials, this process may present high productivity with good results and low costs. If the variability of the pavement structure is considerable, this technique may present very different outcomes from one section to another.

## 2.1 COLD RECYCLING

Cold recycling is the process, in which the materials involved are not heated, with the whole process being conducted at ambient temperature (Bonfim, 1999). Although the costs involved are lower due to the smaller amounts of energy consumed, the final outcome of the process still has a few limitations.

As it is not possible to mix the asphalt binder and aggregates at ambient temperature, the use of asphalt emulsion or foamed bitumen is needed to stabilize the recycled material (ARRA, 2001). Cold recycled mixes should have similar behaviour to that of conventional Hot Mix Asphalt (HMA) to be used as a surface layer. Therefore, parameters such as abrasion, roughness and shear resistance become limiting factors for this application.

The literature refers to the procedure of application of cold recycling techniques for rehabilitating deep pavement layers as FDR – Full Depth Reclamation (ARRA, 2001). This process is performed without any heating of the materials involved, and can be done either in plant, or in situ. Since more than one layer may turn into reclaimed material, not only RAP, but also soil, crushed cement treated layers, graded crush stone and other granular materials may be used in the foaming process. Due to this variability, the end product is usually applied as base, or subbase, in the pavement structure.

The main objective in processing the milled material is to build a new layer with better performance than the previous existing one. One simple way of recycling is incorporating new materials, to increase the granular stability. During the milling process, an abundance of fines may be obtained due to the crushing and breaking of aggregates. The RAP may also come in the form of lumps and, therefore, a coarser material. The addition of virgin aggregates can be necessary to fit the design gradation, and promote a better aggregate interlocking and a higher layer density.

The addition of hydrated lime and cement is also common in the recycling process. The addition of these materials affects directly the performance of

the final mixture, acting as active filler if added in low percentages or as a stabilizing agent as the percentage becomes higher. The addition of cement to recycled layers in percentages higher than 1.0% may lead to a highly cohesive behaviour, with higher stiffness and brittleness. At lower rates, the material may preserve the behaviour previously presented in the layer. (Asphalt Academy, 2009).

## 2.2 RECYCLED LAYERS

The use of recycled materials in the surface layer is done in fewer applications when compared to its use in deeper pavement layers. In these cases, the recycled materials, usually RAP, is added to high quality virgin aggregates, in order to fit the mixture gradation specification.

For surface layers, West (2010) says that the average RAP incorporation rate in new asphalt mixes in the United States is between 12% and 15%, with a rate up to 30% resulting in the same performance as conventional mixtures that only use virgin aggregates. Other authors, as Rahman et al. (2014), have obtained good results studying permanent deformation in the Hamburg Wheel Tracking Device with RAP percentages of up to 50%, surpassing some of the results of mixes with rates of 10% and 30%.

The addition of high percentages of RAP in the production of hot in plant recycled mixtures require the adaptation of conventional hot mix plants, for the reclaimed aggregates mixing to be more efficient. Besides, to seize and activate the remaining binder in RAP, heating is needed to reduce its viscosity, with the possibility to add rejuvenating agents to the mix to recover its original properties, and reverse the process of asphalt oxidation.

Asphalt emulsion is commonly used in the cold recycling process of asphalt layers, since its viscosity is much lower than that of asphalt cement at ambient temperatures. The use of foamed bitumen in the cold recycling process doesn't result in the complete coating of the aggregates, with only the finer particles being covered by asphalt particles, turning those in the ones



responsible for stabilizing the material (Asphalt Academy, 2009). Since the bonds created by the foamed bitumen, or by the asphalt emulsion, are more fragile, the application of these materials as surface layers should be restricted to low traffic and low speed roads, reducing the impacts of pavement deterioration due to abrasive processes.

The decision for recycled surface layers should be made for correction of functional aspects, associated to the pavement surface layer. To assess distresses in deeper layers, it is recommended the Full Depth Reclamation (FDR), resulting in recovered base or subbase (ARRA, 2001).

For full depth reclamation, both the surface layer and the subjacent layers are milled and combined to stabilizing agents, and also new materials when there is the need to correct the material gradation.

## 2.3 ASPHALT BINDERS IN COLD RECYCLING

The common applications of asphalt binder as stabilizing agent in cold recycling processes are through the use of asphalt emulsion or foamed bitumen. The Asphalt Academy (2009) refers to these mixes as Bitumen Stabilized Mixtures (BSM), separating emulsion and foamed bitumen application only from an executive point of view. They also classify the mix as BSM 1, BSM 2, or BSM 3, depending on the quality of the used materials, with the BSM 1 being the one with highest quality, and BSM 3 the one with the lowest. Classification is done by the evaluation of aggregate gradation, mechanical and physical properties.

Both the emulsion and foamed bitumen stabilization processes can be done in situ or in a mix plant, with each technique deploying specific equipment. Asphalt emulsion is a mix between asphalt binder in a water solution, through a process of shear between bituminous particles that make possible the dispersion of water particles (ABEDA, 2001). Emulsifiers are added to give stability to the mix allowing it to be stockpiled, transported and applied at ambient temperatures.

During the mix process with asphalt emulsion, asphalt binder is dispersed preferably through the fines, although there is interaction with coarser aggregates. Polarity difference between the fines and the emulsion creates a chemical bond, conferring cohesion to the mix (Asphalt Academy, 2009). While the emulsion coats smaller aggregates, when low asphalt contents are used (as it is the case for BSM's) coarser aggregates are partially painted by the emulsion, creating discontinuities in the mix.

The production of foamed bitumen mixes, as described by Jenkins (2000), involves the mixture of asphalt binder at temperatures higher than 160°C with air and water at ambient temperature in an expansion chamber. The heat exchange between the binder and the water results in the increase of the particle surface temperature, exceeding the water's latent heat (100° C), with the formation of vapour. The vapour presses against the asphalt binder, being retained by a thin film's wall, resulting in bubbles and consequently foam, with an increase in volume until the point when the binder film's surface tension is as big as the tension created by the vapour. The loss of heat and the decrease in temperature lead to tension reduction, decreasing the volume of foam. The water content is controlled through the foaming expansion rate and its half-life, which are the volume increase and the time needed for it to reduce by half, respectively, as illustrated in Figure 1.

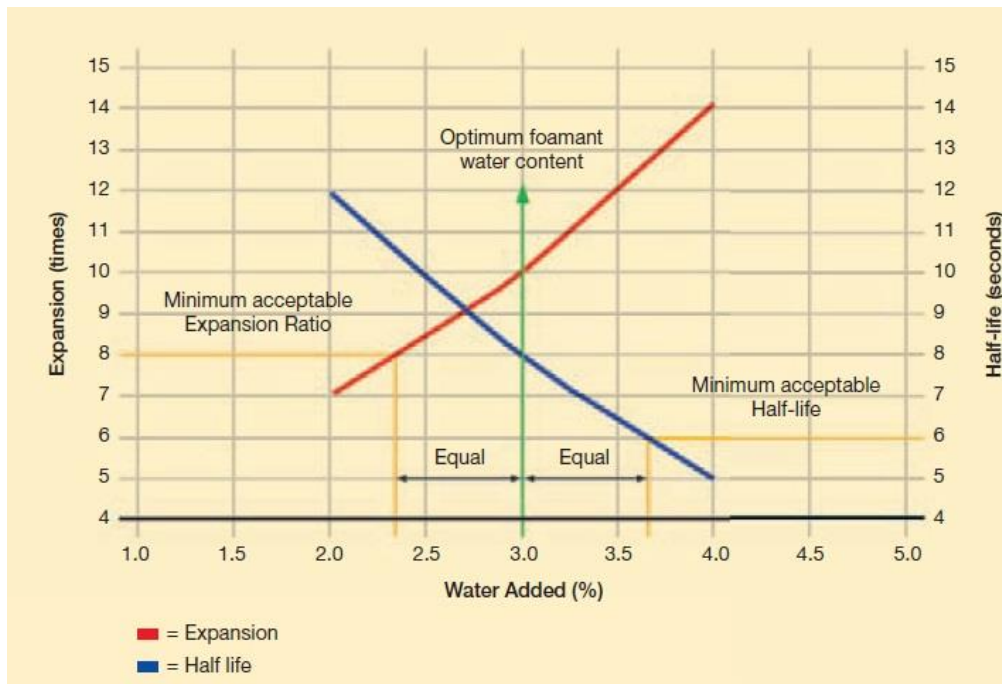


**Figure 1– Optimum water content determination as a function of the expansion rate and half-life of the foamed bitumen (Wirtgen, 2012)**

After the asphalt binder get in contact with air and water particles, the foam is produced at temperature of approximately 100°C, and it is mixed to the aggregates which are at ambient temperature. The energy released from burst of asphalt binder bubbles is only enough to heat the surface of the finer particles, due to its higher surface area/mass relation, making adhesion with the binder possible (Jenkins, 2000), but not to heat the coarser aggregates. Therefore, the mix turns out to have non continuous bonds, with partially coated coarse aggregates that are "spot welded" with fines mortar which provide a higher cohesion to the material.

As there is no binder dispersion throughout the mix, there is no continuous bonding between the aggregates reducing the chances of crack propagation and consequently fatigue failure. For this reason, the Asphalt Academy (2009) considers the material as granular-like, with similar void contents, but with a higher cohesion and lower moisture susceptibility. Schwartz and Khosravifar (2013) have also observed that Graded Crushed Stone and recycled materials stabilized with Foamed Bitumen behave alike regarding permeability, with rates of the same magnitude being found for both materials.

The addition of active filler (such as hydrated lime, or cement) may bring several benefits to the mix. As bitumen dispersion is done primarily through the fines, filler addition may not only improve the dispersion, but also help adjusting the aggregate gradation. Both hydrated lime and cement can reduce moisture susceptibility, aside from conferring a higher stiffness to the material. Since asphalt binder incorporation rates in BSM are low to make it cost effective, filler addition is recommended not to be higher than 1% (Asphalt Academy 2009; Wirtgen, 2012), making sure that the primary mechanism of stabilization are the asphalt bonds.

The water consumption in the exothermic hydration of cement may help the curing mixes stabilized with asphalt emulsion, since water exit accelerates the emulsion break (Heath and Roesler, 1999). As for foamed bitumen, the filler acts as a dispersion catalyst for bitumen particles (Brovelli and Crispino, 2011).

Just as granular materials, BSM must be compacted, promoting layer densification through air voids volume reduction, and increase of stiffness due to the increase of the friction between aggregates. The compaction process compresses the particles forcing the adhesion between the asphalt binder and the aggregate surface, increasing the mix's cohesion, and forcing the water out.

Differently from highly cohesive materials, where the confining stresses have little or no influence in the material stiffness, BSM's show variable resilient modulus depending on the existent stresses (Fu and Harvey, 2007), similarly to granular materials. The influence of confinement in the resistance was also verified by Jenkins (2000) and Schwartz and Khosravifar (2013). Jooste and Long (2007) state that BSM behave like granular materials with higher cohesion for low cement addition rates.

Once BSM's have similar characteristics and behave alike granular materials, permanent deformation may be considered the main criteria for layer failure (Alabaster et al., 2013; Asphalt Academy, 2009; Jooste and Long, 2007; Wirtgen, 2012). Wirtgen (2012) states that moisture susceptibility is also a

damage mechanism. On the other hand, the higher cohesion, due to both the asphalt binder and the active filler, reduce the materials susceptibility to moisture. Moisture damage is nonetheless an important factor to assure the structures life cycle, hence proper draining systems are vital for the long term performance of the structure (Jones et al., 2009).

The importance of proper draining mechanisms is important not only for BSM's, but for any other pavement structural material. In a structure composed by stabilized layers, the subgrade is the most moisture susceptible one, and the most deformable as well (Balbo, 2007), with the biggest contribution in the pavement structural deflection.

After the construction of the recycled layer, a process of material consolidation starts, and in the long term it may lead to the accumulation of vertical permanent deformations, verified in the surface of the pavement.

Although this defect compromises security and rideability, it may be prematurely identified and easily corrected with cold milling and surface overlaying. On the other hand, the more consolidated the material, the more resistant it will be, the less it will deform, and therefore the smaller will be the permanent deformations.

The application of Bitumen Stabilized Materials (BSM), allied to proper, design, execution and maintenance, may result in good pavement structural performance in the long term, reducing costs, time and rehabilitation complexity (Schwartz and Khosravifar, 2013).

## 2.4 INPUTS USED IN RECYCLING WITH FOAMED BITUMEN

Several types of reclaimed materials can be used for recycling purposes with foamed bitumen stabilization, although a few particular characteristics should be observed when looking for a better mix performance.

The usual method for reclaiming pavement material is by milling off the existing pavement, which means cutting off the pavement in a previously

specified depth (Bonfim, 2011). In this process, the material is reclaimed and then processed, either in situ or in plant, to create the constituents of the future recycled layer. Milling procedures may be done in different ways for different outcomes. If the existing structure has multiple layers with different materials, the reclaiming process can be done in parts, or in single pass, resulting in a mix of materials.

The milling equipment and the procedure applied also influence in the final reclaimed material. Depending on the operational speed, milling drums, and bit configuration, the material can have different characteristics (Bonfim, 2011).

The gradation of the reclaimed material, especially for cohesive layers, is very influenced by the process. As observed by West (2010), the breaking of aggregates by the impact of the milling bits may lead to a material of finer gradation.

Bonfim (1999) shows that the direction of the cutting also impacts the size of the reclaimed aggregates. If the milling drum rotates cutting from top to bottom direction, aggregates tend to be smaller, although it demands more power from the machine due to the higher cutting resistance. For this reason most machines are equipped with drums cutting from bottom to top.

Another important factor is the integrity of the layer being milled. The higher the deterioration, the lower the resistance offered against the cutting during the bottom to top process in milling machines. That way, the resulting particles become bigger (large pieces of cohesive material), hence the need for later crushing and gradation correction.

In urban areas, where resurfacing and overlaying existent pavement structures are a common practice, RAP is an abundant material for recycling. Since high quality material is used in HMA layers, RAP aggregates tend to have the same quality.

The presence of asphalt binder leads to the formation of aggregate clumps, resulting in reduced amount of finer particles that creates the need for gradation correction with the addition of finer fractions.

For mixtures with RAP there is the possibility of adding binder rejuvenators, in an attempt to revert the oxidation process of the aged asphalt binder. In cold recycling processes these additives are emulsified and composed by light asphalt fractions rich in malthenes (Bernucci et al., 2010).

Due to the high aggregate quality, the presence of asphalt binder, and the abundance of RAP for recycling, it has become very valuable for these procedures. The use of other materials, however, is not discarded, especially in FDR, where the amount of materials is big and the existing material can be modified to attend the design specifications.

Cement stabilized layers are common in Brazilian highways, more specifically in the State of São Paulo (Bernucci et al., 2010). These layers have high stiffness and their primary failure mechanism is the fatigue cracking, which leads to vertical crack propagation in the material, and also in adjacent layers. When the cemented layer is right beneath a surface asphalt layer, the cracks propagate vertically, and a deeper corrective procedure becomes necessary to address the reflective cracking issue.

Full Depth Reclamation technique is a possible rehabilitation procedure in these cases, recovering aggregates from deeper layers, treating the material and processing it to constitute a new adequate layer. Milling stabilized layers results in the formation of clumps, product of the bonding between particles of different sizes by the stabilizing agent. Once this material is recovered, it must be characterized to verify the need for gradation corrections.

The differences between the various types of materials that can be employed impact directly the mix gradation. Since mix stability is desired, different materials can be combined to fit a proper gradation envelope. As observed by Fu et al. (2008), recycled mixes stabilized with foamed bitumen should contain enough fines to provide a good dispersion of the binder particles, creating more cohesion between the particles. On the other hand, the excess

of fines may lead to the formation of a continuous mineral filler phase, which would result in less cohesion and higher susceptibility to moisture damage (Fu et al., 2011).

Reclaimed granular materials may also be applied, and although well graded material is preferred, the Asphalt Institute (1983) states that various materials can be used, from silty sands to crushed stones, as long as one of the following two criteria are obeyed. The first one is a verification of the product between the Plasticity Index (ASTM D 4318-10e1) and the percentage of material passing the 75  $\mu\text{m}$  sieve, which should be higher than 72. The second criteria is the Sand Equivalent Test (ASTM D 2419-09), where a value over 30 is required.

The differences in the construction processes of the recycled layer should influence the choice of materials to be used. For in situ recycling, the analysis of the reclaimed materials is more complex (Thompson et al., 2009), not being possible for gradation to be controlled precisely along the process. The option for the use of RAP from the surface layers and virgin aggregate incorporation is a common practice, making it easier to control the final mix.

When there is material processing in a mix plant, control and characterization is easier, allowing the combination of different aggregates in order to obtain stability and the desired gradation.

The combination of RAP and different proportions of crushed limerock was studied by Bleakley and Cosentino (2012) with the objective of increasing the resistance and bearing capacity of the recycled mix, to be used as a base layer. It was observed that higher proportions of crushed limerock resulted in smaller deformations and higher stiffness.

Schwartz and Khosravifar (2013) have also studied the performance of recycled mixes from different sources, with incorporation rates from 100% to 40%, combining RAP with graded aggregate base (GAB) and Recycled Concrete (RC). The evaluation of the loss in resistance from the Indirect Tensile Strength before and after conditioning lead to better results for higher RAP incorporation rates, probably due to the higher asphalt binder content. In



a comparison between mixtures of RAP with GAB and RC, higher Indirect Tensile Strength(ITS) was obtained from RAP and RC mixes, difference that the authors attributed to the number of cementitious bonds caused by non-hydrated cement in RC.

Other studies have presented evaluations of foaming stabilization without the use of RAP, with only mixes of reclaimed aggregates and virgin materials (Huan et al., 2010). The mix design and production of these materials in the laboratory for assessment of the simple compressive strength and indirect tensile strength resulted in the determination of an ideal proportion of reclaimed material and virgin aggregates, with superior performance.

The Asphalt Academy (2009) and Wirtgen (2012) do not suggest minimum application rates. The mix design is done with the characterization of the physical and mechanical properties of the materials involved, with performance parameters of minimum standards for different applications of the technology.

## 2.5 CURING OF BSM

The curing of BSM layers is the result of the evaporation process, causing gradual reduction of the layers moisture content, and increase in stiffness and tensile strength of the material (Asphalt Academy, 2009).

Twagira (2010) states that curing is the main process in developing a strong and durable bond between the asphalt binder and the mineral aggregates. The author addresses the curing process in the field as a sum of the effects of the layers temperature gradient, relative humidity, wind speed, and boundary conditions.

Once the moisture content starts to decrease, lubrication between particles also decreases, resulting in a higher friction and therefore higher material strength (Lynch, 2013).

Although it is not part of the evaporation process, traffic may act as another factor affecting the reduction in moisture content, as it generates material compression and layer densification thus helping pump water out of the layer. On the other hand, traffic solicitation only occurs in the field, and could be treated as a separated mechanism.

On the South African Pavement Engineering Manual (SANRAL, 2014), BSM is expected to have an increase in stiffness during its first year in the field, as shown in Figure 2.

Different materials may have different curing times, with some achieving full strength within short periods of only a month, and others requiring more than a year (Mulusa, 2009). Both Lynch (2013) and Martinez et al. (2013) have verified that the curing of BSM layers is still on going after 360 days, with the increase of its stiffness through the analyses of backcalculated FWD data.

The search for a method that simulate the best what happens in the field has led to different procedures in laboratory. Since the constructive process may differ depending on local factors, so will the curing in the field. In the laboratory, on the other hand, conditions are controlled, and the curing procedure is established to produce similar field results in a later stage, when curing is stable.

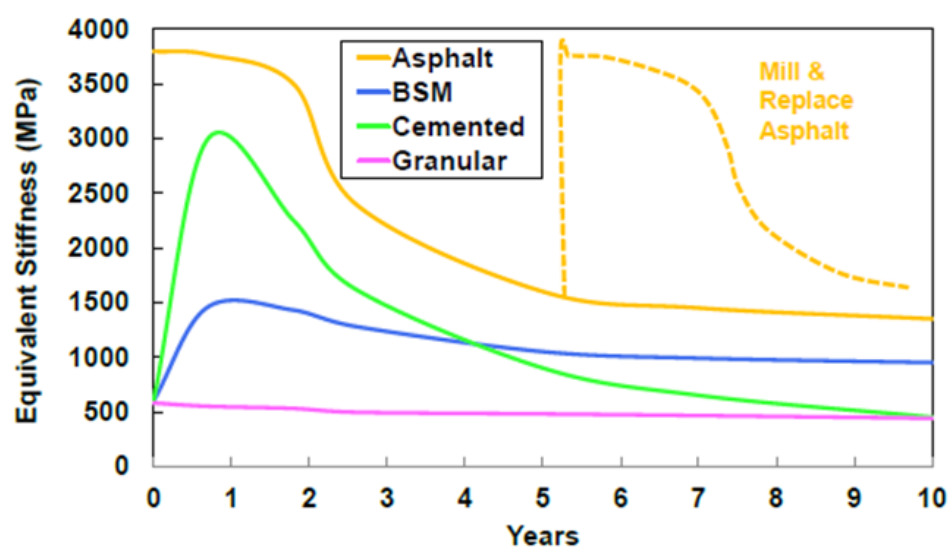


Figure 2– Curing time and long-term performance of different materials (SANRAL, 2014)

As stated in the following paragraphs, there is not a consensus in the international literature regarding the curing procedure of BSM. The Brazilian procedure for BSM mix design determines that Marshall samples should be prepared for Indirect Tensile Strength test (DNIT ME 136/2010), and that they should be cured for 72 hours at 40°C (DNIT ES 169/2014).

The current edition of the Technical Guideline 2 (Asphalt Academy, 2009) recommends that the curing of laboratory ITS specimens should be done unsealed at 30°C for 20 hours, and then sealed at 40°C for 48 hours, while the Cold Recycling Technology manual (Wirtgen 2012), indicates curing for 72 hours at 40°C. After 72 hours of curing, a set of samples should be tested, while another set should be soaked in a water tank at 25°C for 24 hours and then tested.

Some authors have followed these procedures for design and analyses (Ebels, 2008; Dal Ben, 2014; Twagira, 2010). Meanwhile, Fu and Harvey (2007) have conducted experiments after curing the specimens for a week at 50°C, while some of these authors have adopted the curing at 40°C for 72 hours in a later article (Fu et al., 2008).

The curing procedure applied by the Transportation Research Laboratory (TRL), consists of 72 hours of curing at 60°C followed by 12 hours at 20°C. For soaked specimens, an additional 24 hour period is required, with the sample immersed in water at 20°C (Milton and Earland, 1999).

## 2.6 BSM MECHANICAL PERFORMANCE

The analysis of BSM mechanical performance can be done both in laboratory, with tests on prepared specimens, and in the field, with evaluation of in service pavement structures. Since BSM is usually associated with either granular materials or asphalt mixes, laboratory analyses are often made with tests related to those materials, as mentioned in the following subitems.

### 2.6.1 Indirect Tensile Strength Test

Indirect Tensile Strength is one of the most common laboratory tests for BSMs (Dal Ben, 2014), as it is used as a mix design parameter in some methodologies.

Both, the Wirtgen Cold Recycling Technology Manual (Wirtgen, 2012) and the TG2 (Asphalt Academy, 2009) require ITS tests for mix design. Both classify BSM in three categories, BSM1, BSM2 and BSM3, from higher to lower resistance, with minimum values of ITS for dry specimens being specified at 225 kPa, 175 kPa and 125 kPa respectively. For soaked conditions the minimum values are specified at 100 kPa, 75 kPa and 50kPa for BSM1, BSM2 and BSM3 respectively BSM2 or BSM3.

The asphalt binder content on BSM mixes has a direct effect on resistance and moisture susceptibility. Although some design procedures look for the binder content that would result in the higher strength, some others just look for minimum parameters to be achieved. With that in mind, ITS minimum values for design may range from a 125 kPa for a dry specimen (Asphalt Academy, 2009) up to 400 kPa (DER/PR ES-P 32/05).

Although the BSM behaves mainly as a granular material and the fatigue may not be the major concern, the material still presents some viscoelastic behaviour due to the asphalt binder, what makes it susceptible to the temperature and loading frequency (Jenkins; 2012; Collings and Jenkins, 2011; Fu and Harvey, 2007). Dal Ben (2014) tested different mixes at different temperatures, obtaining a variety of results from around 300 kPa for mixes at 40°C until over 1000 kPa for samples conditioned at -10°C.

### 2.6.2 Triaxial Resilient Modulus Testing

The triaxial resilient modulus test has been used in many studies to address the effect of confining pressure in BSM materials. In this test, cylindrical samples are tested applying a dynamic deviatoric stress of short

duration(0,1s), while through a rubber membrane and a pressurized chamber, the confining stress is applied (Figure 3(a) and (b)). Varying both the confining and the deviatoric stresses, one can assess how the material responds to different stress states.



(a)



(b)

**Figure 3—(a) Specimen with the rubber membrane inside the pressurized chamber; (b) Servo-pneumatic test machine**

Highly cohesive materials, such as cement treated layers and asphalt mixes are expected to similar resilient modulus regardless the samples confinement, whereas granular layers present higher stiffness with the increase in confinement.

Twagira (2010) conducted a few triaxial resilient modulus tests to investigate the effect of moisture damage on stiffness for both foamed and emulsion mixtures, with asphalt binder contents of 2.0% and 1% of either cement or lime. The results presented modulus from 300 MPa to 700 MPa for 100% saturated samples for different mixtures. The moduli were twice as high for the dry condition.

Dal Ben (2014) also conducted triaxial resilient modulus tests, with foamed stabilized specimens containing from 2.0% to 2.3% of asphalt binder and 1% of cement cured in the laboratory according to the TG2 procedure prior to testing, and also brought in from the field for testing. While the laboratory samples presented average modulus of 600 MPa, the 6 months old field samples presented higher modulus with some of them reaching 6000 MPa.

Another work analysed the performance of nine different mixtures, varying the stabilization process from foamed bitumen to emulsion, two different asphalt binder contents (2.4% and 3.6%) with the addition or not of cement (Ebels, 2008). The results show all the mixtures with modulus around 1000 MPa, regardless of the stabilization agent, emulsion or foamed bitumen.

### 2.6.3 Monotonic Triaxial Testing

The monotonic triaxial test may use the same confining apparatus used for the triaxial resilient modulus test. In this test, a displacement rate is applied, while measuring the load reaction from the specimen. The Asphalt Academy has a test procedure, the Method 7 - Simple Triaxial Test Procedure, to determine the materials angle of internal friction and cohesion.

On the Cold Recycling Technology Manual (Wirtgen, 2012) the cohesion requirements for BSM range from 50 kPa to 250 kPa, depending on the material classification. As for the angle of internal friction, it should range from 25° to 40°. These characteristics and classification are the same in the TG2 (Asphalt Academy, 2009).

Jenkins et al. (2002) performed monotonic triaxial tests for different mixes, varying asphalt binder and cement contents. When comparing non stabilized mixes (0% asphalt binder) with foamed mixes, it is possible to observe the reduction in the angle of friction value, whereas cohesion practically doubles. Cohesion on stabilized mixes varied from around 150 kPa to 300 kPa, while the angle of friction ranged from 30° to 45°.

Dal Ben (2014) verified the variation of cohesion and friction angle for foamed mixtures with 100% of RAP, 50% RAP and 50% crushed aggregates and 100% crushed aggregates with respectively 2.0%, 2.1% and 2.3% of binder content. Although cohesion values varied from 350 kPa to 500 kPa, no trend relating RAP content was verified. For the friction angle, on the other hand, it appeared that higher RAP contents produced mixtures with smaller friction angles.

Mulusa (2009) studied the development of a simpler monotonic triaxial test that could be applied in lieu of the traditional one. The traditional test uses a more sophisticated apparatus, such as a pressurized chamber where the sample is confined while protected by a rubber membrane. The simpler procedure uses an iron chamber only to confine a bladder that involves the sample and is filled with air until the desired confining pressure is obtained. The test results showed cohesion between 95 kPa and 246 kPa, and a friction angle between 40° and 50° while presenting a very good relation between the simple triaxial test results and the traditional triaxial test.

#### 2.6.4 FWD Testing

Falling Weight Deflectometer (FWD) testing is a non-destructive method of analysing pavement deflection, and in situ stiffness through backcalculation. Several studies have been done with deflection analysis, often followed by backcalculation and stiffness evaluation (Collings et al., 2004; Martinez et al., 2013; Jones et al., 2014).

A series of FWD test were conducted at Ayrton Senna Highway in São Paulo, with the objective of assessing material stiffness increase and pavement deflection decrease. In the study conducted by Martinez et al. (2013) the deflections had dropped from over  $200 \times 10^{-2}$  mm to around  $30 \times 10^{-2}$  mm in 6 months. Material stiffness also increased drastically, from 300 MPa to an average 1900 MPa.

Lynch (2013) conducted a series of FWD tests to evaluate trends of seasonal variation and temperature flotation and its effects on backcalculated stiffness. It was verified that typical values of in service BSM layer stiffness varied between 600MPa and 1100 MPa for layers stabilized with foamed bitumen and between 600MPa and 1600 MPa for layers stabilized with emulsion.

Loizos et al. (2012) evaluated the stress dependency of BSM through the FWD data. The authors made a series of tests varying the applied load from 40 kN to approximately 75 kN. The results showed that the material stiffness

increased up to 18% with the load increase. The stiffness also varied considerably with climate conditions and the type of mixtures studied, ranging from 4780 MPa to 12260 MPa.

## 2.7 MIXTURE AND STRUCTURAL DESIGN OF BSM LAYERS

Although recycling is not a new technique, experiences in the United States date from the early 1910's (Zelaya, 1985 apud Castro, 2003), the first application of foamed bitumen stabilization was done by the French Company Jean Lefebvre in 1981 (Goacolau et al., 1996 apud Castro, 2003).

The technology has been under development, with different design methods being used around the world. Since the material is essentially a bitumen stabilized layer, parallels have been drawn with HMA Design procedures, on the other hand, have been adapted specifically for these bitumen stabilized layers, differentiating it from HMA, with each method having its particularities.

Austroroads (2011) reviewed different design methods for foamed bitumen stabilization before proposing an interim design method for Australia. Some of the procedures discussed in that report, and others that are used around the world, are discussed in the next subitems.

### 2.7.1 Departamento Nacional de Infraestrutura de Transportes (DNIT)

The Brazilian National Department of Transportation does not have a specific design procedure for foamed bitumen stabilized layers, only having a specification for the material properties. The recycled foamed BSM should have minimum ITS of 0.25 MPa for the dry condition and a minimum of 0.10 MPa for the soaked condition (DNIT ES 169/2014). Aside from ITS, and a recommended gradation envelope, not much is specified for the layer design. The structural design parameters, primarily for mechanistic analysis, are chosen by the designer.



The flexible pavement design procedure in Brazil dates from the early 1960's and is based on the CBR Design Procedure, with an update in 1981 (Balbo, 2007). This method has the equivalent thickness approach, with different coefficients being attributed to different materials to protect the underlying layers and the subgrade. No recommendation is made to which coefficient should be used for BSM layers, with that decision left for the pavement designer.

The mechanistic approach with a linear elastic layered system is also very used in Brazil, although no specific procedures are defined for BSM layers on how to analyse its distress and failure criteria.

### 2.7.2 Departamento de Estradas e Rodagem do Paraná (DER-PR)

As what happens in the national level, the Department of Transportation of the State of Paraná establishes only executive procedures, and material specifications for BSMs. The specification, however, request higher ITS values for both Dry and Soaked specimens, 0.40 MPa, and 0.20 MPa, respectively (DER/PR ES-P 32/05). No design procedure is defined specifically for the BSM layers.

### 2.7.3 Transportation Research Laboratory (TRL) – United Kingdom

The TRL design procedure assumes that the foamed bitumen stabilized layer behaves similarly to conventional hot mix asphalt layer. The method determines the pavement's structural need, depending on the foundation and traffic, and empirically through tables and graphs the minimum thickness for the layers is determined (Figure 4). The specification for the use of foamed bitumen mixtures request the Indirect Tensile Stiffness Modulus (ITSM) for cured specimens between 2000 MPa and 2500 MPa, depending on the road classification. The primary mode of distress considered for the material is

fatigue, with around 4% of bitumen content for usual mixture designs (Milton and Earland, 1999).

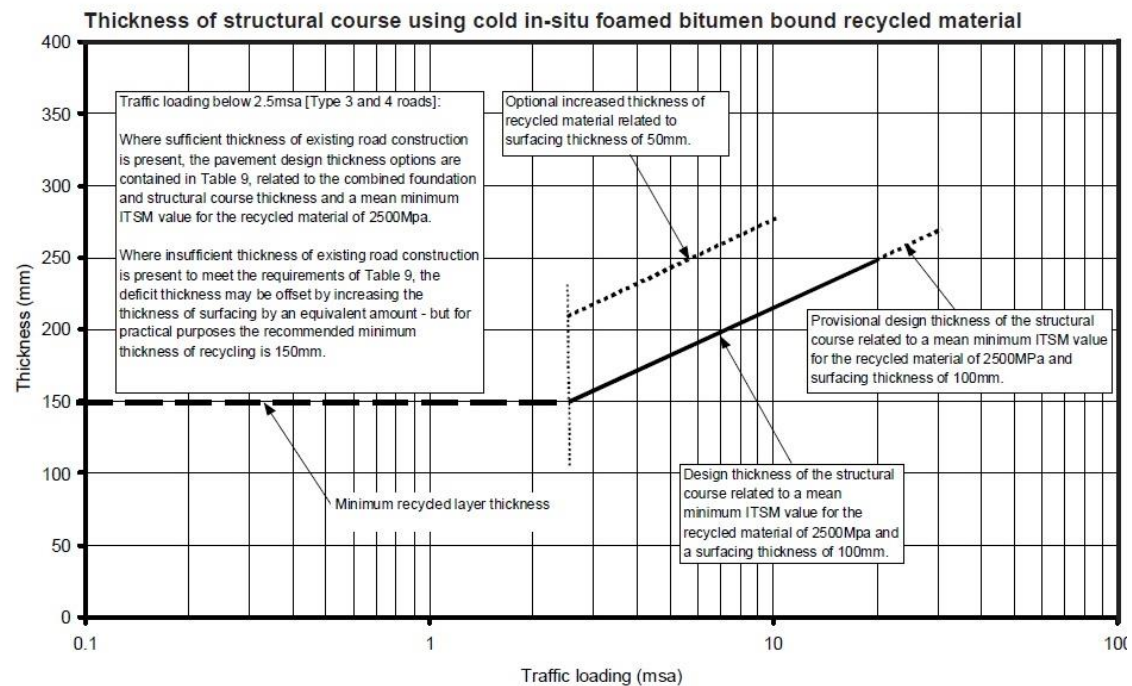


**Figure 4 – Pavement layer thickness using cold in-situ foamed bitumen recycling (Milton and Earland, 1999)**

Nunn and Thom (2002) have later suggested that Foamed Bitumen stabilized materials fatigue behavior would be more similar to Dense Bitumen Macadam (DBM) than with HMA, but would still have fatigue as the primary distress mechanism. Figure 5 show a chart relating traffic to the required thickness of foamed bitumen layer.

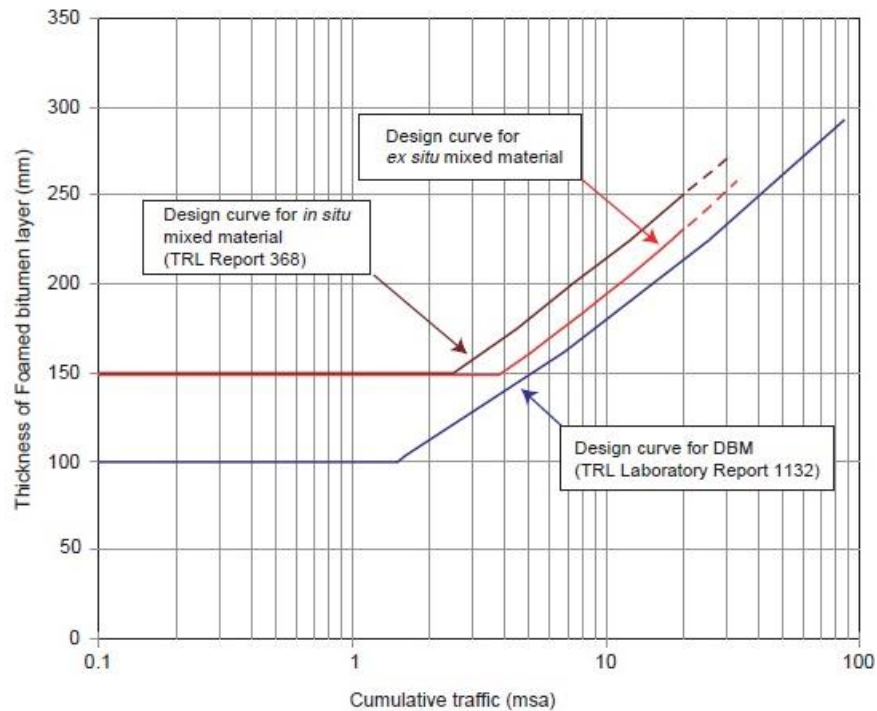


**Figure 5 – Layer Thickness of *in situ* and *ex situ* (plant mix) foamed bitumen recycled material, with 100 mm of asphalt surfacing required for all cases (Nunn and Thom, 2002)**

#### 2.7.4 Department of Transport and Main Roads (TMR), Queensland – Australia

The procedure involves the incorporation of 3.0% to 4.0% of foamed bitumen and 1.0% to 2.0% of lime, aiming for a higher fatigue performance, without compromising the rut resistance (Ramanujam and Jones, 2007; TMR 2012). The mechanical behavior is considered to have two distinct phases, one before cracking and the second one post cracking, when the BSM is said to behave similarly as a granular material (TMR, 2012).

The volumetric properties of the mix, its stiffness, and the tensile strain at the bottom of the layer are then related to an admissible number of load cycles in a fatigue relationship, which is considered the primary distress mode (Austroads, 2011). The fatigue equation is presented as follows:

$$N = \left[ \frac{6918 \times (0.856V_b + 1.08)}{S_{mix}^{0.36} \mu\epsilon} \right]^5 \quad (1)$$

where:      N = the allowable number of load repetitions to fatigue;  
               V<sub>b</sub> = asphalt binder percentage by volume in the mix;  
               S<sub>mix</sub> = mixture stiffness (modulus) MPa;  
               μϵ = tensile strain at the bottom of the layer (microstrains);

#### 2.7.5 City of Canning – Australia

The design method from the City of Canning also defines fatigue as the primary mode of distress, but develops a modified criteria from the one used in Queensland (discussed above) based on the results of flexural beam fatigue tests (Leek, 2010). Although the volumetric properties and the mixture stiffness are not taken into account in the fatigue criteria, the characteristics of the materials used for both the Canning procedure and the Queensland procedure are similar. The fatigue equation is defined as follows:

$$N = \left( 1558 / \mu\epsilon \right)^6 \quad (2)$$

where:      N = the allowable number of load repetitions with strain level μϵ;  
               μϵ = tensile strain at the bottom of the layer (microstrains)  
                       applied by a 80 kN axle load;

#### 2.7.6 New Zealand Transport Agency – New Zealand

Differently from the design procedures of the TRL, the TMR and that from the City of Canning, the New Zealand procedure do not consider fatigue as the main distress mode. Alabaster et al. (2013) state that it is unclear whether the fatigue life occurs in the foamed asphalt stabilized materials, and therefore only the equivalent granular phase is accounted for the design. Once foamed material is considered as granular, the primary mode of failure is permanent

deformation, and the mechanistic verification is done analysing the vertical strain on top of the subgrade with the following equation:

$$N = (9300/\mu\varepsilon_v)^7 \quad (3)$$

where:        N = the allowable number of standard axle loads;  
                $\mu\varepsilon_v$  = the maximum vertical strain at the top of the subgrade;

During mechanistic design it is recommended that the foamed bitumen layer shall be considered with 800 MPa of elastic modulus, and poisson's ratio of 0.30 (Alabaster et al., 2013).

Although fatigue is not considered the primary distress mode as in the other methods, it is important to observe that New Zealand mixtures have 2.7% to 3.0% of asphalt content, and around 1.0% of cement (Alabaster et al., 2013). On the other hand, all the other methodologies recommend asphalt application rate between 3.5% and 4.0%, and up to 2.0% of cement (Austroads, 2011).

#### 2.7.7 TG2 2009 – Structural Design Method – South Africa

The Technical Guideline 2 (TG2) was first published in 2002 with the objective of providing guidelines on how to design and use Bitumen Stabilised Materials (BSM), whether using emulsion or foamed bitumen (Asphalt Academy, 2002).

The 2002 edition was based on a series of different pavement structures and trial sections subjected to accelerated testing with the Heavy Vehicle Simulator (HVS). After these experiments, performance models were developed for the material (Asphalt Academy, 2002). BSM layer was considered to perform in two distinct phases, (i) fatigue life phase, when it behaves as cohesive material subject to fatigue damage, and (ii) equivalent granular phase, when permanent deformation became the main mode of distress, as for the granular materials. As the industry felt that the report did not properly represent the material real performance in the field, further

research was developed, resulting in the document published in 2009 (Austroads, 2011).

The mixtures studied in the 2002 edition had approximately 2.0% of cement, and it was later suggested that the cohesive behaviour prone to fatigue damage was a result of the high cement content. Later research resulted in the 2009 edition limited the maximum content of either cement or lime in 1.0%, and the material was considered as granular for design purposes. Although BSM was considered to behave as a granular material, because of the bitumen bonds it would have a higher cohesive strength, and smaller moisture susceptibility (Asphalt Academy, 2009).

TG2 recommendations indicate asphalt binder contents in the mix from 1.5%, when using graded and coarser aggregates, to 3.0% for finer mixtures and soil applications. This application rates contrast with those of the Australian and British practices that range from 3.5% to 4.0%, and as a result so differs the approach for layer analysis.

One other aspect is that optimum binder content for BSMs is determined by assuring that material ITS results are higher than minimum limits, and although a higher content may lead to a higher resistance, it would also make the material more cohesive, thus subject to fatigue damage.

The 2009 edition of the TG2 presents the Pavement Number Design procedure, which is a knowledge based structural design method. In this method, an index, called Pavement Number (PN), is calculated for the designed pavement structure and a minimum PN is required for a given traffic and confidence level. Figure 6 shows a graph where PN is related to the design traffic and reliability, where A is 95% reliability, and B represents 90%. Traffic is expressed in MESA, which stands for Million Equivalent Single Axles.

The existing information that culminated in the graph presented in Figure 6 was based on three data sets (described in the following paragraphs), that along with the proposed rules for pavement behavior presented in the method formed the knowledge based procedure (Jooste and Long, 2007).

The first data set came from the Technical Recommendation for Highways Design Catalogue (CSRA, 1985), and served as the base for developing the procedure. A series of structures provided for Category A and B (reliability of 95% and 90%, respectively) and recommended for traffic between 1 and 30 MESA were used to calibrate climate factors and material constants.

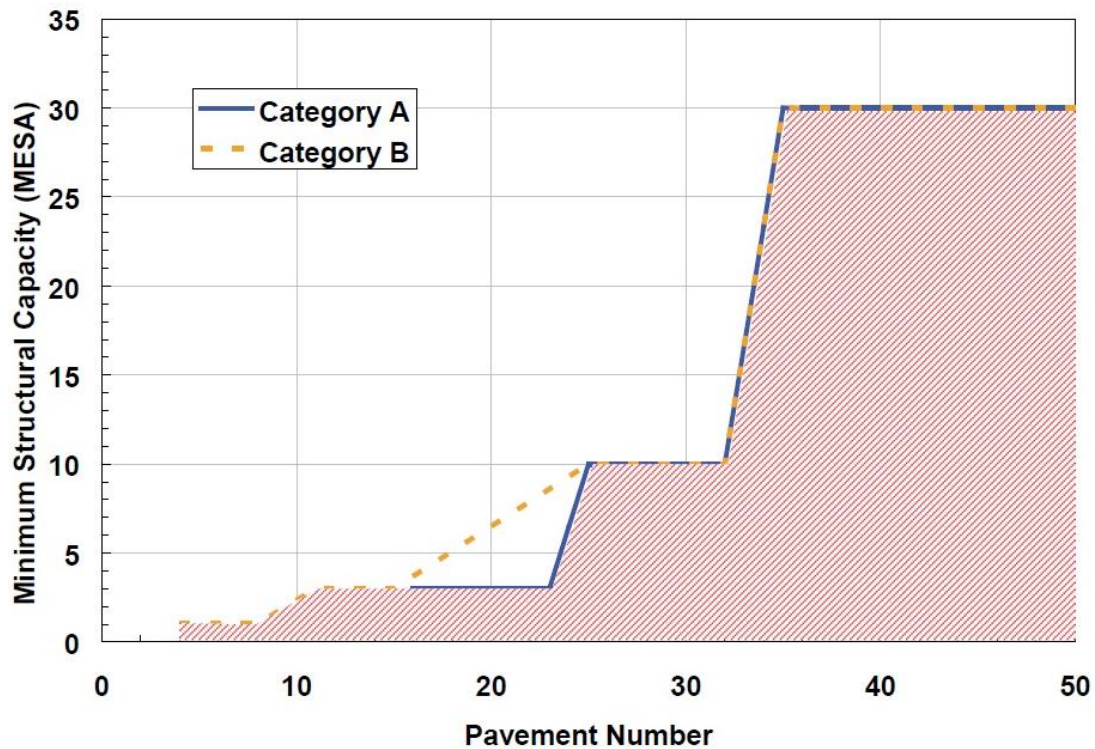


**Figure 6 – Criteria for Determining Allowed Capacity from PN (Asphalt Academy, 2009)**

The second data set used in the process was the one from the LTPP (Long-Term Pavement Performance) program on bitumen stabilized pavements. The historic data from this set helped determine which in service structures were reliable for specific traffic and climatic conditions. The last set of data came from the HVS tests conducted on bitumen stabilized materials.

The concepts of the design method are based on the Effective Long-Term Stiffness (ELTS) model, in which a material is modeled with the average of its long term in situ stiffness (Asphalt Academy, 2009). The realistic ELTS values are calculated based on the analysis of the BSM stiffness and the stiffness of its support. Although for highly cohesive materials the support does not influence that much on its stiffness, it may be relevant on the fatigue analysis

and the long term performance. For that reason, the modular ratio was introduced in the method, as an index of the how many times the layers stiffness can be in comparison to the stiffness of its support.

The ELTS for each material is calculated considering the smaller value between a pre-defined maximum stiffness, and the product between the materials modular ratio and the stiffness of the immediate underlying layer.

The modeling of the subgrade ELTS is subject to the climatic conditions and the pavement thickness (cover thickness) protecting it. Afterwards, ELTS is calculated for each of the other layers from bottom to top considering the smaller value between a pre-defined maximum stiffness, and the product between the materials modular ratio and the stiffness of the immediate underlying layer.

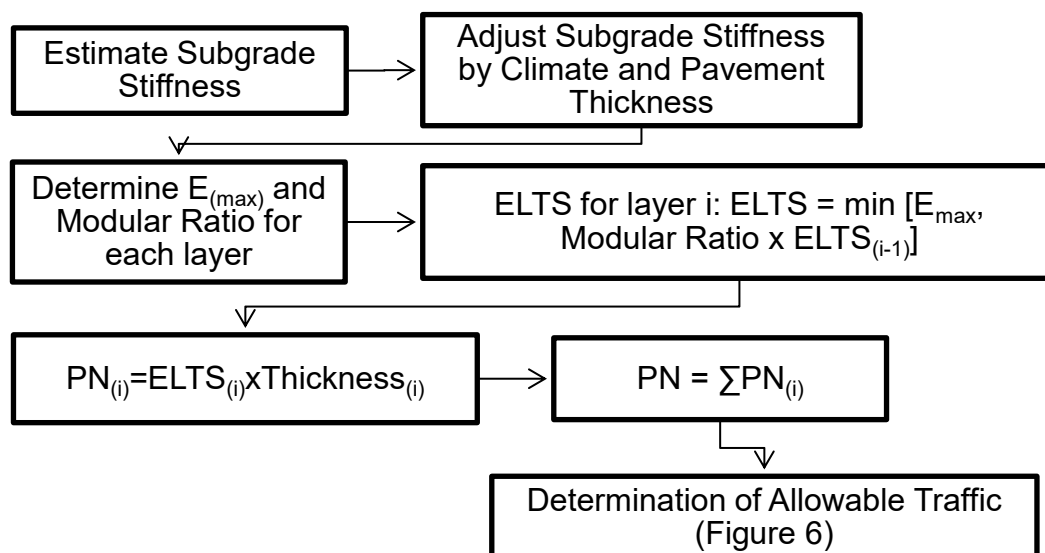


**Figure 7 – Flow chart of the PN design methodology (adapted from Austroads, 2011)**

After calculating the ELTS for each layer, the individual  $PN_{(i)}$  for each layer is calculated as a product of ELTS by its thickness. The sum of all  $PN_{(i)}$  results in the PN, that should be verified in the graph shown in Figure 6 to determine the allowable traffic for that pavement structure.



### 2.7.8 SAPEM 2014 – South African Pavement Engineering Manual

The South African Pavement Engineering Manual is a reference manual for all aspects of pavement engineering, and is subdivided in 14 chapters (SANRAL, 2014). Chapter 10 is Pavement design, where many aspects of it are covered, including traffic evaluation, economic assessment and structural capacity evaluation.

The South African Mechanistic-Empirical Design is described in this chapter, and also the approach for analyzing BSM layers. The method evaluates all the layers that compose the pavement structure, analyzing for each layer the stress, or strain, at a specific point, as shown in Figure 8.

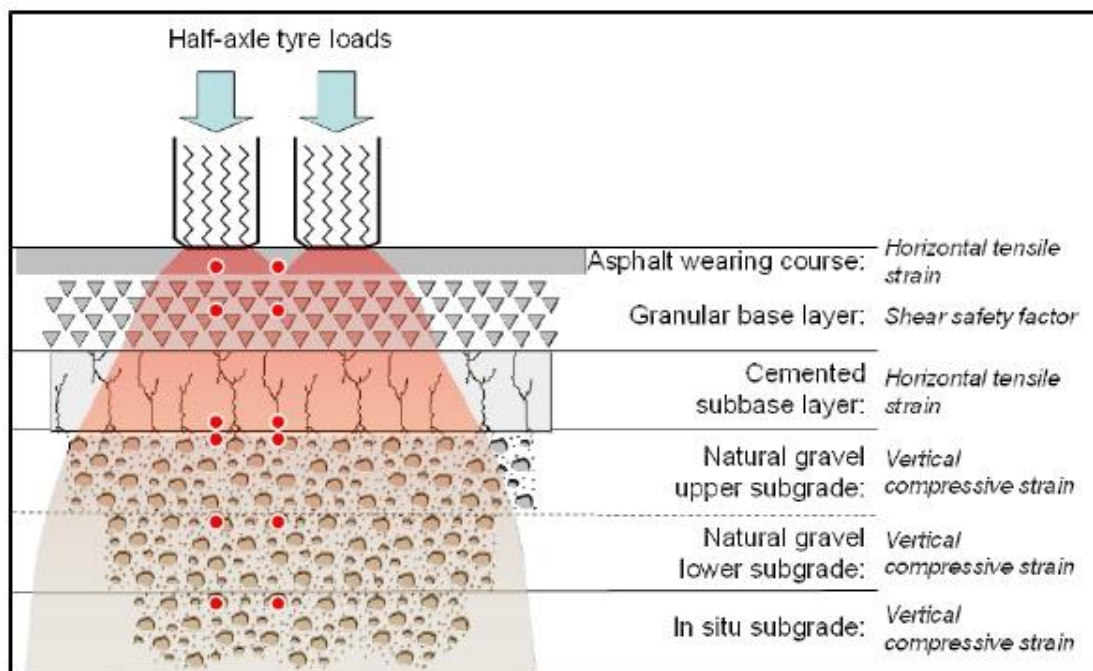


**Figure 8 – Position of analysis for each layer and parameter (SANRAL, 2014)**

For BSM layers, evaluation is done similarly to granular materials, as their behavior is considered to be alike. The primary failure criterion for granular base and BSM layers is permanent deformation, and for that analysis a transfer function relates allowable number of load repetition to a Shear Safety Factor.

This factor used for granular bases is analyzed at 75% of layer depth, and is a relation between the material resistance and the active stresses on the layer. The material resistance is represented by its cohesion and friction angle, and can be obtained by Mohr-Coulomb theory (Theyse et al., 1996). The equation for Shear Safety Factor calculation presented in the SAPEM (SANRAL, 2014) for granular layer analysis is presented as follows:

$$F = \frac{\sigma_3 \left[ K \left( \tan^2 \left( 45 + \frac{\phi}{2} \right) - 1 \right) \right] + 2KC \tan \left( 45 + \frac{\phi}{2} \right)}{(\sigma_1 - \sigma_3)} \quad (5)$$

where:

F = Shear Safety Factor;

$\sigma_1$  and  $\sigma_3$  = Major and minor principal stresses;

C = Cohesion;

$\phi$  = Internal Friction Angle;

K = Moisture content, with 0.65 for moist conditions, 0.80 for moderate moisture conditions, and 0.95 for dry conditions.

Once the Shear Safety factor is determined, the allowable number of load repetitions (N) before failure can be calculated using a transfer function. For granular base materials equations (6 to 9) are applied to determine N:

$$N = 10^{(2,605122F + 3,480098)} - \text{Category A (95\%)} \quad (6)$$

$$N = 10^{(2,605122F + 3,707667)} - \text{Category B (90\%)} \quad (7)$$

$$N = 10^{(2,605122F + 3,983324)} - \text{Category C (80\%)} \quad (8)$$

$$N = 10^{(2,605122F + 4,510819)} - \text{Category D (50\%)} \quad (9)$$

For BSM layers, instead of using the shear factor as an input parameter, a Stress Ratio that can be calculated using equation (10) is applied:

$$SR = \frac{(\sigma_1 - \sigma_3)}{\sigma_3 \left[ K \left( \tan^2 \left( 45 + \frac{\phi}{2} \right) - 1 \right) \right] + 2C \tan \left( 45 + \frac{\phi}{2} \right)} \quad (10)$$

where:      SR = Stress Ratio;  
 $\sigma_1$  and  $\sigma_3$  = applied major and minor principal stresses;  
C = Cohesion;  
 $\phi$  = Internal Friction Angle (degrees);

After the determination of the SR, equation (11) is applied to determine the allowable number of South African standard load repetition N:

$$N = 10^{(A+B(RD)+C(Sat)+D(PS)+E(SR))} \quad (11)$$

where:      N = the allowable number of standard load repetitions;  
RD = relative density of the material, compared to its maximum density (%);  
Sat = layer saturation (%);  
PS = allowed plastic strain (%);  
SR = stress ratio, which is the inverse of the shear safety factor (SR = 1/F);

The coefficients A, B, C, D and E are calibration factors for the equation and they are currently under revision. For this reason, they are not disclosed in this dissertation.

The allowable number of load repetitions (N) corresponds to the amount of Equivalent Single Axles Loads of 80 kN that the pavement can withstand before meeting a specific failure criterion.

### 3 TRIAL SECTION

The evaluation of trial section presents the possibility of comparison between the theory behind the design and the practical result in the field. When talking about pavement structures, field conditions are not always replicable with perfection in the laboratory, which makes trial sections even more significant for parameters calibration and empirical data collection.

A trial section at Ayrton Senna (SP-070) highway was the subject of the field study. The highway is a major point of entry to the Brazil's biggest city, São Paulo, connecting the city to the southeast region of the State. The highway has two roadways in its entire length, with segments resending between 2 and 4 lanes for each direction.

Ayrton Senna Highway is under the toll concession of Ecopistas, part of the Ecorodovias Group, since 2009. To comply with the performance demands of the São Paulo State Transportation Agency (ARTESP), rehabilitation interventions have been successively performed for the highway maintenance.

As it represents an important connection between São Paulo and the Paraíba Valley, an important industrial region in the state, the SP-070 absorbs a considerable amount of the commercial traffic destined to the ports of São Sebastião, Itaguaí and Rio de Janeiro. Besides, the proximity with the city of São Paulo results in intense low speed traffic, as a result of the traffic jams formed in the city's access.

Along the rehabilitation process in the Ayrton Senna Highway (SP-070), a cold recycling with foamed bitumen stabilization was applied in the lane with heaviest commercial traffic. In this process, a trial section comprised of 2 segments (with the same pavement structure) was monitored, as detailed in the following items.

### 3.1 TRIAL SECTION CHARACTERIZATION

The test section consists in two segments located in the third lane (heavy traffic lane) of the West Track of the highway, coming into the city. The segments are located near the off-ramp that comes from the Helio-Smidt Highway (SP-019), as shown in Figure 9.

For the driver coming into the city, after passing the off-ramp giving access to the SP-019 and the Guarulhos International Airport, the first segment is right after the 19<sup>th</sup> km sign. In this section, the west track has 3 traffic lanes so the third lane receives the majority of the heavy traffic. The first segment is located between the kilometers 18.950 and 18.830.

The second segment corresponds to the third lane between the kilometers 18.620 and 18.480. In this section the west track has 4 lanes due to the off-ramp coming from the SP-019, although the third lane is still the one receiving the majority of the heavy traffic on the road.



**Figure 9 – Location of the Trial Section**

Prior to the rehabilitation, the pavement structure consisted of 160 mm Hot Mix Asphalt (HMA) on top of a 200 mm Cement Treated Base (CTB) in poor condition, and 260 mm Granular material (Figure 10).

The CTB layer was in an advanced stage of deterioration with block cracking that had already reflected through the asphalt layer. A series of asphalt overlays had been done in previous rehabilitations, with reflective cracks in only 6 months.

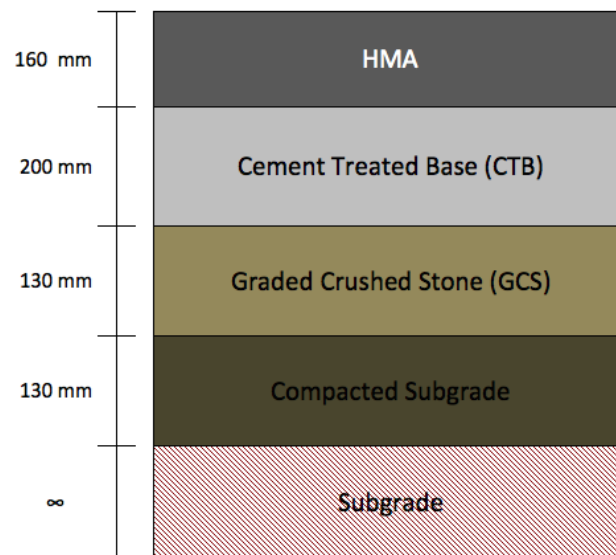


**Figure 10 – Existing structure in Highway SP-070 prior to rehabilitation**

The CTB layer can be therefore identified as a structural weakness, with the possibility of differential displacements happening when subject to traffic loading, compromising the support of overlying layers. Therefore, the CTB layer removal became important to the pavement performance after the rehabilitation process.

Another significant factor in the definition of the rehabilitation procedure is that the intervention affects directly the traffic between the cities of São Paulo and Guarulhos. In this sense, the rehabilitation procedures are limited by logistic impositions for lane closing and opening.

For that reason, all the interventions in the highway in the areas close to São Paulo could only be done at night. The reduction of the traffic at night allowed the closing of lanes for rehabilitation, without considerable impact on the city traffic flow.

### 3.2 REHABILITATION SOLUTION

With the time constraint to the restoration procedures between 10 PM and 6 AM, it was necessary to select a solution that could be performed in that time frame, and also able to withstand the demands of the highway's high traffic volume.

Once cement stabilization requires the curing period for stiffness and strength increase, that solution was discarded, as it would not be possible to pave the wearing course and open for traffic in the pre-determined time.

To increase pavement stiffness, without compromising the traffic operation, bitumen stabilization was chosen through cold recycling with foamed bitumen. To assure that the operational procedures would be done and the lanes open in time, it was decided that the work would be conducted in segments of 100 to 200 meters per day.

The reclaimed material from the highway was taken to a mix plant, where it was processed and foamed to be then applied in the road. Due to time limitations, the milled material of a segment was taken to the plant, processed, foamed and then stockpiled for further application. This way it was possible to perform the procedure faster, paving the recycled layer right after milling the pavement.

The mix plant used in this job was a KMA 220 manufactured by Wirtgen and owned by FREMIX (ANE Group), which is the company responsible for the rehabilitation works. During the construction of the trial section, the plant was positioned in a work site located in the kilometer 11 of the Ayrton Senna Highway, on the west track as detailed in Figure 11, resulting in a material transportation distance of approximately 10 kilometers.

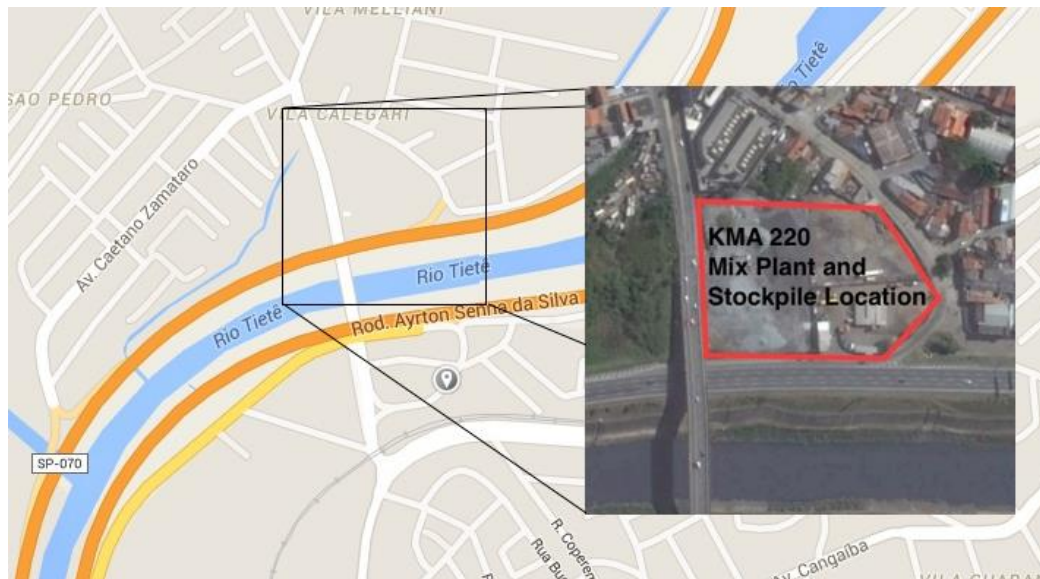


**Figure 11 – Location of the KMA 220 mix plant**

### 3.3 REHABILITATION PROJECT

The rehabilitation project was prepared in a partnership between the Brazilian company JBA Engineering and Consultancy LTDA and the Loudon International, a South African company.

Loudon International prepared the report “Technical Proposal for the Construction of a Trial Section – 600m of Slow Lane, Westbound Carriageway (km 15+650 to km 16+250)” in October of 2011 after visual inspections. In the document, there was a proposition for cold recycling with foamed bitumen stabilization and the application of an asphalt layer as a wearing course.

The construction of the recycled layer was then considered to be applied in two layers to assure proper compaction. The foamed mix was designed by JBA. Due to the abundance of stockpiled RAP material and the possibility of its use, the design was at first made for two mixtures (JBA, 2012). The first mixture was composed by 100% of RAP and would be applied as the bottom layer, and the second mixture had 85% of RAP (by mass) and 15% of Stone Crusher Dust stone dust and would be applied as the top layer. For both mixtures, 1% of cement was added as the active filler, aiming to gain resistance, improve bitumen dispersion, and reduce moisture susceptibility.



As described on the Technical Report RT/120323/0129/1023, the grading of the mixtures followed Asphalt Academy (2009) recommendations as presented in Table 1 and Figure 12.

**Table 1 – Gradation envelope for BSM (Asphalt Academy, 2009)**

Sieve (mm)	Percentage passing (by mass)			
	Ideal		Less Suitable	
	Minimum	Maximum	Minimum	Maximum
50	100	100	100	100
37,5	87	100	100	100
26,5	77	100	100	100
19,5	66	99	100	100
13,2	57	87	87	100
9,6	49	74	74	100
6,7	40	62	62	100
4,75	35	56	56	95
2,36	25	42	42	78
1,18	18	33	33	65
0,6	14	28	28	54
0,425	12	26	26	50
0,3	10	24	24	43
0,15	7	17	17	30
0,075	4	10	10	20

The mix design followed the TG2 procedure (Asphalt Academy, 2009), which later gave place to the Cold Recycling Technology Manual (Wirtgen, 2012). In this procedure, the Indirect Tensile Strength test is performed in order to determine the optimum (minimum) bitumen content that provides the minimum strength necessary to the mixture. Aside from that, tests are performed for a fixed bitumen content to determine the appropriate active filler to be used, whether its cement, hydrated lime, or if it is not necessary.

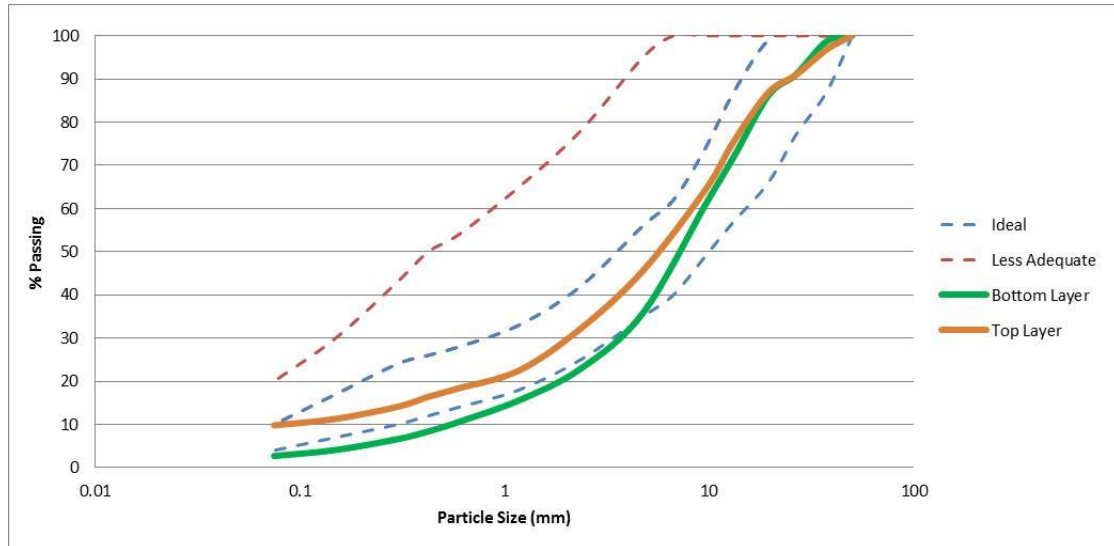


**Figure 12 – Foamed Stabilized Recycled Mixture Gradation**

Optimum asphalt binder content was determined in two stages. At first, variations from 1.75% to 2.25%, increasing 0.25% per sample, were prepared. Then a refinement was done with contents ranging from 2.0% to 2.3%, increasing 0.1% per sample.

All ITS tests were performed in cylindrical specimens with 100 mm diameter and 63 mm height. The samples were tested for both dry and soaked condition, according to Wirtgen curing procedure. Optimum bitumen content was defined as the mixture with lower content that was able to achieve 225 kPa for the dry sample, and 100 kPa for the soaked one.

The results of the ITS tests can be used as an indicator of the mix quality. For high Tensile Strength Ratio (TSR) values, that corresponds to the relation between dry and soaked tensile strength, it is verified that the mix is enough stabilized, and if moisture susceptibility is low. For Low TSR values, moisture susceptibility is high, caused by insufficient amount of bitumen, inappropriate dispersion or even flawed gradation.

The composition was then defined for the two mixtures as shown in Table 2.

**Table 2 – Initial designed mixture for the recycled layers**

<b>Cold Recycled Mix Composition</b>		
<b>SP-070 - West</b>		
<b>Material</b>	<b>Layer 1 - Bottom</b>	<b>Layer 2 - Top</b>
RAP	100%	85%
Stone Crusher Dust	-	15%
Portland Cement	1%	1%
Asphalt Binder Content	2,0%	2,2%

Once RAP stockpiles started to get depleted, there was the need of mixture alteration. Due to the existing pavement constitution, with a CTB layer under the asphalt surface layer, a new mixture was developed using these materials. Initially a composition of 95% RAP and Crushed CTB with 5 % of Stone Crusher Dust was selected. Later, with the change in the milling process, with finer reclaimed material produced, it was possible to compose the mixture with 100% of RAP and Crushed CTB (between 30% and 40% RAP, and the remaining part crushed CTB). The active filler adopted for the mixture composition was the hydrated lime, which allowed it to be stockpiled prior to field application.

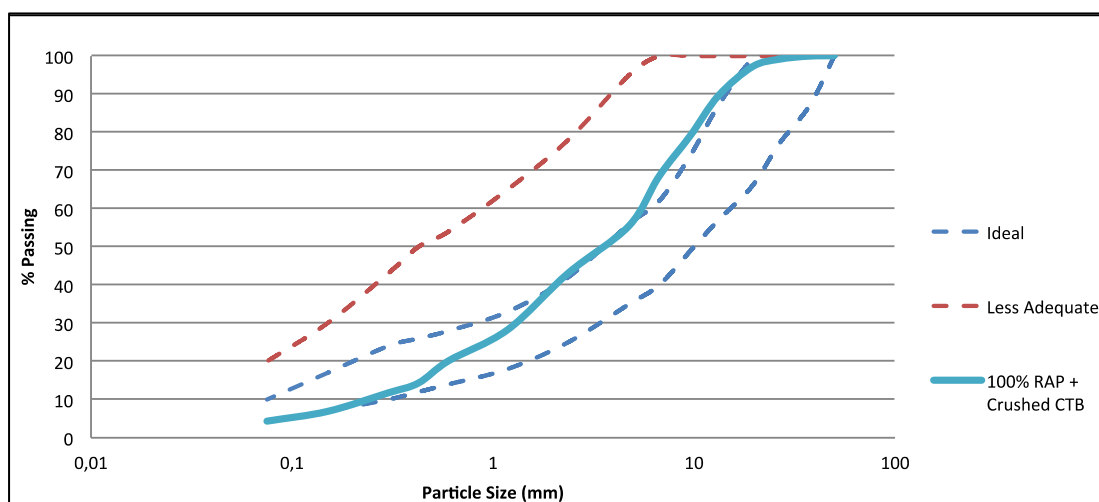
The mixture containing 95% of RAP and Crushed CTB was designed for a bitumen content of 2.2%, resulting in high Tensile Strength values ( $ITS_{SOAKED} = 450$  kPa and  $ITS_{DRY} = 500$  kPa) (JBA, 2013). As the tensile strength was too high, the design for the mix containing 100% of RAP and crushed CTB was made for lower bitumen contents, ranging from 1.7% to 2.0%.

Table 3 presents the ITS results for samples containing 1.8% of bitumen content, that was considered the minimum content for the 100% of RAP and Crushed CTB mixture.

**Table 3 – ITS tests for the mixture containing 100% RAP + Crushed CTB and 1% of Hydrated Lime**

RESULTS FOR DRY SPECIMENS	SAMPLE			MEAN
	1	2	3	
ITS <sub>DRY</sub> (kPa)	262	286	287	278
Dry Density (kg/m <sup>3</sup> )	2072	1988	2069	2043
ITS <sub>DRY</sub> minimum limit (kPa)	225	225	225	225
RESULTS FOR SOAKED SPECIMENS	SAMPLE			MEAN
	4	5	6	
ITS <sub>SOAKED</sub> (kPa)	184	184	185	184
Dry Density (kg/m <sup>3</sup> )	2084	2099	2113	2099
ITS <sub>SOAKED</sub> minimum limit (kPa)	100	100	100	100

As previously defined, the gradation followed the Asphalt Academy (2009) recommendation, as presented in Figure 13 and Table 4.



**Figure 13 – Gradation for Recycled mixture containing 100% RAP + Crushed CTB and 1% Hydrated lime**

**Table 4—Gradation for Recycled mixture containing 100% RAP + Crushed CTB and 1% Hydrated lime**

Sieve (mm)	% Passing
	100% RAP + BGTC plus 1% hydrated lime
50,0	100,00
37,5	100,00
25,0	99,16
19,5	92,20
12,5	89,61
9,5	79,19
6,3	68,52
4,75	55,55
2,36	43,10
1,18	28,27
0,600	20,13
0,425	14,32
0,300	11,74
0,150	6,91
0,075	4,36

Once the gradation and the bitumen content (1.8%) were defined, the pavement structure design was done based on the South African Mechanistic Design Procedure, described in chapter 2, item 2.7.

The structural modelling and mechanistic analysis was performed using the software Rubicon Toolbox. The software models the pavement structure as an elastic layered system in which the materials are characterised by its Young's modulus of elasticity and Poisson's ratio. The program then uses multi layered linear elastic system to calculate stresses and strains resulting from traffic loading.

After the stresses and strains are calculated, the program applies different failure criteria to each pavement layer, to obtain the service life of each layer in terms of the number of standard load repetitions.

The pavement structure was modelled with the default materials in the program. These materials follow the South African Material Classification, according to the TRH14, Guidelines for Road Construction Materials, from the Committee of State Road Authorities (CSRA, 1985).

The proposed pavement structure for rehabilitation was composed of at least 300 mm of foamed BSM layer, topped by a thin Gap Graded HMA layer of 20 mm. The remaining pavement structure that was not going to be recycled, composed of a Graded Crushed Stone layer in moderate moisture conditions and a compacted subgrade were treated as one single G4 layer (CSRA, 1985) with 200 mm. The subgrade was modelled as a G7 material, meaning a gravel soil material of California Bearing Ratio smaller than 15% (Theyse et al., 1996). Figure 14 shows the proposed rehabilitation structure.

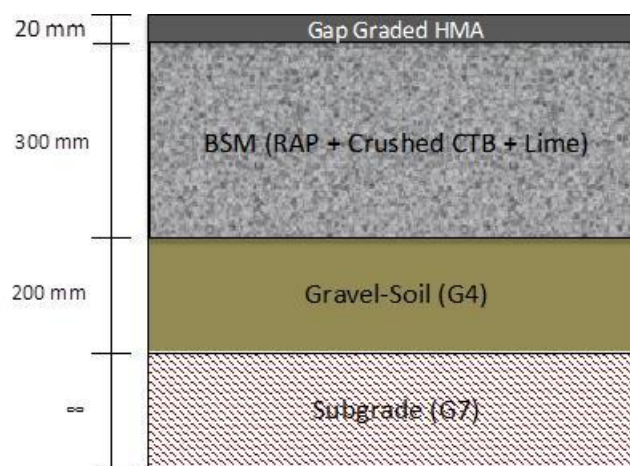


**Figure 14 – Proposed pavement structure**

The Asphalt mix layer was designed as a Gap Graded mix, with 5.1% of void content, to provide riding comfort to the users and to protect the BSM Layer underneath it. The thickness of the layer was defined as 20 mm to provide a thin cover, making it easier for water to ascend, in such a way that would help in the curing process of the BSM layer. Once the asphalt layer was very thin, it was considered as a functional layer with no structural contribution.

Based on the South African Design Methods (SANRAL, 2014; Asphalt Academy, 2009) and the Cold Recycling Technology Manual (Wirgten, 2012)

the main failure criteria for the BSM layer was considered to be permanent deformation.

According to the material classification by the CSRA (1985), the input parameters for the G4 and G7 material were obtained, as presented in Table 5, along with the parameters for the BSM layer. The foamed stabilized layer parameters were obtained from the Wirtgen Cold Recycling Manual (2012), based on the ITS results and the material characterization from the mixture design. No triaxial tests were performed for this material, and, therefore, cohesion and friction angle were based on literature and field experience by the consultants.

**Table 5 – Material properties defined for structural analysis modelling on Rubicon Toolbox Software**

Material	Parameter	
<b>BSM Layer</b>	Cohesion (kPa)	300 / 280 / 250
	Friction Angle (degrees)	42 / 40 / 38
	Relative density (compared to the density which results in the maximum friction resistance)(%)	86 / 84 / 82
	Saturation (%)	70
	Allowable Plastic Strain (%)	10
	Stiffness (MPa)	1000 / 700 / 400
	Poisson Ratio	0.35
<b>Gravel - Soil (G4)</b>	Cohesion (kPa)	34.4
	Friction Angle (degrees)	43.4
	Stiffness (MPa)	200
	Poisson Ratio	0.35
<b>Subgrade (G7)</b>	Stiffness (MPa)	100
	Poisson Ratio	0.35

The definition of the material stiffness was defined based on ELTS concept from the Pavement Number Method described on Chapter 2, item 2.7.7. The BSM material was modelled in the Rubicon Software in three layers, to get a better representation of field conditions. Since it behaves like a granular

material, it is subject to the effect of confining pressure, which means that layers positioned closer to the surface and therefore subject to higher tensions are more confined. In this sense, the cohesion, friction angle, relative density and stiffness for the three layers were defined differently.

Figure 15 presents the Rubicon Software analysis, with the material properties on the left, and design outputs on the right for each layer.



**Figure 15 – Structural analysis results for a segmented recycled layer using Rubicon Toolbox Software**

After the first analysis, another structure was simulated in the software, this time evaluating the BSM response in a single 300 mm layer. A 50 mm Hot Mix Asphalt layer was also introduced on top of the structure. This layer was designed to substitute the initial Gap Graded wearing course after curing had been finished providing a greater structural capacity and already assessing any distresses caused by the initial consolidation of the structure. This second analysis is presented in Figure 16.





**Figure 16 – Structural analysis results for a unified recycled layer using Rubicon Toolbox Software**

Both software analyses showed that the pavement was able to withstand 100 million load repetitions or more, which is the software design traffic limit. Once the structure can withstand that amount of load repetitions, the software is not able to accurately predict how much more the structure will support, considering it already an extremely efficient pavement.

### 3.4 TRIAL SECTION CONSTRUCTION

The construction of the trial section was done in one night, from 31<sup>st</sup> of August to the 1<sup>st</sup> of September of 2013, with all the procedures and materials applied identical for the two segments. Once traffic is lower on Saturdays after 12 PM, rehabilitation works started around 6 PM on the 31<sup>st</sup>, with lane closing and pavement milling.

Milling was executed at a 300 mm depth (Figure 17(a) and (b)), but it was verified that part of the CTB layer remained at the top of the remaining structure. For that reason, the structure was milled again for another 60 mm depth.



(a)



(b)

**Figure 17 – Pavement milling of the Trial Section**

After HMA and CTB milling, the remaining infrastructure was subject to passings of the Pneumatic Compaction Roller at low speed to verify its stability, moisture, and support condition.

On top of the remaining infrastructure a series of Falling Weight Deflectometer tests were conducted. The tests were performed with the FWD model Dynatest 8000 owned by Dynatest Engenharia LTDA with a 10 meter spacing alternating from the internal to the external wheel path, as presented in Figure 18.

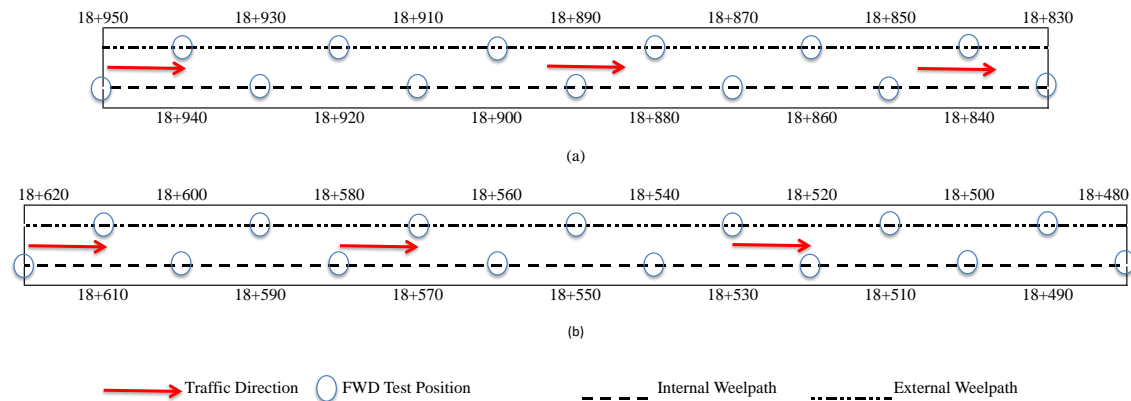


**Figure 18 – Location of FWD evaluation points**

The geophones used in the FWD tests were located at the following distances from the load application point: 0 cm, 20 cm, 30 cm, 45 cm, 60 cm, 90 cm and 120 cm. All the tests were executed for an approximately load of 42 kN.

Afterwards came the execution of the recycled BSM layer. Due to the additional 60 mm that were milled off, it was necessary to make an adjustment to the designed structure. The BSM layer absorbed the adjustment, being executed in two layers, the bottom one with 200 mm and the top one with 140 mm. Figure 19(a) and (b) shows the comparison between the previously existing structure and the final rehabilitated one.

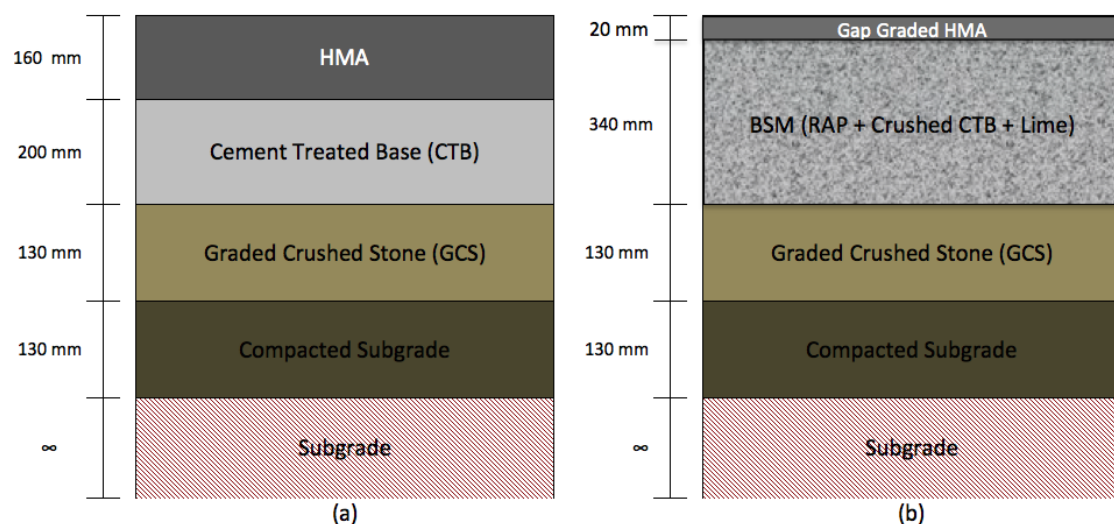
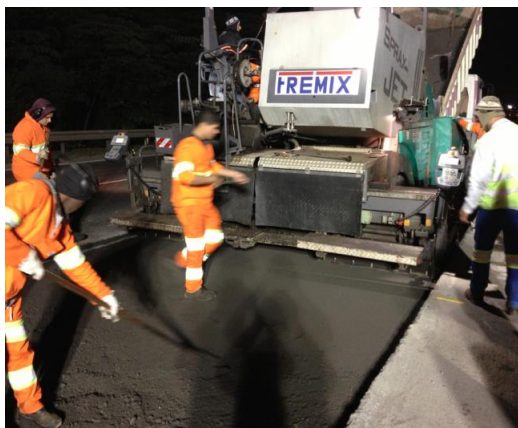


**Figure 19 – (a) Existing pavement structure; (b) Recycled pavement structure**

The construction of the bottom BSM layer (Figure 20(a)) was done with a paver, followed by compaction with the Tandem Compaction Roller (TCR) and then with the Pneumatic Compaction Roller (PCR). The thicknesses of the layer before and after compaction were 260 mm and 200 mm, respectively. For the designed compaction to be achieved were necessary 8 passes of the TDR of 15 tons followed by 4 passes of the PCR SP-55. In the end, the padfoot roller was introduced to create grooves in the surface and promote the bonding between BSM layers.

The second layer was constructed with the same sequence of procedures, except for compaction that required 6 passes of the TCR with 15 tons (Figure 20(b)) and 4 passes of the PCR SP-55. The thicknesses of the layer, before and after compaction, were 200 mm and 140 mm, respectively.



(a)



(b)

**Figure 20 – (a) Recycled layer execution; (b) Compaction with the TCR (15 tons)**

After compaction was concluded for each layer, the Sand Equivalent Test (ABNT NBR 7185/86) was performed for in situ determination of the layer density. For each layer, 50 kg of recycled mix was also collected to determine the compaction curve with modified compaction energy, and to run the ITS tests in Marshall specimens. Table 6 presents the results of the quality control tests.

**Table 6 – ITS results from mixture quality control**

Sample condition	Sample	Asphalt Binder Content (%)	ITS (kPa)	Dry Density
Dry	1	2	153,1	1,99
	2	2	199,6	1,99
	3	2	168,8	2,00
	Average		173,8	1,99

Compaction was determined through the Sand Equivalent Test (Figure 21(a)) and the result of one Proctor sample (ABNT NBR 7182/86) compacted at field moisture content, executed right before the truck transporting the material left the mix plant (Table 7). Moisture determination was done in the field with the Frying Pan Method (DER M 28/61) and on the mix plant using the Oven drying Method (ABNT NBR 6457/86) (Table 7).

**Table 7 – Construction quality control results**

Location	Parameter	km 18+950to km 18+830		km 18+620to km 18+480	
		Bottom Layer	Top Layer	Bottom Layer	Top Layer
Field Evaluation	Moisture Content (%)	7,70	7,70	7,70	7,70
	Dry Density (g/cm <sup>3</sup> )	2,011	1,971	1,932	1,967
	Design Dry Density (g/cm <sup>3</sup> )	1,966	1,966	1,966	1,966
	Compaction (%)	102	100	98	100
Proctor Compaction – Mix Plant	Dry Density (g/cm <sup>3</sup> )	1,965		1,958	
	Optimum Moisture Content (%)	7,7		8,6	
	Compaction Energy	Modified		Modified	

As FWD tests were performed on top of the remaining infrastructure, they were also executed on top of each BSM layer applied (Figure 21(b)), on the same positions shown before (Figure 18).



(a)



(b)

**Figure 21 – (a) Sand Equivalent Test; (b) FWD evaluation of stipulated points**

After both BSM layers were constructed and the FWD tests performed, the thin Gap Graded mixture was applied, with the objective of protecting the recycled layer and allowing early lane opening.

### 3.5 FWD MONITORING

To evaluate and monitor the structural performance of the trial section, FWD tests were conducted during rehabilitation, and after it was concluded. As previously described, FWD control was performed in specific positions of the trial section, spaced 10 metres apart from each other, alternating from the internal to the external wheel path.

The first series of FWD tests were conducted during pavement rehabilitation, initially on the top of the remaining infrastructure, then on the top of the first BSM layer applied, and in the end on the top of the second BSM layer applied. Once the HMA wearing course was still cooling when it opened for traffic, it wasn't possible to do tests on top of it in the construction day.

Figure 22 present the deflection bowls for the 90<sup>th</sup> percentile of the D0 results from measurements made on the rehabilitation day on top of each layer. As can be observed, the maximum deflection on top of the BSM layers remained



similar to the deflection on top of the remaining infrastructure. This phenomenon can be explained by the fact that right after execution, the BSM layers are highly deformable (high deflections), due to the high moisture content needed for compaction.

Another influencing factor is the temperature throughout the tests, as pavement surface was at average 20°C when testing over the remaining infrastructure, 18°C when testing over the bottom layer, and when testing over the top layer 13° for the first segment and 29°C for the second one. This temperature variation may have influenced the measurements, especially the readings for the sensors closer to the load application point.

Three months after the rehabilitation of the trial section, new FWD tests were conducted on the same positions previously analysed. The objective of these new tests in beginning of December of 2013 was to verify changes in structural behaviour due to the exit of water due to material curing.

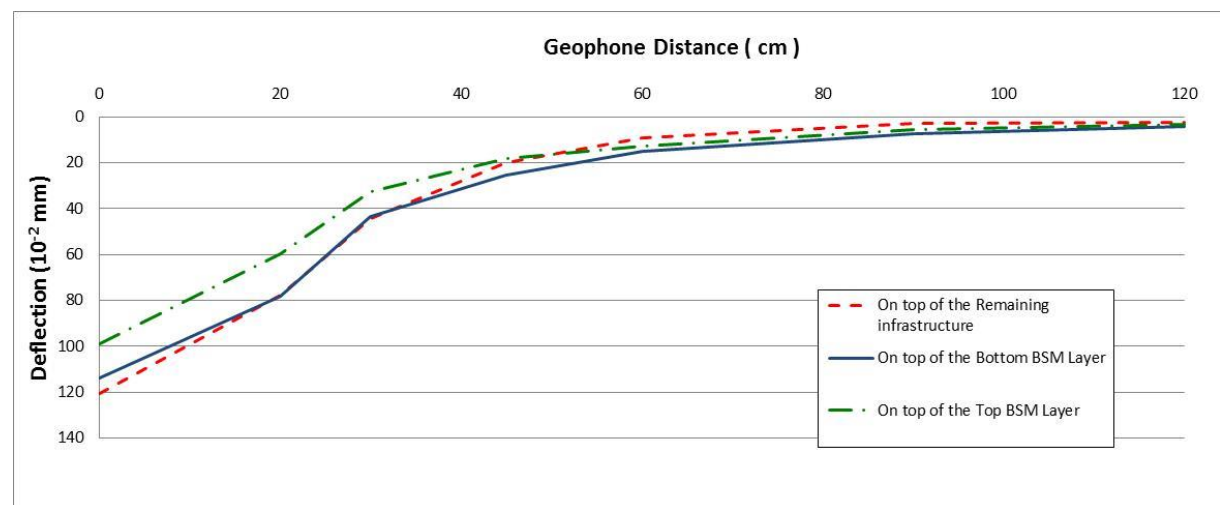


**Figure 22 – Deflection bowls for the 90th percentile of D0 for the FWD tests performed on different layers on rehabilitation day**

With the same objective, two other FWD evaluations were made in the trial section, one in October of 2014 (after 13 months), and the other in June of 2015 (after 22 months). It was expected that with material curing, the layer stiffness would increase, resulting in smaller deflections with time. Figure 23 shows a comparative of the 90<sup>th</sup> percentile for the different deflection bowls measurements through time.

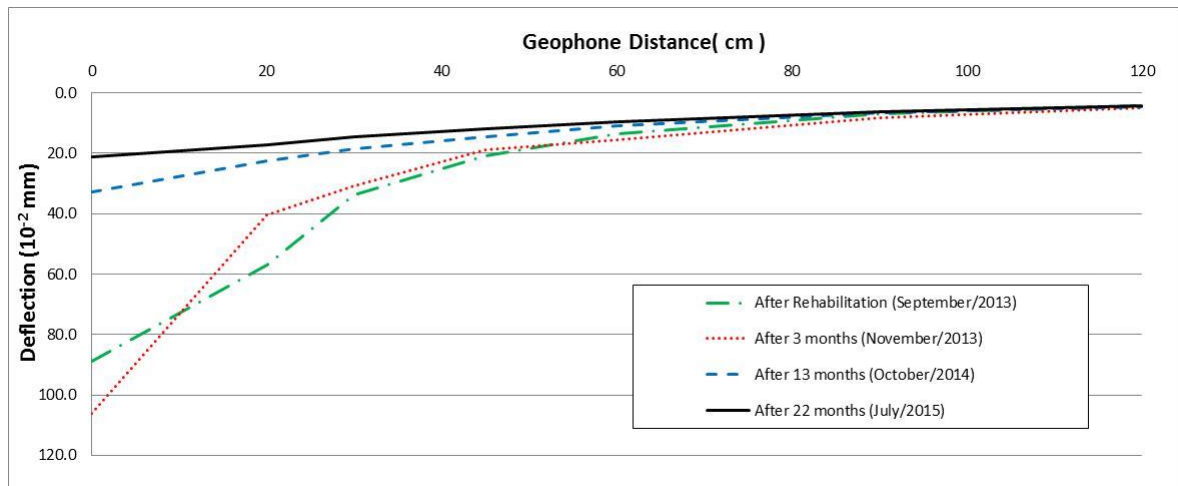


**Figure 23 – Deflection bowls for the 90th percentile of D0 for different FWD evaluations**

When analysing the 90<sup>th</sup> percentile deflection bowls and its evolution along the different measurements with time, one can observe the increase in structural capacity of the pavement, with curve flattening. As time passed, the capacity of stress distribution increased due to the stiffening of the foamed recycled base layer. Although curing is understood as a period in which the layer is increasing its resistance until it reaches a stable phase, the amount of time needed depends on the materials used, the pavement configuration, and seasonal and climatic effects.

As can be observed, after the second FWD evaluation, deflections reduce considerably, especially for the geophones closer to the loading point. The small variability for the deflections on the geophones further from the loading point mean a small variation on the subgrade and deeper layer behaviour.

The maximum deflections obtained throughout the monitoring period are presented in Figure 24, where can be seen that pavement deflections decreased, an average of 63% from rehabilitation until October/2014 and 76% until July/2015, without any intervention. From the same Figure, it is also possible to observe the decrease in the variability among the points tested.



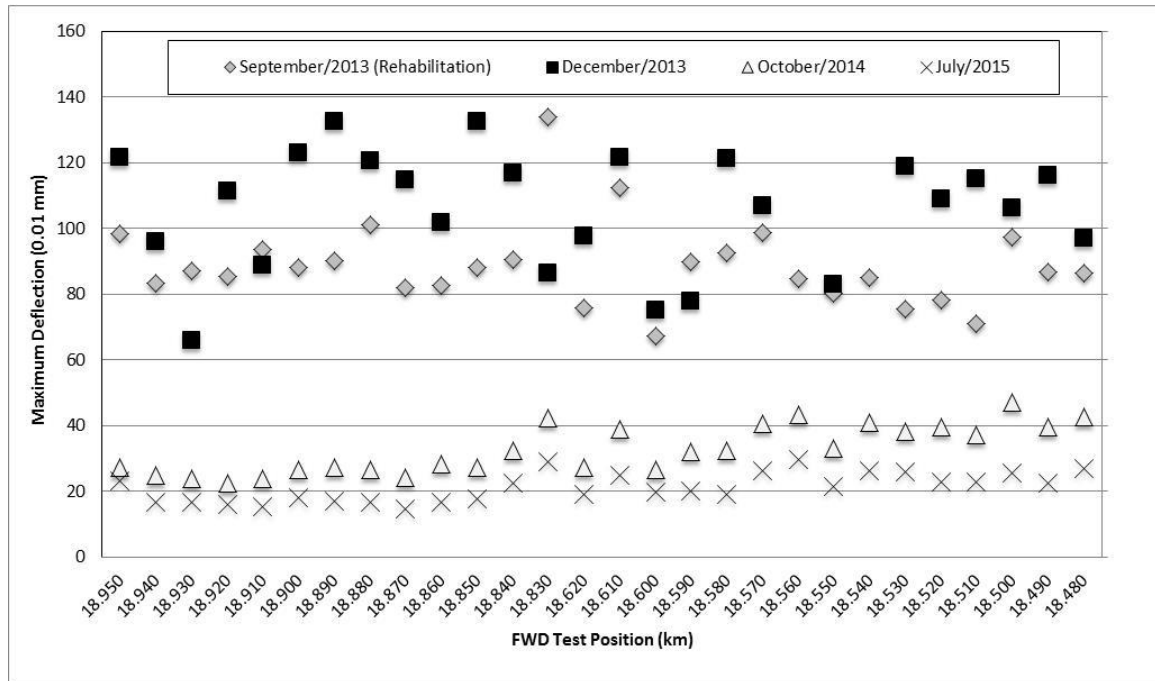


**Figure 24 – Maximum deflection (D0) evaluation of the trial section on different occasions**

One possible reason why the deflections measured in December/2013 were higher than right after rehabilitation is a seasonal influence, affecting the pavement and the materials moisture content. December is in the beginning of the rainy season in Brazil, which would explain the increase in the deflections, associated with moisture ingress. The same reason could justify part of the deflection decrease from October/2014 to July/2015, which is in the dry season.

### 3.6 FWD BACKCALCULATION

Currently there is no field equipment designed to determine the resilient modulus of base materials, or subgrade soils, for construction quality control purposes. Falling Weight Deflectometer (FWD) has been widely used in pavement engineering. Backcalculated moduli from FWD data have been used extensively in pavement design, and other management activities. Although using the FWD on top of surface layer might induce nonlinear displacement, a linear-elastic program was used to analyse the foamed

recycled layer moduli. In this study, the software ELMOD 6, from Dynatest Consulting Inc., was selected to backcalculate the moduli of the tested pavement sections.

The software analyses the measured deflection bowls, comparing it to theoretical bowls created by an elastic linear analyses iteration process, where the elastic modulus for the layers are changed until a similar bowl to that measured is obtained.

For the analysis, the 20 mm HMA layer was not considered a structural layer, but a wearing course. Since the asphalt layer is only 20 mm thick, it was not considered to have any structural function, with its displacement behaviour on the field conditioned to that of the underlying layer.

As the focus of the analysis was the BSM layer, everything underlying it was treated as single semi-finite layer, named "Remaining Infrastructure". The adoption of a single semi-finite layer for the remaining infrastructure was done to minimize the effect of variability from the remaining existing structure on the analysis of the BSM layer. With the layer unification, it was possible to obtain a smaller variation of the elastic modulus of the remaining infrastructure layer, hence a better homogeneity for the BSM layer results.

In this way, it was possible to isolate the BSM layer to verify its modulus variation along the research period. The modulus of the Remaining Infrastructure did not change significantly, whereas the BSM layer's stiffness has increased from 240 MPa after construction to 2.400 MPa 22 months after construction.

Contrary to the laboratory specimens, which are cured to steady state, the BSM layer in the field is curing under traffic loading. Although this loading causes distress and loss of stiffness to the layer in the long term, it also acts as a compaction mechanism, increasing the density of the layer, while forcing aggregates against each other, which may strengthen its bitumen bonds. This way, during the curing period the material is not only stiffening through the migration of moisture, but also by its densification due to traffic loading and by strengthening of aggregate bitumen bonds (Figure 25). This can, however, be

offset by a reduction in dissipated energy within the material under repeated loading. In addition, moisture variation due to seasonal changes should be accounted for stiffness variation through the year.

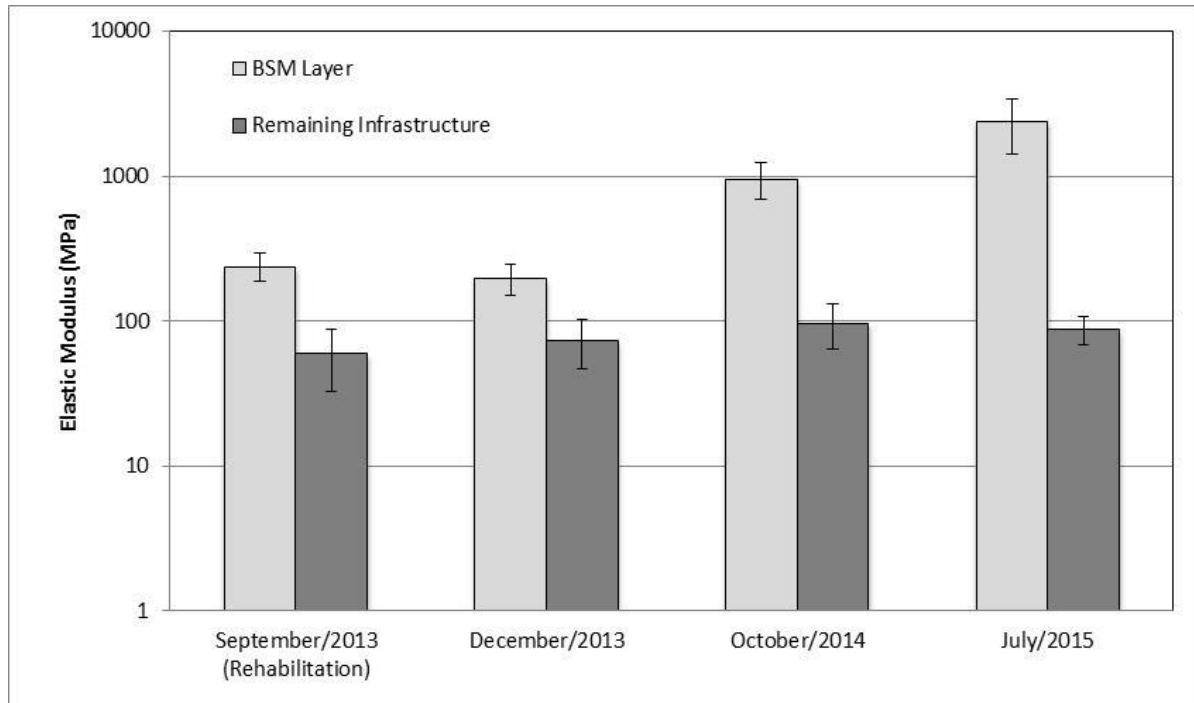


**Figure 25 – Backcalculated Elastic Modulus for the BSM layer and the remaining infrastructure along the curing period**

All the backcalculated results, as well as all the FWD measurements are presented in the Appendix .

## 4 LABORATORY ANALYSIS

The laboratory analysis in this thesis was done to investigate the behaviour of the recycled foamed BSM mixture in a more controlled environment than in the field. The material used in most of the experiments is the same as the one used in the Ayrton Senna Highway trial section.

Monitoring the trial section allowed the evaluation of pavement performance when subject to several factors than cannot be controlled, such as climate conditions and traffic loading. On the other hand, laboratory evaluation makes possible a greater control of the factors influencing the material behaviour, reducing possible interferences on the results. A flowchart with the summary of the tests and activities undertaken in the laboratory is presented in Figure 26.

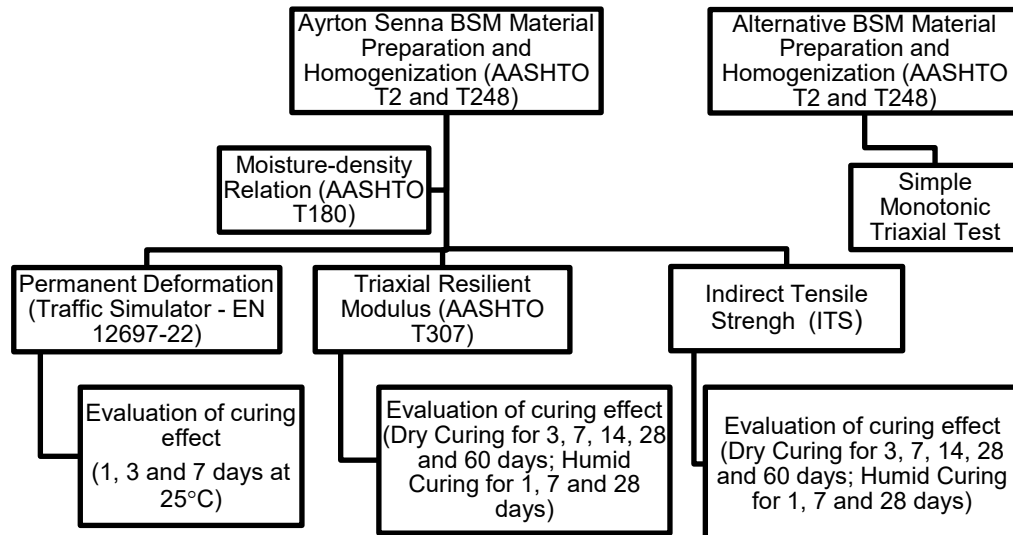


Figure 26 – Flow chart with a summary of laboratory proceedings

#### 4.1 TRIAL SECTION MATERIAL

The trial section material used in the laboratory experiments is the same material used to pave the BSM layer in the night of 31<sup>st</sup> of August of 2013 in SP-070 Highway. The material was collected in the plant during the loading of the trucks that were transporting the material to the job site.

After the material was processed in the KMA 220, with the aggregates already mixed to the foamed bitumen, part of the material was separated for laboratory analysis. The mixture was sealed in resistant plastic bags (1,5 mm thick), so moisture would be preserved. Each plastic bag was then placed inside a fabric bag, to enhance the protection of the bags, preventing the plastic bags from shredding and losing moisture.

The material (total of 43 bags) was then taken to Laboratory of Pavement Technology (LTP) in the Polytechnic School of the University of São Paulo for analysis. Each bag had approximately 30 kg of the RAP and crushed CTB mixture already foamed.

When received, all the bags were opened and mixed in the laboratory for material homogenization (Figure 27(a) and (b)). Once mixed, the material was quartered according to AASHTO T2 and T248 and then sealed again in plastic bags to avoid further moisture loss (Figure 27(c) and (d)). Although some moisture was lost in this process, material homogenization was done with the objective of making each bag a representative sample, with similar characteristics, especially in terms of aggregate gradation.



(a)



(b)



(c)



(d)

**Figure 27 – Material (a) reception; (b) homogenization; (c) separation; (d) storage**

Since hydrated lime was used as active filler in the mixture, material storage was allowed, once its moisture was preserved, whereas storage would not have been possible if the active filler used in the process had been cement (Wirtgen, 2012). As tests were carried on and as the plastic bags were opened for use, moisture content analyses were made for every material sample, in order to guarantee that moisture was at least between 50% and 60% of Optimum Moisture Content (OMC). Moisture content evaluation was done oven drying a sample previously weighted, leaving it at 110° C for at least 24 hours, and then weighting it again. The verified mass difference indicates the amount of water lost, and therefore the samples moisture content.

## 4.2 MOISTURE DENSITY RELATION

Before specimens' preparation for testing, the maximum dry density of the material, and the mixture's optimum moisture content were determined. The compaction tests were conducted according to ASSHTO T99 and T180 and were performed in two stages.

In the first stage, compaction was done in cylindrical samples of approximately 152 mm of diameter and 127 mm height, commonly used for California Bearing Ratio tests (AASHTO T193-99). Five samples were compacted for moisture contents increments of 1% per sample, from 6% to 10%. The obtained compaction curve is presented in Figure 28, resulting in optimum moisture of approximately 7.3%, and dry density of 2.03 g/cm<sup>3</sup>.

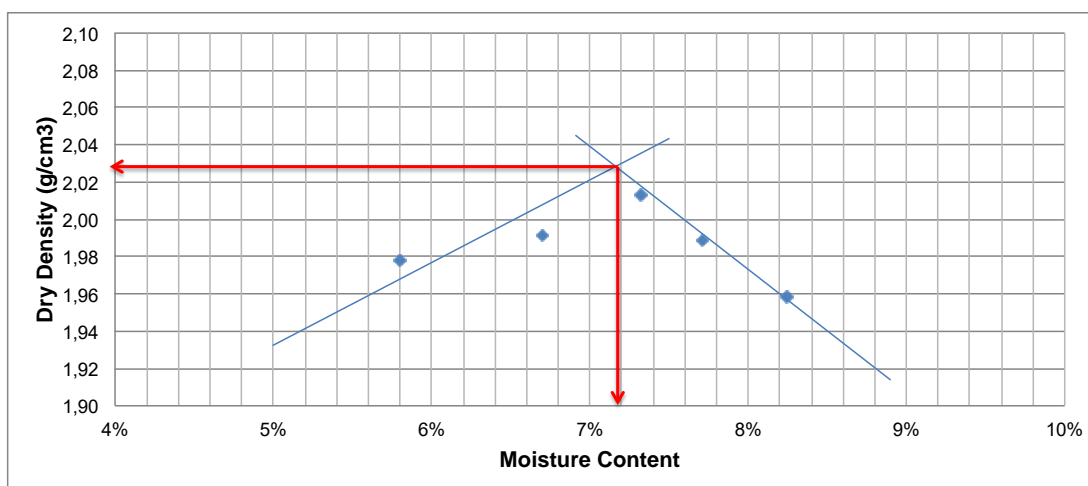


**Figure 28 – Moisture Density relation determination (Specimens with 152 x 127 mm)**

After the optimum moisture content was estimated in 7.3%, new samples were compacted for moisture contents of 7.0%, 7.5% and 8.0%. At this time, the samples were compacted in cylindrical specimens of 100 mm diameter and 200 mm height, which would be the sample size used for some of the mechanical tests performed. The optimum moisture content, and the maximum dry density were the same as previously determined.

The material used in the compaction tests was screened through the 19 mm sieve (3/4") for aggregate separation according to ABNT NBR 6457 (1986)

regarding compaction test preparation. Moisture determination for each moulded specimen was done oven drying small samples (Figure 29(b) and (d)), and then adding the needed amount of water to the mixture to achieve the desired content (7.3%).



(a)



(b)



(c)



(d)

**Figure 29 – (a) specimen with 152 x 127 mm; (b) material drying in the oven; (c) specimen with 200 x 100 mm; (d) sample of oven dried material**

For both specimen dimensions, modified energy was applied in compaction (Asphalt Academy, 2009; Wirtgen, 2012).

### 4.3 PERMANENT DEFORMATION EVALUATION

One important characteristic of BSM layers with low percentage of foamed asphalt binder is that the bonding between particles in the mixture is dispersed. Once the nature of these non-continuously bound materials may



prevent crack propagation and therefore material fatigue, permanent deformation becomes the primary mode of distress, caused by the shear stress between particles.

Assuming that permanent deformation is the primary failure criterion for this BSM layer, the laboratory analysis proceeded with a test that would allow the mixture evaluation from that point of view. After the determination of the moisture density relation, slab samples were moulded to be tested in the LCPC traffic simulator.

The compaction machine used to compact the slabs is manufactured by the LCPC (*Laboratoire Centrale de Ponts et Chaussées*), according to the European specification EN 12697-33 (2003) (Figure 30). The method consists in the compaction of slab-shaped specimens of 100 x 180 x 500 mm through the passing of a standard pneumatic tire with tire pressure varying from 0.1 to 0.6 MPa.



**Figure 30 – LCPC compaction machine**

After compaction the slabs were subjected to different curing periods (1, 3 and 7 days), left inside the moulds at ambient temperature, with only its upper surface exposed. After the curing period, the samples were tested in the traffic simulator for evaluation of the accumulation of permanent deformation.

The traffic simulator used was the French one, developed by the LCPC for wheel path rutting determination of the evaluated sample. This test is conducted according to the European specification EN 12697-22 (2003), with two specimens being tested at the same time subjected to the loading of an axle with two pneumatic tires rolling over each specimen, in cycles of two passes and 1 Hz frequency.

The tire pressure on the pneumatics is standardized on 0.6 MPa (6 bar), and the applied loading is defined in 5.9 kN. As the test was developed primarily for HMA analysis, the procedure is usually conducted at 60° C. In this case, as the material is going to serve as a base layer, all the simulations were conducted at ambient temperature of approximately 25°C. The procedure involves the measurement of the surface condition prior to the beginning of the test, and then after the accumulation of deformations caused by 100, 300, 1000, 3000, 10000 and 30000 cycles. The test should be stopped at 30000 cycles, or for deformations higher than 15%. Figure 31 shows the simulator with the doors open, during the test on the specimens at ambient temperature.



**Figure 31 – LCPC Traffic Simulator operating at ambient temperature**

The first two specimens were compacted to verify if the compaction procedure had achieved the desired dry density by moulding the slabs with the

approximate material mass that would result in that density. Meanwhile, a sample of the material was oven dried for moisture determination, so the slabs dry density could be verified. As results turned to be positive, those specimens were tested after a 7 day curing period, and both of them resisted the 30000 cycles accumulating only 2.7% of permanent deformation.

Due to the low deformation level verified, a more critical condition was evaluated. For that, two more specimens were moulded and tested after 3 days of curing period. This time the accumulated permanent deformation was higher, but still smaller than 5.0%, which is a relatively low deformation for the end of the test.

Another pair of specimens were compacted and cured for only 24 hours in the same conditions as the previous samples. Even though the accumulated permanent deformation has doubled from the 3 day curing specimens to the 24 hour curing ones, it is still smaller than 8% after 30000 cycles.

Although the test with only 24 hours of curing may not represent the material field condition during its service life, it does represent a more critical condition that may occur in the first days after pavement construction. Considering that the trial section at Ayrton Senna Highway was opened to traffic right after rehabilitation, the simulated condition with 24 hours of curing may occur. During this first period after rehabilitation, traffic loading is already underway, but the moisture content is still high, which may allow higher particle lubrication and consequently a higher accumulation of permanent deformations.

Table 8 presents the results of accumulated permanent deformation for each curing period. On Figure 32 the curves of accumulated permanent deformation by the number of cycles are plotted for the different curing periods. In the first 1000 cycles, for the specimens cured for 3 days, a higher initial deformation was observed, which may suggest that the initial density could have been lower than that of the other specimens.

**Table 8 – Accumulated Permanent Deformation per curing, based on the LCPC Simulator tests**

Curing Period	% of Accumulated Permanent Deformation			
	1,000 cycles	3,000 cycles	10,000 cycles	30,000 cycles
24 hours	2.69%	3.77%	5.47%	7.67%
3 days	2.80%	3.30%	3.95%	4.66%
7 days	1.38%	1.72%	2.19%	2.73%

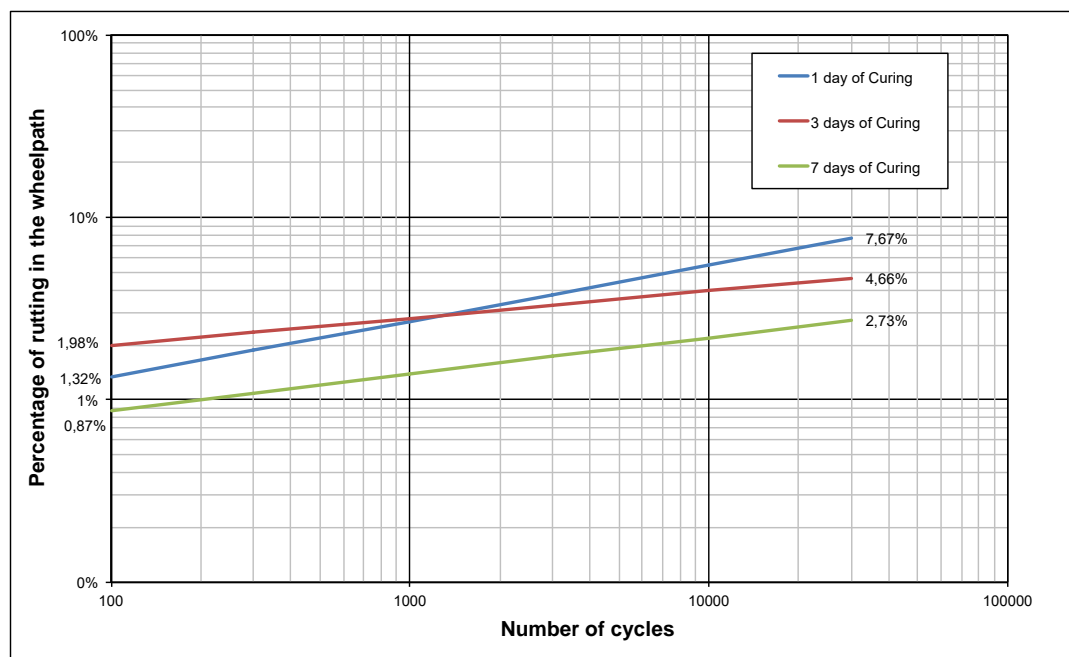


**Figure 32 – Percentage of rutting accumulated in the wheelpath in terms of the number of load cycles**

#### 4.4 TRIAXIAL RESILIENT MODULUS

Jenkins (2000) and Fu and Harvey (2007), mention the sensibility of the BSM's stiffness to the stress state to which it is subjected. Aiming towards improving the understanding of the mechanical properties of the material, the triaxial resilient modulus test was conducted, so the effect of confinement could be verified. Not only the effect of confinement was observed, but also how moisture into the specimens affected its behaviour and the materials stiffness.

The triaxial resilient modulus test was conducted according to the Brazilian specification DNIT ME 134/2010, from the National Department of Transportation and Infrastructure (DNIT). This procedure is similar to the AASHTO T-307 (2011), but with broader loading combinations. All the samples were tested in a servo-pneumatic testing machine, used to characterize the laboratory prepared mixtures in terms of triaxial resilient modulus.

Table 9 presents the combinations of confining and deviatoric stresses applied in the test.

The samples used for the test were 200 x 100 mm cylindrical specimens and were compacted according to ABNT NBR 7182 (1986) with modified compaction energy. After compaction, the samples were weighted and a small amount of material was taken for moisture content verification.

The specimens remained into a controlled chamber at 25°C for curing. Inside the chamber, the specimens remained with its surface exposed, without any protective bags or membrane, and cured for periods of 3, 7, 14, 28 and 60 days. This curing process was named “dry curing”, and 12 samples were tested after this procedure, with at least 2 specimens for each curing period.

**Table 9 – Stress combinations for the Resilient Modulus Tests**

$\sigma_3$ (kPa)	$\sigma_d$ (kPa)	$\sigma_1/\sigma_3$
20.7	20.7	2
	41.4	3
	62.1	4
34.5	34.5	2
	68.9	3
	102.9	4
50.4	50.4	2
	102.9	3
	155.2	4
68.9	68.9	2
	137.9	3
	206.8	4
102.9	102.9	2
	206.8	3
	309	4
137.9	137.9	2
	274.7	3
	412	4

The objective of the curing procedure was to evaluate the effect of the decrease in the moisture content in the mixture, instead of trying to accelerate curing to simulate field conditions after its stabilization.

After curing, the specimens were weighted again to determine the approximate residual moisture, and then were prepared for the test. To make sure that the stress distribution on the specimen was homogeneous throughout the test, all specimens were capped on the bottom and on the top with a thin layer of plaster, as can be seen in Figure 33(a) and (b).

To apply the confining stress on the specimen during the test a latex membrane was used and strapped to it with rubber rings. The specimen was

then placed inside the chamber where air pressure was applied, pressing the latex membrane against the specimen's surface, creating confinement.



(a)



(b)



(c)



(d)

**Figure 33 – Specimen preparation and triaxial test: (a) bottom capping; (b) Top capping; (c) capped specimen with top cap positioned; (d) specimen during the test**

Figure 33(c) shows the specimen preparation for the triaxial resilient tests while Figure 33(b) shows the specimen with the membrane inside the confining chamber.

Figure 34 presents the results obtained from the triaxial resilient modulus tests, with different curing periods, showing the stiffness variation in terms of the applied confining pressure ( $\sigma_3$ ).

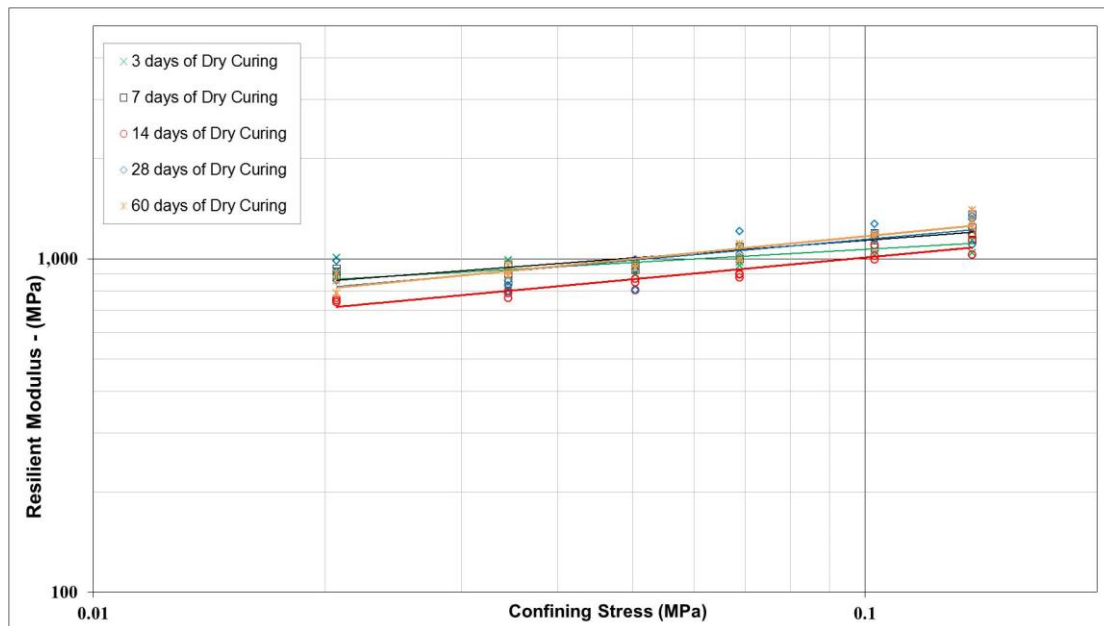


**Figure 34 – Resilient Modulus for dry cured specimens with different periods in terms of the confining stress ( $\sigma_3$ )**

As it can be seen from the results, although the material seems to be influenced by the variation in the confining pressure, it was not possible to efficiently assess the effect of curing on the resilient modulus. Regarding the effect of confinement, a clear trend can be noticed in stiffness increase for all curing periods. As  $\sigma_3$  increased, so did resilient modulus, with maximum increase ranging from 50% to 78%.

Observing the results per condition in Table 10, it can be verified that most part of moisture is lost in the first few days, with moisture dropping to 50% of OMC after 3 days of curing, while the moisture decrease rate reduced after that period. That could explain why the resilient modulus increase from 3 to 60 days was not significant.

In order to better understand the foamed recycled material behavior in its initial curing stage, when moisture content is high, one specimen was tested without curing, with the test being conducted right after compaction.

This specimen presented high deformability, with low loading resistance, even for high levels of confining pressures (137.9 kPa). Figure 35 shows the deformation on the specimen after the test, being possible to verify the



diameter increase in the middle of the sample (Figure 35(a)) and then material crumbling when trying to remove it from the test base (Figure 35(b)).



(a)



(b)

**Figure 35 – Specimen tested without curing resulting in (a) deformation along the diametral line; (b) material crumbling when removed from test apparatus**

As a way to understand the effect of moisture during the curing period, and its effect on the resilient modulus, the curing method was changed. At this time the specimens were sealed in plastic bags right after compaction, in an attempt to confine the water inside. This second method was named “humid curing” and 7 samples were cured for 1, 7, and 28 days, with at least 2 specimens tested for each condition.

Figure 36 shows the results obtained for the different humid curing periods showing the resilient modulus variation in terms of the applied confining pressure ( $\sigma_3$ ).

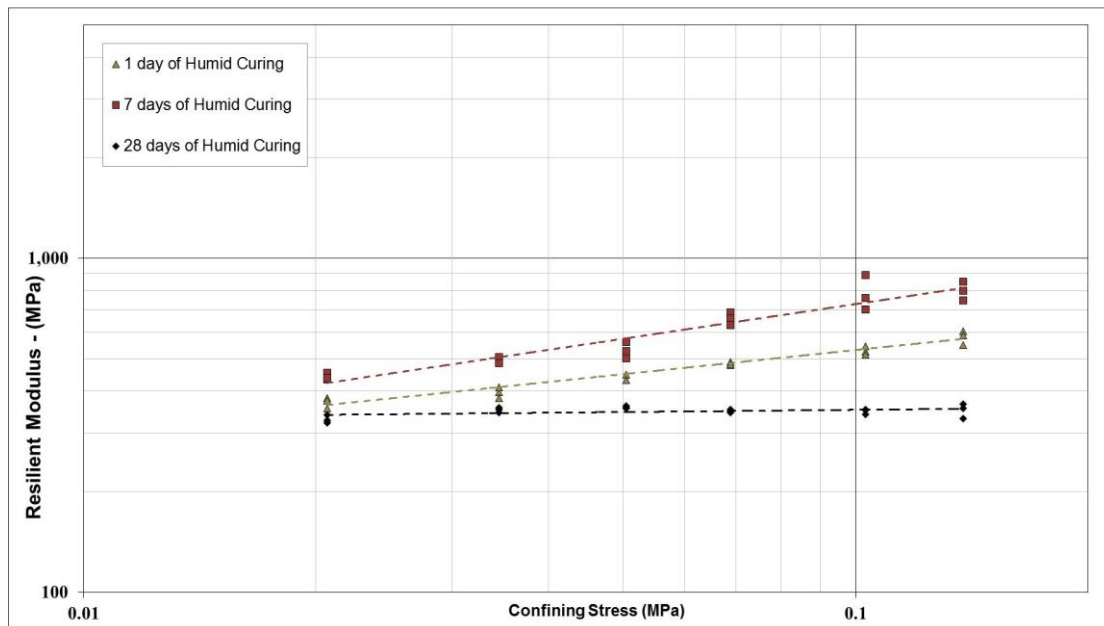


**Figure 36 – Resilient Modulus for humid cured specimens with different periods in terms of the confining stress ( $\sigma_3$ )**

Although the moisture in these specimens was between 95% and 99% of OMC, since they were sealed during the curing process, the modulus is higher for 7 days then for 1 day. This may suggest that some chemical reaction may have occurred, although the hydrated lime percentage is very low, or even that hydrogenesis has resulted in a change in moisture content and distribution, even though the specimens were sealed, leading to a higher resilient modulus. The results obtained after 28 days of humid curing show a drop in the material stiffness that could be related to moisture damage, once an extended humid curing time could deteriorate the bond between binder and aggregate.

Figure 37 compares the average resilient modulus of each curing procedure for a specific stress combination. A slight improvement in the material resilient modulus can be seen for longer curing periods, although a low stiffness was also verified for the specimens cured for 28 days in humid condition.

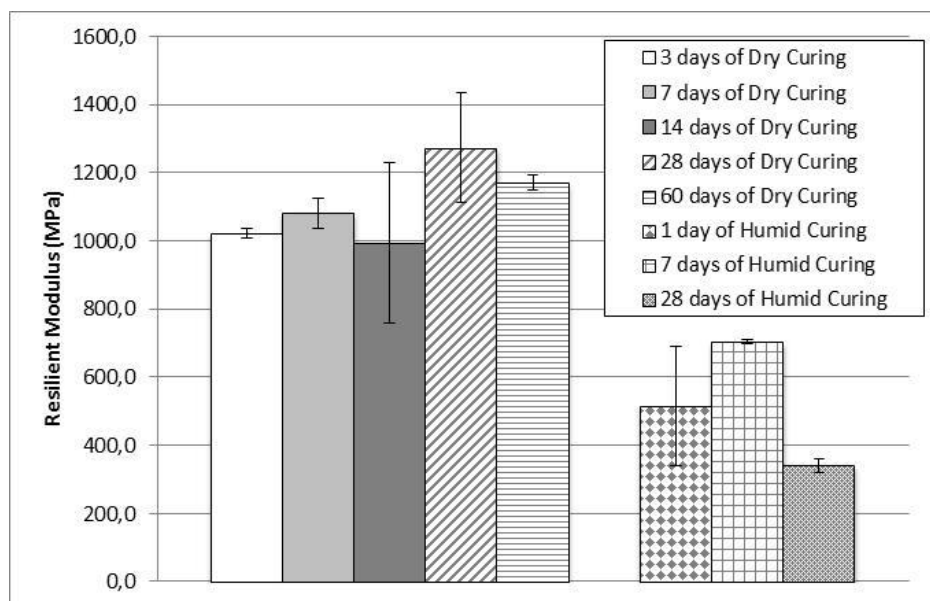


**Figure 37– Resilient Modulus obtained for stress combination of  $\sigma_d = 0,309$  MPa and  $\sigma_3 = 0,103$  MPa**

In Table 10 it is shown a comparison between material stiffness verified in tests with the different curing periods and procedures.

**Table 10 – Resilient modulus Increase rate per different curing periods**

Curing		Minimum Resilient Modulus (MPa)	Maximum Resilient Modulus (MPa)	Resilient Modulus Increase Rate
Dry	3 days	803.3	1210.1	51%
	7 days	857.3	1360.7	59%
	14 days	740.7	1185.4	60%
	28 days	798.4	1341.7	68%
	60 days	788.3	1399.6	78%
Humid	24 hours	354.8	604.9	70%
	7 days	433.5	890.2	105%
	28 days	320.9	365.5	14%

The moisture effect in the materials behaviour can also be observed through the difference in the average resilient modulus results for the "dry" and the "humid" curing, and consequently the residual moisture remained in the

sample presented in Table 11. Table 11 also presents the resilient modulus equations as a function of the confining stress.

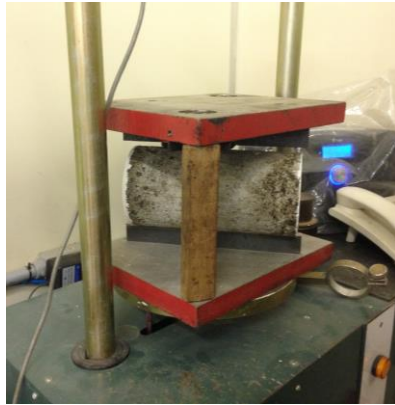
**Table 11 – Residual moisture content and resilient modulus equations**

Curing Period	Curing Method	Residual Moisture (% OMC)	RM	R <sup>2</sup>
3	Dry	38.7%	$RM = 1413.04 * \sigma_3^{0.1229}$	0.407
	Dry	40.7%	$RM = 1467.1 * \sigma_3^{0.1383}$	0.565
7	Dry	39.4%	$RM = 1597.9 * \sigma_3^{0.1637}$	0.547
	Dry	38.5%	$RM = 1684.0 * \sigma_3^{0.1562}$	0.699
	Dry	38.8%	$RM = 1822.7 * \sigma_3^{0.207}$	0.897
14	Dry	20.4%	$RM = 2123.5 * \sigma_3^{0.2566}$	0.850
	Dry	28.5%	$RM = 1938.0 * \sigma_3^{0.2363}$	0.799
	Dry	25.0%	$RM = 973.1 * \sigma_3^{0.1303}$	0.624
28	Dry	23.1%	$RM = 2385.5 * \sigma_3^{0.3236}$	0.778
	Dry	11.0%	$RM = 1486.0 * \sigma_3^{0.1109}$	0.246
60	Dry	-	$RM = 2010.1 * \sigma_3^{0.2387}$	0.897
	Dry	-	$RM = 1914.3 * \sigma_3^{0.2121}$	0.849
0	No Curing	-	$RM = 37.3 * \sigma_3^{0.616}$	0.381
1	Humid	-	$RM = 1419.1 * \sigma_3^{0.3446}$	0.924
	Humid	-	$RM = 1316.9 * \sigma_3^{0.3152}$	0.846
	Humid	-	$RM = 273.1 * \sigma_3^{-0.054}$	0.329
7	Humid	99.1%	$RM = 1557.9 * \sigma_3^{0.346}$	0.913
	Humid	96.6%	$RM = 1669 * \sigma_3^{0.3443}$	0.886
28	Humid	98.1%	$RM = 276.9 * \sigma_3^{-0.075}$	0.519
	Humid	98.4%	$RM = 494.7 * \sigma_3^{0.1215}$	0.531

#### 4.5 INDIRECT TENSILE STRENGTH TEST

After the triaxial resilient modulus test, each sample was tested for Indirect Tensile Strength. Each specimen was placed in a metallic support as shown in Figure 38(a), resulting in stress application in the diametral line along the specimen. Then the specimen was loaded at a constant displacement rate of

50.8 mm/min. Along the test, the equipment records load and displacement, that increase up to the point where the material resistance starts to decrease. At this point (maximum load), the tensile strength is determined and the sample, as shown in Figure 38(b).



(a)



(b)

**Figure 38 – (a) Specimen positioning for ITS test; (b) specimen after failure**

The increase in the strength due to the curing can be observed in Figure 39, and it follows the same trend observed in the triaxial test (with the same decrease in resistance observed between 7 and 28 days for the humid curing procedure).

For the specimens that went through the dry curing procedure, tensile strength increased as the length of the curing period increased. However, within the specimens that went through the humid curing procedure the specimens cured for 28 days presented a smaller resistance than that of 7 days.

As previously discussed, an extended curing period with moisture confined in the specimen could lead to the deterioration of the asphalt bonds in the mixture. That moisture damage process could have been more significant to the specimens than the benefits of chemical curing, resulting in the reduction of the tensile strength.

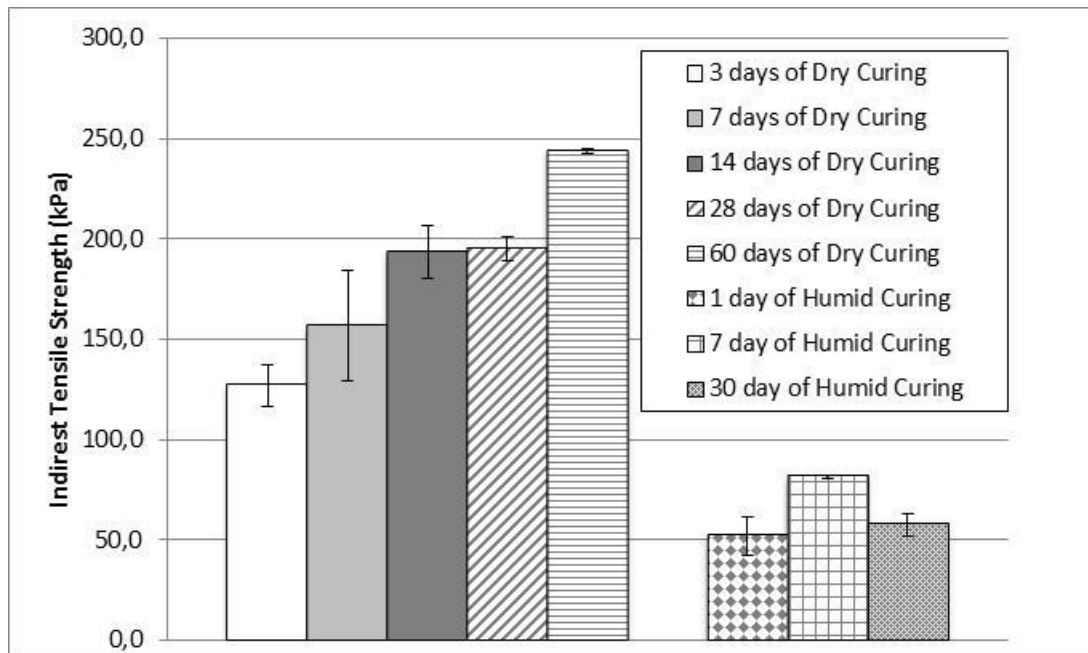


**Figure 39 – ITS results for different curing periods and procedures**

One thing that can be observed is the low magnitude of the resulting tensile strengths. The dry samples would be expected to have ITS results greater than 225 kPa, which was the minimum limit used for design. One possible reason for that could be that the samples were tested right after being subject to the resilient modulus test. Although that test is considered as non-destructive, the stress combinations applied may have been too severe, especially the last set of stress combinations with  $\sigma_3=137.9$  kPa, and  $\sigma_d$  values as high as 412 kPa.

#### 4.6 MONOTONIC TRIAXIAL TEST

Since an important part of BSM mechanical characterization consists in the determination of its cohesion and angle of internal friction, Simple Monotonic Triaxial Tests were conducted in this study.

The procedure was carried out in a MTS hydraulic machine (Figure 40(a)). Cylindrical specimens with 150 mm diameter per 300 mm height were subjected to a compressive, monotonic loading while confined inside a pressurized chamber (Figure 40(b)).

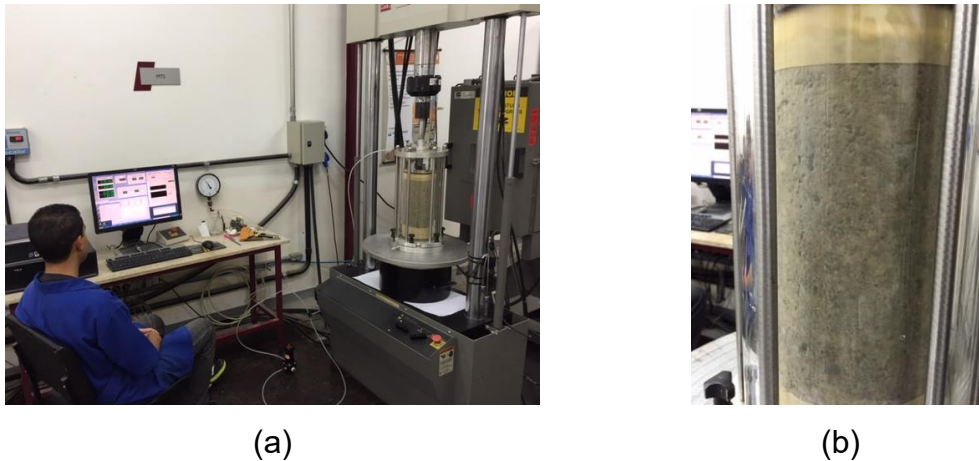


**Figure 40 – (a) Specimen during the monotonic triaxial test; (b) effect of air confinement on latex membrane**

The testing apparatus must have an acquisition system that allows for load and displacement recording, so material failure can be identified and properly characterized. The acquisition rate was defined at 10 Hz as recommended by Asphalt Academy's Method 7.

The displacement rate applied in the test was 3 mm/min, until the point where the material resistance started decreasing, or 18 mm of displacement (6 % of total specimen deformation) was achieved. Although Method 7 recommends and Mulusa (2009) applies a displacement rate of 6.3 mm/min, Ebels (2008) uses a 1 mm/min rate. In this study, a specific recommendation from BSM Laboratories Ltd test procedure was followed, resulting in the 3 mm/min rate.

By the time it was possible to execute the tests, the Ayrton Senna Highway Foamed BSM mixture had a very low moisture content, around 2% (approximately 30% of OMS). In this case, the material was considered not suitable for tests, as it was not possible to assess how deteriorated and aged the mixture was.

As a result, this test was conducted with a different mixture, in order to analyze how the test could be run to obtain the desired parameters (cohesion and friction angle) for design considerations.

The BSM mixture used for the tests was designed by Fremix Engenharia e Comércio LTDA., and was composed of 84% reclaimed pavement (RAP + granular material), 15 % Stone Crusher dust and 1 % of hydrated lime.

The material gradation is presented in Table 12 and Figure 41, fitting in Wirtgen (2012) gradation envelope for foamed BSM mixtures.

**Table 12 – Gradation of the BSM mixture used for the Monotonic Triaxial Tests**

Sieve (mm)	% Passing	Wirtgen	
	84% reclaimed pavement + 15% Stone Crusher dust + 1% Hydrated lime	Ideal	
		Minimum	Maximum
50	-	100	100
37.5	-	87	100
26.5	100.0	76	100
19	68.0	65	100
13.2	-	55	90
9.5	51.5	48	80
6.7	-	41	70
4.75	40.5	35	62
2.36	33.0	25	47
1.18	-	18	36
0.6	17.0	13	28
0.425	-	11	25
0.3	-	9	22
0.15	8.5	6	17
0.075	5.0	4	12



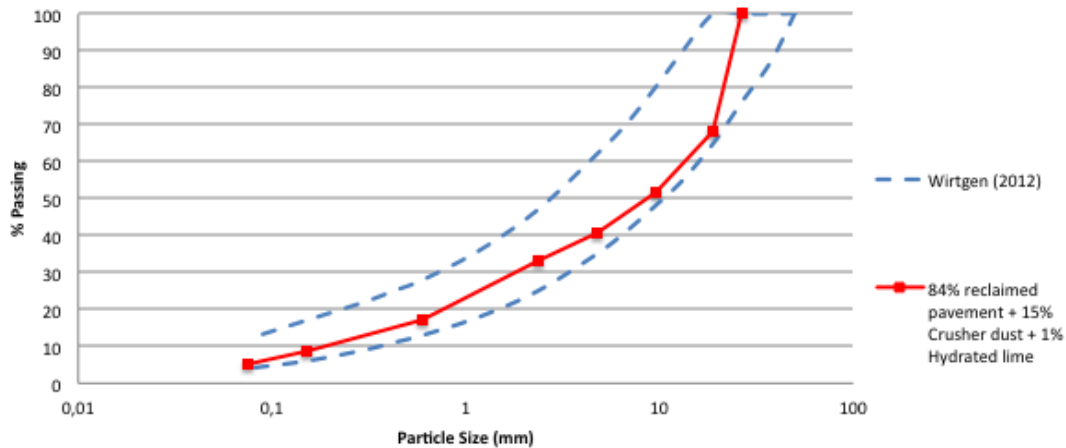


**Figure 41 – Gradation envelope for the BSM material used in the Monotonic Triaxial Test**

As described in the Technical Report “ARVEK DP BARROS0 1/14” (Fremix, 2014), OMC was defined at 7.5% for a maximum dry density of  $1.845 \text{ g/cm}^3$ . Mix design resulted in an optimum asphalt binder content of 2.2% and 1% addition of hydrated lime as the active filler.

For manufacturing the specimens for the monotonic triaxial tests the material was screened through a 19 mm (3/4”) sieve to avoid that coarse aggregates interfered creating variability due to the scale of the modeled sample. The retained material was then substituted for material retained at the 4,75 mm (#4) sieve. The cylindrical 150 x 300 mm specimens were manually compacted with modified energy.

The objective of the test was to obtain the material cohesion and angle of internal friction. The tests were performed with 4 different conditions of confining pressure ( $\sigma_3$ ): 0 kPa, 50 kPa, 100 kPa and 140 kPa. Although usual confining pressure for the test would include 200 kPa, there was a concern if the confining chamber would support that amount of pressure. As a security issue, this condition was replaced by  $\sigma_3 = 140 \text{ kPa}$ .

For this test, all specimens were cured according to Wirtgen (2012) procedure, in which specimens are kept unsealed at  $30^\circ\text{C}$  until they reach between 60% and 70% of OMC (usually takes 24 hours), which is considered as the field equilibrium moisture. Then, they were sealed in a plastic bag and

kept at 40°C for 48 hours. After this process, two specimens were soaked in water at 25°C for 24 hours, after which they should be tested at soaked condition.

The specimens at soaked condition should be tested with a confining pressure of 100 kPa, so retained cohesion may be calculated afterwards comparing soaked and equilibrium specimens. The retained cohesion ratio was calculated after the test, reaching the minimum recommended value of 50% (Asphalt Academy, 2009). Table 13 presents the results of the monotonic triaxial tests separated by confinement conditions.

**Table 13 – Monotonic Triaxial Test results**

	Units	SET 1	SET 2	SET 3	SET 4
Dry Density	(g/cm <sup>3</sup> )	1.865	1.881	1.883	1.898
Applied Failure Load	(kN)	4.1	5.7	7.3	7.8
Displacement	(mm)	3.5	9.0	11.6	11.6
Applied Failure Stress	(kPa)	228	316	400	432
<b>Applied Confining Stress (<math>\sigma_3</math>)</b>	<b>(kPa)</b>	<b>0</b>	<b>50</b>	<b>100</b>	<b>140</b>
<b>Major Principle Stress at failure (<math>\sigma_{1,f}</math>)</b>	<b>(kPa)</b>	<b>231</b>	<b>369</b>	<b>502</b>	<b>575</b>

It can be observed that as the applied  $\sigma_3$  increases, so does  $\sigma_{1,f}$ , showing how the material is stress dependent. It should be noticed that even though the mixture design defined the maximum dry density for the material as 1,845 g/cm<sup>3</sup> and the obtained dry density for all samples seem to be close to that, a higher density would be expected for a BSM mixture composed essentially by RAP material. As an example, the mixture used in the Ayrton Senna Highway, and characterized in Chapter 3, section 3.3, had 2.03 g/cm<sup>3</sup> dry density. Since higher densities would result in a better material interlocking and, consequently, a higher friction angle, lower densities could result in a weaker material, reducing its failure load.

Figure 42 shows the test results presented as Mohr-Coulomb Circles, and the resulting failure envelope. Material cohesion is the intercept between the failure envelope (a line tangent to the four Mohr-Coulomb circles) and the angle of internal friction is the failure envelope angle with the Normal Stress axis.

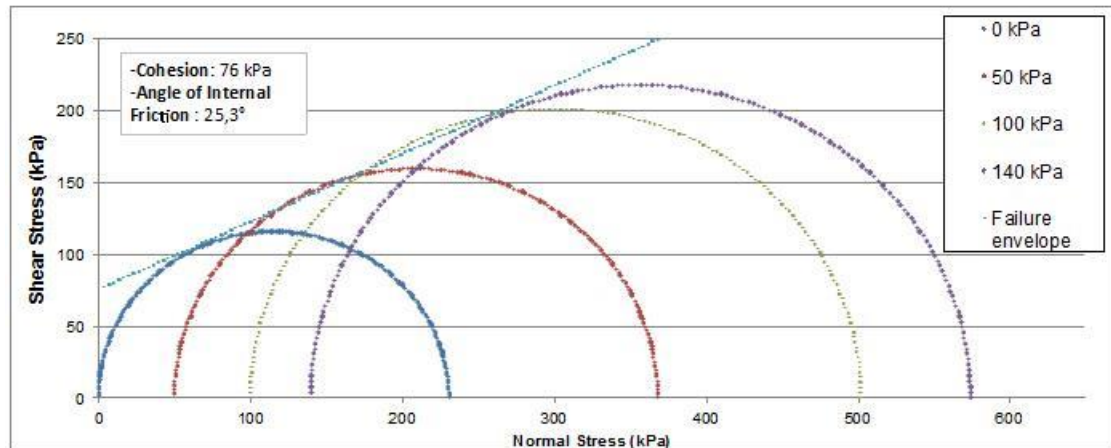


**Figure 42 – Mohr-Coulomb failure envelope**

A cohesion of 76 kPa and an angle of internal friction of 25.3° was calculated for the material. Both are considered to be low values for BSMs, what would result in a BSM3 classification by Wirtgen (2012). Since the 300 x 150 mm specimen is considerably bigger than the CBR and 200 x 100 mm specimens used in the other tests, it demands more effort from the hammer operator. The desired compaction may not have been achieved due to the fatigue of the operator in the later stages of compaction. This could have led to insufficient compaction and therefore the low dry densities obtained. Usual compaction procedures for BSM mixtures in South Africa apply Vibrating Compaction Hammers (Mulusa, 2009). This change would reduce variability from manual compaction, while guaranteeing that the right amount of energy was applied.

## 5 SUMMARY AND CONCLUSIONS

After a review of the existing literature on the theme of cold recycling, it can be observed that the number of studies about it have been increasing since the beginning of the century. Although it is not a new technique, the search for sustainable use of natural resources, allied to the necessity of cost reduction on road maintenance and construction have mobilized the industry into the development of the existing recycling techniques. As new construction techniques and more sophisticated equipment are developed, more researches aim to understand in detail the behaviour of the different mixtures and materials.

The foam bitumen stabilization technique for recycling purposes is particularly under development. Although procedures for mixture design, material characterization and structural analysis exist, the mechanical behaviour and distress mode are still being discussed.

Once recycled layers may be made out of different materials, the best way to standardize procedures may be treat them all as reclaimed aggregates. Therefore for every different project the material characterization process shall be done, resulting in common design parameters independently of the recycled material.

As for foamed mixes, a line may need to be drawn between a non-continuously bonded material, which is the concept between South African and New Zealand methodologies, and continuously bound bitumen layers, as the case of United Kingdom and many Australian methods. Once those two concepts are differentiated, the material may be treated by their characteristics instead of their construction/production procedure.

As a result, the mix design and the structural design are intimately related, as material characteristics will have direct impact on its structural performance.

When BSM mixtures are treated as non-continuously bonded materials, as was the case for this study, low asphalt binder contents are used. In the process of foam stabilization, the asphalt binder only covers the finer particles, which turn out responsible for the formation of weak non-continuous bonds between particles, increasing material cohesion and reducing moisture susceptibility. However, BSM stress dependency is not suppressed, making it behave similarly to granular materials when subject to loading, but with a higher resistance due to the increased cohesion.

Once crack propagation is difficult in BSMs due to the nature of its bonds, a more appropriate approach for structural design is the analysis of the accumulation of permanent deformation.

In this study laboratory tests were performed to analyse the accumulation of permanent deformation on BSM slabs with the LCPC traffic simulator. The verified deformations, however, have been very low, with all tested samples easily resisting the total amount of cycles of the tests. The laboratory conditions may be considered more severe than in the field since the slab is directly loaded by the contact of the pneumatics, while in the field BSM layers are usually used as base layers. Other factor is the uninterrupted and channelized nature of the loading, whereas in the field it occurs with variable frequencies and with a broader spatial distribution.

On the other hand, the BSM slabs were tested inside their iron moulds, a material of high resistance and low deformability, what could have created unreal confining pressures when compared to a field situation. As the repeated triaxial tests showed, BSM are stress dependent and high confinement stresses could result in a greater stiffness than that verified in the field.

Moisture content variability has influenced material stiffness, fact that could be verified when comparing dry cured samples and humid cured samples. Moisture content was considerably higher in the later and as result, stiffness was drastically smaller.

If the curing procedures for cylindrical specimens and slab-shaped specimens are compared, while the former was cured with its entire surface exposed, except from the bottom, the later was cured inside the mould with only its top surface exposed. That may explain why curing seemed to be slower for the slabs, with smaller curing periods resulting in the double or triple of the other deformations. On the other hand, the relation between increased stiffness and longer curing periods was not clearly identified in the resilient modulus tests. This increase in stiffness was identified to be related to the curing stage as a function of moisture reduction in the mixture.

Material curing due to chemical reactions was also verified, as specimens with similar moisture content, but higher curing periods, presented higher resilient modulus.

Material curing was also observed in the field, as the deflections measured in the trial section were drastically reduced during the evaluated time span. Even though seasonal variations are expected when analysing pavement behaviour in the field, the stiffness increase verified by the FWD analysis was in accordance with the results obtained from laboratory analysis. When analysing moisture loss as a major factor for material curing and thus stiffness increase, laboratory tests results can be compared to those obtained from the trial section evaluation.

Considering that in the first FWD evaluation with material undergoing cure, and with high moisture content, and in the third one with curing at advanced stage and lower moisture content, backcalculated elastic modulus can be compared to the resilient modulus from humid cured and dry cured specimens, respectively.

Resilient modulus results obtained for dry cured specimens presented values between 740 MPa and 1400 MPa, while humid cured specimens showed values ranging from 240 MPa up to 890 MPa. Those results are in good agreement to those obtained for material elastic modulus in the field, which resulted in an average of 240 MPa in the first FWD evaluation, and an average of 960 MPa for the third one.

This thesis has attained its specific objectives for successfully assessing all proposed analysis.

- Backcalculated FWD elastic modulus was compared to resilient modulus from Triaxial Repeated Load Testing, with a good relation between the results for material stiffness before and after curing;
- The effect of confinement was successfully quantified as material increasing stiffness rate can achieve over 100%. Therefore, BSM mechanical behaviour was defined as similar to granular material due to its significant stress dependency;
- Curing influence on material behaviour was well evaluated through its resulting stiffness variation and permanent deformation accumulation reduction.

## 6 SUGGESTIONS FOR FUTURE RESEARCH

As the evaluation performed in this study assess some of the questions regarding BSM, several others remain unanswered.

From a field performance evaluation point of view, a few suggestions are:

- FWD evaluation of existing performing BSM structures along with climate monitoring to assess the effects of seasonal variation on layer performance.
- FWD analysis for different load applications so in situ effect of confinement can be verified.
- Permanent deformation monitoring of performing BSM structures for failure criteria determination and evaluation;

From a laboratory point of view, some suggestions are:

- Permanent deformation evaluation through the shakedown method, where field confining stresses can be achieved simulating service conditions.
- Evaluation of viscoelastic properties in BSMs through temperature dependency and load frequency evaluation;
- Comparison between the effect of temperature dependency and moisture content on BSMs performance, as a way of assessing the different factors involved in seasonal variation;
- Evaluation of aggregate material influence on BSM properties;
- Analysis of moisture induced damage on BSM materials as a result of seasonal variation.

At last, from a theoretical point of view the suggestions are to:

- Compare the differences between a linear elastic mechanistic design approach and a non-linear one, considering the material stress dependency and the impacts of different approaches on pavement lifetime expectancy;



- Finite Element / Linear Elastic / Non-linear modelling for calculating BSM particle stress state dependence on vehicle configuration and loading, as a way of evaluating different material damage levels.

## 7 REFERENCES LIST

ABEDA. Associação Brasileira das Empresas Distribuidoras de Asfalto. Manual básico de emulsões asfálticas: Soluções para pavimentar sua cidade. Rio de Janeiro. 2001.

ALABASTER, D., PATRICK, J., ARAMPAMOORTHY, H., GONZALEZ, A., The design of stabilized pavements in New Zealand, New Zealand Transport Agency research report 498, Wellington, New Zealand. 2013.

ARRA. Asphalt Reclaiming and Recycling Association – Basic Asphalt Recycling Manual. 2001.

ASPHALT ACADEMY, Technical Guideline: Bitumen Stabilized Materials, A Guideline for Design and Construction of Bitumen Emulsion and Foamed Bitumen Stabilized Materials. Pretoria, South Africa, 2009.

ASPHALT ACADEMY, Interim Technical Guideline: The Design and Use of Foamed Bitumen Treated Materials , TG2, Pretoria, South Africa, 2002.

ASPHALT INSTITUTE, Asphalt Cold-Mix Recycling (MS-21). Maryland, USA. 1983.

AUSTROADS, Review of Structural Design Procedures for Foamed Bitumen Design, Austroads Technical Report - AP-T188/11, Sidney, Australia, 2011.

BALBO J.T. Pavimentação Asfáltica: materiais projeto e restauração. São Paulo: Oficina de Textos. 2007.

BANG, S., LEIN, W., COMES, B., NEHL, L., ANDERSON, J., KRAFT, P., DESTIGTER, M., LEIBROCK, C., ROBERTS, L., SEBAALY, P. and others, Quality Base Material Produced Using Full Depth Reclamation on Existing Asphalt Pavement Structure--Task 4: Development of FDR Mix Design Guide. 2011.

BERNUCCI, L. B.; MOTTA, L. M. G.; CERATTI, J. A. P.; SOARES, J.B. Pavimentação Asfáltica: Formação básica para engenheiros. Rio de Janeiro. 2010.

BLEAKLEY, A., M., COSENTINO, P., J., Improving the Properties of Reclaimed Asphalt Pavement for Roadway Base Applications through Blending and Chemical Stabilization. 92nd Annual Meeting of the Transportation Research Board. 2012.

BONFIM, V. Estudo da granulometria resultante da fresagem de revestimentos asfálticos com vistas à reciclagem “in situ” a frio. Master of Engineering Degree Thesis, EPUSP, USP. São Paulo. 1999.

BONFIM, V. Fresagem de pavimentos asfálticos. 3ª Edição. Ed Exceção. São Paulo 2011.

BROVELLI, C., CRISPINNO, M., Bitumen emulsion and foam bitumen for cold recycled and bitumen stabilized materials: a comparison based on performances, costs and safety. 8th International Conference on Managing Pavement Assets. Paper ICMPA068. Santiago, Chile. 2011.

CASTRO, L. N. Reciclagem a frio “in situ” com espuma de asfalto. Master of Engineering Degree Thesis, COPPE/UFRJ, Rio de Janeiro. 2003.

CASTRO NETO, A. M., Proposta de Projeto de Dosagem de Concreto Betuminoso Reciclado a Quente. Master of Engineering Degree Thesis, EPUSP, USP. São Paulo. 2000.

CSRA Committee of State Road Authorities, Technical Recommendations for Highways (TRH) 14, Guidelines for Road Construction Materials, from the Committee of State Road Authorities. Pretoria, South Africa, 1985.

COLLINGS, D., LINDSAY, R., SHUNMUGAM, R., LTPP Exercise on a Foamed Bitumen Treated Base – Evaluation of almost 10 years of heavy trafficking on MR504 in KwaZulu-Natal, Conference on Asphalt Pavements for South Africa (CAPSA04), Sun City, South Africa, 2004.

COLLINGS, D., JENKINS, K. J., The Long-term behavior of Bitumen Stabilised Materials (BSMs), 10<sup>th</sup> Conference on Asphalt Pavements for South Africa (CAPSA11), KwaZulu-Natal, South Africa, 2011.

DAL BEN, M., Resilient Response and Performance of Bitumen Stabilized Materials with Foam incorporating Reclaimed Asphalt. PhD Dissertation. Stellenbosch University, South Africa, 2014.

DNIT, Departamento Nacional de Infra-Estrutura de Transportes, SNV publication of 03/12/2014. Available at <http://www.dnit.gov.br/sistema-nacional-de-viacao/sistema-nacional-de-viacao> in 05/09/2015.

EBELS, L. J., Characterization of Material Properties and behavior of Cold Bituminous Mixtures for Road Pavements. PhD Dissertation. Stellenbosch University, South Africa, 2008.

FREMIX, Fremix Engenharia e Comércio LTDA., Verificação do Projeto de Dosagem Reciclagem em Usina a frio com espuma de asfalto, Technical Report ARVEK DP BARROS 01/14, São Paulo, 2014.

FU, P., HARVEY, J. T., Temperature sensitivity of foamed asphalt mix stiffness: field and lab study. International Journal of Pavement Engineering, Vol. 8, No. 2, 137-145, 2007.

FU, P., HARVEY, J. T., JONES, D., CHAO, Y. Understanding internal structure characteristics of foamed asphalt mixes with Fracture Face Image Analyses. Transportation Research Record: Journal of the Transportation Research Board, No 2057. Transportation Research Board of National Academies. Washington. D.C., 2008.

FU, P., JONES, D., HARVEY, J. T., The effects of asphalt binder and granular material characteristics on foamed asphalt mix strength, Construction and Building Materials, Volume 25, Issue 2, February 2011, 1093-1101, 2011.

HEATH, A., ROESLER, J., Shrinkage and Thermal Cracking of Fast Setting Hydraulic Cement Concrete Pavements in Palmdale, California. Davis and Berkeley, CA: University of California Research Center. 1999.

HUAN, Y., SIRIPUN, K., JITSANGIAM, P., NIKRAZ, H., A preliminary study on foamed bitumen stabilization for Western Australian pavements. Scientific Research and Essays Vol. 5 (23), Perth, Australia. 2010.

JBA ENGENHARIA E CONSULTORIA LTDA., Rodovia Ayrton Senna – Restauração do Pavimento com RAP Espumado, São Paulo, March/2012.

JBA ENGENHARIA E CONSULTORIA LTDA., Estudo para definição do traço de RAP+BGTC com espuma de asfalto – Rodovia Ayrton Senna SP-070, São Paulo, June/2013.

JENKINS, K. J., Mix Design Considerations for cold and half-warm bituminous mixes with emphasis on foamed bitumen. PhD Dissertation, Stellenbosch University. South Africa, 2000.

JENKINS, K. J., Cracking Behaviour of Bitumen Stabilised Materials (BSMs): Is there such a thing? 7<sup>th</sup> RILEM International Conference on Cracking in Pavements. Volume 4 of the series RILEM Book series pp1007-1015. 2012.

JENKINS, K. J., VAN DER VEN, M. F. C., MOLENAAR, A. A. A., GROOT, J. L. A., Performance prediction of cold foamed mixes, Proceedings 9<sup>th</sup> International Conference on Asphalt Pavements, Copenhagen, Denmark, 2002.

JONES, D., FU, P., HARVEY, J., MINE T., Full-Depth Recycling with Foamed Asphalt in California: Guidelines for Project Selection, Design, and Construction. Institute of Transportation Studies, University of California, Davis, Research Report UCD-ITS-RR-09-50. 2009.

JONES, D., WU, R., LOUW, S., Comparison of Full Depth Reclamation with Foamed Asphalt and Full Depth Reclamation with No Stabilizer in an Accelerated Loading Test, 93<sup>rd</sup> Transportation Research Board Annual Meeting, Paper 14-15144, Washington, 2014.

JOOSTE, F., LONG, F., A Knowledge Based Structural Design Method for Pavements Incorporating Bituminous Stabilized Materials. Technical Memorandum. Gauteng Department of Public Transport, Roads and Works

and South Africa Bitumen Association (SABITA), Pinelands, South Africa. 2007.

LEEK, C., Review of the performance of insitu foamed bitumen stabilised pavements in the City of Canning, 5<sup>th</sup> Australian Road Engineering and Maintenance Conference, Melbourne, Victoria, Australia, 2010.

LOIZOS, A., PAPAVALIOU, V., PLATI, C., Investigating In-situ Stress-Dependent Behaviour of Foamed Asphalt Treated Pavement Materials, Road Materials and Pavements Design, Volume 13, Issue 4, 678-690, 2012.

LOUDON INTERNATIONAL, Technical Proposal for the Construction of a Trial Section – 600m of Slow Lane, Westbound Carrieway (km 15+650 to km 16+250), South Africa, October of 2011.

LYNCH, A. G., Trends in Back-calculated Stiffness of in-situ Recycled and Stabilized Road Pavement Materials. Master of Engineering Degree Thesis. Stellenbosch University, South Africa, 2013.

MARTINEZ, R. M., BONFIM, V., PAIVA, C. E. L de., Retroanálisis para Estimar los Módulos de las capas de un Pavimento Reciclado con Espuma de Asfalto, 01/2013, XVII Congreso Ibero-Latinoamericano del Asfalto, Vol. único, pp.205-215, Guatemala, Guatemala, 2013.

MILTON, L. J., EARLAND, M., Design guide and specification for structural maintenance of highway pavements by cold in-situ recycling, Prepared for CSS, Colas Limited and the Pavement Engineering Group, Highways Agency, TRL Report 386. United Kingdom, 1999.

MULUSA, W. K., Development of a Simple Triaxial Test for characterising bitumen stabilized materials, Master of Engineering Degree Thesis. Stellenbosch University, South Africa, 2009.

NUNN, M., THOM, N., Foamix: Pilot scale trials and design considerations, Viridis Report VR1, Transportation Research Laboratory, United Kingdom, 2002.

RAHMAN, F., HOSSAIN, M., HOBSON, C., SHIEBER, G., Performance of Superpave Mixtures with High RAP Content in Kansas. 93rd Annual Meeting of the Transportation Research Board, Washington D.C., 2014.

RAMANUJAM, J. M., JONES, J. D., Characterization of foamed-bitumen stabilization, International Journal of Pavement Engineering, 8:2, 111-122, 2007.

ROBERTS, F., L., KANDHAL, P., S., BROWN, E., R., LEE, D., KENNEDY, T., W., Hot Mix Asphalt Materials, Mixture Design, and Construction. National Asphalt Pavement Association Research and Education Foundation, 2<sup>nd</sup> Edition, Lanham, Maryland. 1996.

SANRAL. South African National Roads Agency Ltd. South African Pavement Engineering Manual. Second Edition, 2014.

SCHWARTZ, C., W., KHOSRAVIFAR, S., Research Report: Design and Evaluation of Foamed Asphalt Base Materials. Project Number SP909B4E. Maryland. 2013.

STROUP-GARDINER; M., NCHRP Synthesis 421, Recycling and Reclamation of Asphalt Pavements Using In-Place Methods – A Synthesis of Highway Practice. Washington D.C., 2011.

TANG, S., CAO, Y., LABUZ, J., F., Structural Evaluation of Asphalt Pavements with Full-Depth Reclaimed Base. Report no. MnDOT 2012-36. 2012.

THEYSE, H., L., DE BEER, M., RUST, F., C., Overview of South African Mechanistic Pavement Design Method. Transportation Research Record 1539. 1996.

THEYSE, H., L., MUTHEN, M., Pavement analysis and design software (PADS) based on mechanistic-empirical design method.. South African Transport Conference 'Action in Transport for the New Millennium'. Pretoria. 2000.

THOMPSON, M., R., GARCIA, L., CARPENTER, S., H., Cold In-place Recycling and Full-Depth Recycling with asphalt products (CIR & FDRwAP) Research Report ICT-09-036. Illinois Center for Transportation. 2009.

TMR, Transportation and Main Roads, Pavement Rehabilitation Manual, Brisbane, Australia, 2012.

TWAGIRA, E. M., Influence of Durability Properties on Performance of Bitumen Stabilized Materials. . PhD Dissertation, Stellenbosch University. South Africa, 2010.

WEST. R., C., Reclaimed Asphalt Pavement management: Best Practices. National Center for Asphalt Technology, Auburn, AL. 2010

WIRTGEN GMBH. Manual de Tecnologia de Reciclagem a Frio. 1ª Edição. 2012.



## APPENDIX

**Table 14 – FWD data and backcalculation results for measurements made on September/2013, on top of the remaining infrastructure**

Test Position (km)	Applied Stress (kPa)	Applied Load (kN)	D1 (μm)	D2 (μm)	D3 (μm)	D4 (μm)	D5 (μm)	D6 (μm)	D7 (μm)	Air Temperature (°C)	Pav. Temperature (°C)	E1 (Mpa)	E2ref (Mpa)	H1 (mm)	H2 (mm)
18.950	594	42.0	1299	953	702	514	358	196	114	19	21	130	30	1000	-
18.940	590	41.7	942	760	599	447	315	167	99	19	20	198	31	1000	-
18.930	593	41.9	1062	787	600	430	289	154	88	18	21	165	36	1000	-
18.920	601	42.5	979	789	590	392	240	110	60	18	21	176	40	1000	-
18.910	603	42.6	1089	803	558	339	176	59	29	18	21	154	52	1000	-
18.900	609	43.0	1028	717	422	239	119	42	28	18	22	167	12	1000	-
18.890	611	43.2	1000	704	475	266	132	42	26	18	21	182	10	1000	-
18.880	601	42.5	1205	777	442	202	90	27	23	18	22	136	14	1000	-
18.870	608	43.0	1049	663	371	179	75	28	26	18	21	163	13	1000	-
18.860	603	42.6	1032	685	434	230	120	52	38	18	21	164	12	1000	-
18.850	601	42.5	1081	744	445	230	122	52	34	18	20	155	13	1000	-
18.840	600	42.4	1115	704	436	246	123	48	35	18	22	149	13	1000	-
18.830	612	43.3	1416	970	612	316	131	29	29	18	21	120	10	1000	-
18.620	615	43.5	777	519	294	144	67	30	27	16	20	217	16	1000	-
18.610	606	42.8	1077	675	353	165	73	34	29	16	19	158	10	1000	-
18.600	610	43.1	799	485	276	136	66	36	29	16	20	219	16	1000	-
18.590	600	42.4	1191	717	437	197	80	33	28	16	19	139	11	1000	-
18.580	609	43.0	908	620	437	202	104	49	37	16	20	193	12	1000	-

Test Position (km)	Applied Stress (kPa)	Applied Load (kN)	D1 (μm)	D2 (μm)	D3 (μm)	D4 (μm)	D5 (μm)	D6 (μm)	D7 (μm)	Air Temperature (°C)	Pav. Temperature (°C)	E1 (Mpa)	E2ref (Mpa)	H1 (mm)	H2 (mm)
18.570	604	42.7	1049	734	465	219	95	38	31	16	20	163	8	1000	-
18.560	613	43.3	934	603	387	194	84	40	29	16	20	189	11	1000	-
18.550	602	42.5	871	495	277	125	58	32	29	16	20	196	11	1000	-
18.540	604	42.7	913	600	353	188	75	31	24	16	20	186	14	1000	-
18.530	616	43.5	817	533	314	140	62	30	26	16	20	216	14	1000	-
18.520	606	42.8	706	495	296	149	69	34	26	16	20	240	20	1000	-
18.510	616	43.5	654	441	278	147	73	37	29	16	19	267	21	1000	-
18.500	618	43.7	942	623	305	127	55	25	20	16	20	176	18	1000	-
18.490	610	43.1	1027	647	400	194	84	39	28	16	20	160	18	1000	-
18.480	613	43.3	820	565	343	160	83	42	29	16	20	214	15	1000	-

**Table 15 –FWD data and backcalculation results for measurements made on September/2013, on top of the bottom BSM layer**

Test Position (km)	Applied Stress (kPa)	Applied Load (kN)	D1 (μm)	D2 (μm)	D3 (μm)	D4 (μm)	D5 (μm)	D6 (μm)	D7 (μm)	Air Temperature (°C)	Pav. Temperature (°C)	E1 (Mpa)	E2ref (Mpa)	H1 (mm)	H2 (mm)
18.950	604	42.7	1187	858	593	420	301	177	108	17	20	381	35	200	-
18.940	610	43.1	903	618	420	306	228	142	96	16	20	413	64	200	-
18.930	610	43.1	987	695	465	328	241	148	97	16	20	397	51	200	-
18.920	614	43.4	1088	741	443	292	201	105	65	16	19	389	32	200	-
18.910	612	43.3	1137	783	434	256	152	73	41	16	20	489	17	200	-
18.900	620	43.8	1075	680	412	247	143	63	34	16	20	438	24	200	-
18.890	618	43.7	976	649	378	226	133	57	32	16	20	560	21	200	-
18.880	578	40.9	2085	1470	904	496	214	43	21	16	20	110	44	200	-
18.870	613	43.3	1018	683	400	222	115	43	31	16	20	602	15	200	-
18.860	618	43.7	986	632	376	224	137	69	48	16	19	436	31	200	-
18.850	613	43.3	1094	706	448	255	148	68	41	16	19	448	22	200	-
18.840	617	43.6	1082	716	432	266	156	73	44	16	20	444	24	200	-
18.830	561	39.7	2370	1869	1307	851	439	54	18	16	19	116	30	200	-
18.620	635	44.9	806	511	262	142	81	42	32	14	17	308	69	200	-
18.610	626	44.3	1082	723	403	216	114	48	34	14	17	309	31	200	-
18.600	631	44.6	745	470	263	151	86	45	33	14	17	391	64	200	-
18.590	625	44.2	1029	658	376	208	107	45	30	14	17	337	31	200	-
18.580	626	44.3	1000	675	413	243	131	52	33	14	17	441	28	200	-
18.570	624	44.1	994	675	387	220	119	51	35	14	17	363	33	200	-
18.560	624	44.1	1018	657	359	190	99	42	30	14	17	309	34	200	-
18.550	631	44.6	880	557	304	166	90	40	29	14	17	352	44	200	-

Test Position (km)	Applied Stress (kPa)	Applied Load (kN)	D1 (μm)	D2 (μm)	D3 (μm)	D4 (μm)	D5 (μm)	D6 (μm)	D7 (μm)	Air Temperature (°C)	Pav. Temperature (°C)	E1 (Mpa)	E2ref (Mpa)	H1 (mm)	H2 (mm)
18.540	620	43.8	942	581	321	172	87	33	22	14	16	350	33	200	-
18.530	630	44.5	836	527	283	152	81	37	28	14	17	335	49	200	-
18.520	630	44.5	786	483	261	145	85	41	28	14	17	360	57	200	-
18.510	629	44.5	785	477	268	151	87	45	30	14	17	369	59	200	-
18.500	623	44.0	1006	640	334	164	81	32	23	14	17	314	31	200	-
18.490	621	43.9	984	628	339	181	97	43	31	14	17	306	38	200	-
18.480	625	44.2	910	536	307	180	104	48	31	14	17	347	46	200	-

**Table 16– FWD data and backcalculation results for measurements made on September/2013, on top of the top BSM layer**

Test Position (km)	Applied Stress (kPa)	Applied Load (kN)	D1 (μm)	D2 (μm)	D3 (μm)	D4 (μm)	D5 (μm)	D6 (μm)	D7 (μm)	Air Temperature (°C)	Pav. Temperature (°C)	E1 (Mpa)	E2ref (Mpa)	H1 (mm)	H2 (mm)
18.950	616	43.5	984	702	478	339	249	153	102	14	17	235	70	340	-
18.940	620	43.8	832	555	364	258	194	128	90	14	16	269	93	340	-
18.930	620	43.8	870	606	395	280	207	133	91	14	16	263	85	340	-
18.920	616	43.5	853	573	366	250	175	103	64	14	16	250	95	340	-
18.910	614	43.4	935	601	366	239	160	83	49	14	16	212	98	340	-
18.900	616	43.5	882	550	350	222	142	70	39	14	16	330	22	340	-
18.890	614	43.4	902	566	345	212	137	71	43	14	17	310	22	340	-
18.880	618	43.7	1011	685	417	248	152	71	41	14	16	192	93	340	-
18.870	619	43.8	819	528	316	196	123	59	36	14	17	392	16	340	-
18.860	618	43.7	826	546	321	200	132	70	45	14	17	368	20	340	-
18.850	613	43.3	882	581	357	223	147	78	49	14	16	228	101	340	-
18.840	615	43.5	907	589	366	230	149	76	45	14	17	220	101	340	-
18.830	604	42.7	1339	1009	664	440	291	125	64	14	17	158	52	340	-
18.620	612	43.3	757	473	268	163	102	53	36	24	27	251	64	340	-
18.610	591	41.8	1125	738	462	275	159	70	39	24	27	193	24	340	-
18.600	613	43.3	673	393	220	136	92	54	35	24	27	271	94	340	-
18.590	607	42.9	899	559	319	185	105	49	31	24	27	212	43	340	-
18.580	601	42.5	925	584	309	173	106	59	38	24	28	183	58	340	-
18.570	597	42.2	988	597	327	184	127	54	32	28	31	200	38	340	-
18.560	600	42.4	849	526	292	167	102	50	28	28	31	228	44	340	-
18.550	600	42.4	804	485	269	157	95	43	27	28	30	239	48	340	-

Test Position (km)	Applied Stress (kPa)	Applied Load (kN)	D1 (μm)	D2 (μm)	D3 (μm)	D4 (μm)	D5 (μm)	D6 (μm)	D7 (μm)	Air Temperature (°C)	Pav. Temperature (°C)	E1 (Mpa)	E2ref (Mpa)	H1 (mm)	H2 (mm)
18.540	599	42.3	851	511	280	160	98	47	28	28	31	217	49	340	-
18.530	602	42.5	756	464	247	143	89	45	30	28	30	233	67	340	-
18.520	601	42.5	782	456	235	137	89	47	31	28	32	216	76	340	-
18.510	597	42.2	711	443	238	143	88	48	30	29	31	250	72	340	-
18.500	590	41.7	974	574	318	176	103	49	30	29	31	185	41	340	-
18.490	592	41.8	868	556	313	169	100	48	29	29	31	216	43	340	-
18.480	599	42.3	866	524	297	170	105	53	34	29	31	210	54	340	-

**Table 17– FWD data and backcalculation results for measurements made on December/2013**

Test Position (km)	Applied Stress (kPa)	Applied Load (kN)	D1 (μm)	D2 (μm)	D3 (μm)	D4 (μm)	D5 (μm)	D6 (μm)	D7 (μm)	Air Temperature (°C)	Pav. Temperature (°C)	E1 (Mpa)	E2ref (Mpa)	H1 (mm)	H2 (mm)
18.950	604	42.7	1216	532	440	278	263	153	107	19	27	155	87	360	-
18.940	608	43.0	960	398	319	209	191	119	84	19	26	201	116	360	-
18.930	602	42.5	659	408	318	208	197	133	94	19	27	324	106	360	-
18.920	606	42.8	1114	357	293	186	168	110	78	19	27	168	131	360	-
18.910	605	42.8	889	369	298	193	162	93	58	19	27	243	84	360	-
18.900	601	42.5	1231	480	376	245	199	108	60	19	27	168	56	360	-
18.890	599	42.3	1327	456	358	224	186	97	51	19	27	153	57	360	-
18.880	603	42.6	1205	411	320	198	159	79	45	20	28	166	66	360	-
18.870	609	43.0	1149	449	279	166	141	79	50	20	28	142	102	360	-
18.860	606	42.8	1018	387	325	198	165	82	47	20	28	221	61	360	-
18.850	603	42.6	1327	456	347	218	175	90	49	20	28	149	62	360	-
18.840	598	42.3	1170	494	365	221	179	90	49	20	27	179	47	360	-
18.830	601	42.5	865	384	294	182	155	88	56	20	28	227	87	360	-
18.620	606	42.8	976	323	242	142	115	62	41	19	27	179	123	360	-
18.610	600	42.4	1216	411	314	190	144	66	32	19	26	178	50	360	-
18.600	606	42.8	750	297	221	136	110	60	39	19	27	245	121	360	-
18.590	607	42.9	780	331	252	150	114	55	31	19	27	273	65	360	-
18.580	602	42.5	1212	437	296	164	139	66	38	19	27	142	73	360	-
18.570	601	42.5	1070	448	316	177	140	69	36	19	27	185	52	360	-
18.550	602	42.5	831	365	274	161	125	58	30	19	27	268	53	360	-
18.530	600	42.4	1188	396	301	173	132	60	35	20	28	160	64	360	-

Test Position (km)	Applied Stress (kPa)	Applied Load (kN)	D1 (μm)	D2 (μm)	D3 (μm)	D4 (μm)	D5 (μm)	D6 (μm)	D7 (μm)	Air Temperature (°C)	Pav. Temperature (°C)	E1 (Mpa)	E2ref (Mpa)	H1 (mm)	H2 (mm)
18.520	604	42.7	1090	338	267	150	118	52	30	20	28	172	77	360	-
18.510	602	42.5	1152	352	258	162	116	55	30	20	28	171	70	360	-
18.500	597	42.2	1061	349	329	185	147	59	28	20	28	264	39	360	-
18.490	597	42.2	1162	449	333	192	144	62	28	20	27	198	36	360	-
18.480	600	42.4	969	431	324	179	144	67	36	20	28	214	49	360	-



**Table 18 – FWD data and backcalculation results for measurements made on October/2014**

Test Position (km)	Applied Stress (kPa)	Applied Load (kN)	D1 (μm)	D2 (μm)	D3 (μm)	D4 (μm)	D5 (μm)	D6 (μm)	D7 (μm)	Air Temperature (°C)	Pav. Temperature (°C)	E1 (Mpa)	E2ref (Mpa)	H1 (mm)	H2 (mm)
18.950	609	43.0	27	22	19	16	13	9	7	19	26	1437	102	360	-
18.940	540	38.2	25	16	15	13	11	7	7	19	26	1251	153	360	-
18.930	567	40.1	24	18	16	14	12	8	7	19	26	1411	145	360	-
18.920	580	41.0	23	16	14	12	10	7	6	19	26	1407	172	360	-
18.910	575	40.6	24	17	15	13	10	7	5	19	26	1398	119	360	-
18.900	551	39.0	27	19	17	15	11	7	6	19	26	1215	94	360	-
18.890	572	40.4	27	20	17	14	11	6	5	19	26	1194	88	360	-
18.880	597	42.2	27	19	16	13	10	6	5	19	26	1168	112	360	-
18.870	589	41.6	24	17	15	12	9	6	5	19	26	1237	133	360	-
18.860	551	39.0	29	20	16	13	10	6	5	19	26	951	114	360	-
18.850	604	42.7	27	19	16	13	11	7	5	19	26	1174	127	360	-
18.840	585	41.3	33	22	19	15	11	7	5	19	26	876	99	360	-
18.830	603	42.6	42	30	24	19	14	7	5	19	26	706	62	360	-
18.620	564	39.9	27	19	15	12	9	6	4	19	26	973	119	360	-
18.610	597	42.2	39	25	20	16	11	6	4	19	26	686	83	360	-
18.600	608	43.0	27	18	15	12	9	5	4	19	26	1067	142	360	-
18.590	598	42.3	32	20	16	12	9	5	4	19	26	799	123	360	-
18.580	583	41.2	33	22	18	14	11	6	4	19	26	889	88	360	-
18.570	592	41.8	41	27	22	16	11	6	4	19	26	656	72	360	-
18.560	614	43.4	43	29	23	18	12	7	4	19	26	689	60	360	-
18.550	583	41.2	33	23	19	13	11	6	4	19	26	867	86	360	-

Test Position (km)	Applied Stress (kPa)	Applied Load (kN)	D1 (μm)	D2 (μm)	D3 (μm)	D4 (μm)	D5 (μm)	D6 (μm)	D7 (μm)	Air Temperature (°C)	Pav. Temperature (°C)	E1 (Mpa)	E2ref (Mpa)	H1 (mm)	H2 (mm)
18.540	613	43.3	41	29	23	16	12	6	4	19	26	747	58	360	-
18.530	583	41.2	38	25	20	15	10	6	4	19	25	680	73	360	-
18.520	562	39.7	40	26	21	16	11	6	4	19	26	677	59	360	-
18.510	614	43.4	37	24	19	14	10	7	4	19	25	723	101	360	-
18.500	571	40.4	47	32	25	18	13	7	4	19	26	582	48	360	-
18.490	618	43.7	40	26	22	17	12	6	4	19	25	776	67	360	-
18.480	546	38.6	43	30	23	19	12	7	4	19	26	697	44	360	-

**Table 19 – FWD data and backcalculation results for measurements made on June/2015**

Test Position (km)	Applied Stress (kPa)	Applied Load (kN)	D1 (μm)	D2 (μm)	D3 (μm)	D4 (μm)	D5 (μm)	D6 (μm)	D7 (μm)	Air Temperature (°C)	Pav. Temperature (°C)	E1 (Mpa)	E2ref (Mpa)	H1 (mm)	H2 (mm)
18.950	618	43.7	23	20	18	16	14	10	8	16	10	2453	82	360	-
18.940	618	43.7	17	14	13	12	10	8	6	17	10	3455	136	360	-
18.930	618	43.7	17	15	14	12	11	8	7	16	10	4157	99	360	-
18.920	616	43.5	16	14	13	11	10	8	6	16	10	4633	87	360	-
18.910	617	43.6	16	13	12	11	9	7	5	16	10	4205	90	360	-
18.900	608	43.0	18	16	14	12	10	7	5	16	10	3506	74	360	-
18.890	616	43.5	17	15	13	11	9	6	4	16	10	3591	73	360	-
18.880	616	43.5	17	14	12	10	8	6	4	16	9	2962	106	360	-
18.870	617	43.6	15	12	11	9	8	5	4	16	9	3681	115	360	-
18.860	614	43.4	17	14	12	10	9	6	4	16	10	2944	108	360	-
18.850	614	43.4	18	15	13	11	9	6	4	16	9	3088	88	360	-
18.840	612	43.3	23	18	15	12	10	7	5	16	9	1784	97	360	-
18.830	611	43.2	29	23	19	15	12	8	5	16	10	1356	68	360	-
18.620	616	43.5	19	16	13	11	9	6	4	15	9	2217	106	360	-
18.610	614	43.4	25	19	16	12	10	6	4	15	9	1539	81	360	-
18.600	615	43.5	20	16	13	11	9	6	4	15	9	2110	102	360	-
18.590	612	43.3	20	16	13	10	8	5	4	15	9	1798	116	360	-
18.580	612	43.3	19	16	13	11	9	6	4	15	9	2557	85	360	-
18.570	609	43.0	26	21	17	13	10	6	4	15	9	1419	74	360	-
18.560	609	43.0	30	23	19	15	11	7	4	15	9	1314	59	360	-

Test Position (km)	Applied Stress (kPa)	Applied Load (kN)	D1 (μm)	D2 (μm)	D3 (μm)	D4 (μm)	D5 (μm)	D6 (μm)	D7 (μm)	Air Temperature (°C)	Pav. Temperature (°C)	E1 (Mpa)	E2ref (Mpa)	H1 (mm)	H2 (mm)
18.550	609	43.0	22	17	14	11	9	6	4	15	9	1822	93	360	-
18.540	609	43.0	26	21	17	13	10	6	4	15	9	1551	60	360	-
18.530	608	43.0	26	20	16	12	10	6	4	15	9	1335	85	360	-
18.520	610	43.1	23	17	14	11	9	5	3	15	9	1601	94	360	-
18.510	607	42.9	23	18	15	11	9	5	3	15	9	1683	83	360	-
18.500	608	43.0	26	20	17	13	10	6	3	15	9	1660	57	360	-
18.490	607	42.9	23	18	15	12	9	6	4	15	9	1783	83	360	-
18.480	608	43.0	27	21	18	14	11	6	4	15	9	1515	60	360	-